THE PETROLOGY OF OOLITIC PHOSPHORITES FROM ESPRIT (ALDABRA), WESTERN INDIAN OCEAN

By C. J. R. BRAITHWAITE
Department of Geology, The University, Dundee DD1 4HN, U.K.

(*Communicated by T. S. Westoll, F.R.S.* – *Received* 26 *May* 1978 – *Revised* 8 *August* 1979)

[Plates 1–7]

CONTENTS

The island of Esprit, at the western end of Aldabra lagoon, is capped by two groups of phosphorites. Near the summit, bedded deposits rest on and in cavities within the subaerially eroded surface of the limestones forming the island. The limestones themselves have not been phosphatized. On the lower slopes, and derived from the phosphorites above, are small outcrops of coarse, phosphate-cemented, bioclastic sediments and large, irregular fans of phosphoritic conglomerates.

The phosphorites can be divided into five petrographic groups. Oolitic phosphorites are the most common and are apparently primary. Associated with them are lithoclast-bearing rocks, fine-grained phosphorites, bioclastic deposits and internal sediments, all of which are also wholly phosphatic. There have been numerous reworking episodes in the history of these rocks, such that large volumes now consist only of phosphatic cement sequences (the linings of former cavities) and internal sediments. Up to fourteen changes in the depositional milieu can be seen. The distribution of both cements and internal sediments is restricted, recording the paths of particular transport streams in groundwaters.

The minerals identified are carbonatian hydroxyfluorapatites. Most cements are multilayer colloform crusts with a radially fibrous structure, but, in addition, crystals show a range of morphologies, including hexagonal, monoclinic and cubic forms. Some cements are carbonate, but other minerals that may have been present have been pseudomorphed by phosphates.

The primary source of the phosphate in these rocks is thought to have been avian guano, deposited on a limestone surface at a time when sealevel was 7–8 m above its present position. Phosphate-rich derivatives from this were carried downwards by surface-wash processes and precipitated in a series of caves in the limestones excavated at the water table and drained as sealevel fell. Solution pipes were formed when sea-level was at least 1–2 m below its present position, but marine coquinal sediments deposited within these suggest that it was subsequently higher. Continued erosion of the host limestones, destroying the caves, released both phosphorite detritus, re-deposited as the low-level sediments and transported into beach calcarenites, and phosphatic solutions for precipitation as cements.

The phosphorites are tentatively dated as deposited 170–230 ka B.P.

Introduction

Aldabra is a raised atoll in the western Indian Ocean (latitude 9° 24′ S, longitude 45° 20′ E) that was investigated geologically in 1969 as part of the Royal Society Aldabra Expedition (Braithwaite *et al.* 1973). The islet of Esprit, about 34 ha (0.34 km^2) in area, lies at the western end of the lagoon (figure 1), forming an elongate E–W crescentic ridge about 1 km long, 200 m wide and 8–10 m high, sloping gently to the east. It is densely clothed in vegetation, including quite large trees and a mangrove area on the northern shore. The island is formed by a sequence of limestones, the Esprit Limestones, which are putatively the oldest sediments exposed on Aldabra and are capped by phosphorites, the Esprit Phosphorites. The limestones are cross-bedded calcarenites in thick, tabular sets, generally fine-grained but becoming coarser locally into coquinal calcirudites. A diverse marine fauna has been recovered, dominated by bivalves (*Glycymeris*, *Fragrum* and *Trachycardium*) but including gastropods (*Cassis*, *Strombus*, *Natica* and others) and small corals (*Goniastrea* and *Favia*). This indicates a sublittoral, predominantly soft-bottom environment. In the youngest limestones, forms such as *Cerithidea*, *Terebralia palustris* and *Cerithium morum* indicate a decrease in depth and a restriction of circulation of the waters in which they lived, and the probable establishment of mangroves (Braithwaite *et al.* 1973). These changes are important since they prelude the period of emersion during which the phosphorites were formed.

These limestones have been eroded by prolonged solution, forming, particularly on the north slope, tower-like pinnacles. The Esprit Phosphorites rest unconformably on them and fall into two groups. Those near the summit are generally well bedded oolites believed to have formed *in situ*. In contrast, deposits near sealevel lie in jumbled, roughly conical masses predominantly formed by the weathering and erosion of the older materials. Phosphorites on Esprit and Picard were described by Fryer (1911), who, although he did not separate the two groups described here, did suggest that many of the sediments had formed in caves.

Taken together, these sediments are important for two reasons. (1) The oolites were probably primarily phosphatic and therefore provide evidence on conditions of phosphate precipitation. (2) Although they are 'insular', these phosphorites are petrographically different from those described from other oceanic islands (compare Braithwaite 1968; Roy 1970; and Trueman 1965).

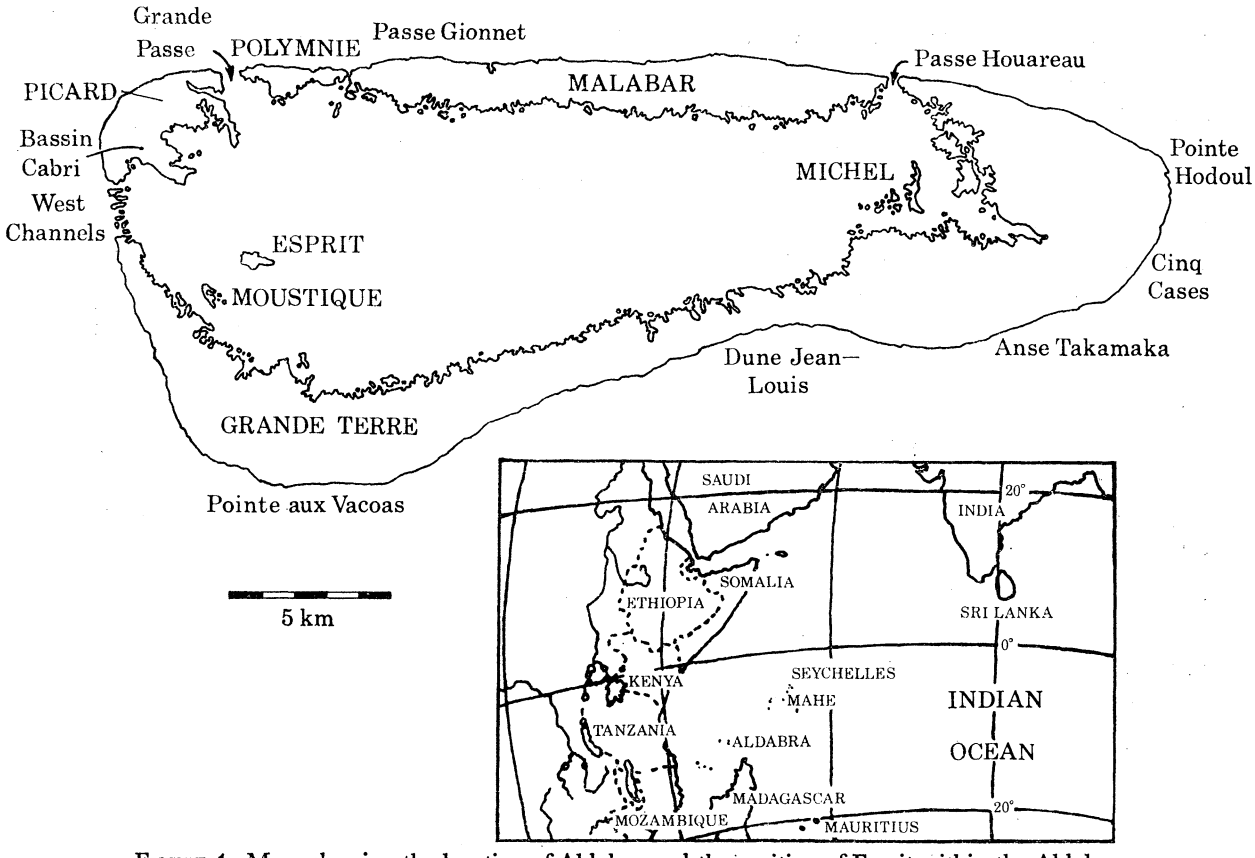

FIGURE 1. Maps showing the location of Aldabra and the position of Esprit within the Aldabra Lagoon.

FIELD RELATIONS

The Esprit Phosphorites form two spatially separated groups, which are probably of significantly different ages. At the summit and along the ridge below it, there are laterally discontinuous outcrops of bedded phosphorites up to 2 m thick. These rest upon a pinnacled limestone surface (figure 2, plate 1), but are also found occupying the floors of caves of 1–2 m horizontal diameter and of up to 50 cm height. It is likely that most of these deposits originally occupied such caverns, which have been unroofed by more recent erosion. Those remaining, open along bedding plane joints and resemble cavities forming above the surface of the present water table. If they are analogous then they must have originated when sealevel stood about 8 m higher than at present.

This group of phosphorites is thinly and sometimes irregularly bedded in units of a few centimetres. Sediments include dense clay-grade, silt and sand-size phosphate deposits. Among the sands oolites are common, together with thin, phosphatic calcarenites containing cerithiid gastropods. Lithoclast-bearing phosphate rocks are also locally common and probably dominate the coarser sediments. However, the most prominent feature of these deposits is the presence within them of numerous horizontally extensive cavities. These are of several centimetres diameter and are floored with fine-grained or oolitic phosphatic internal sediments. Residual spaces are lined with thin, multilaminate, colloform phosphate cements. Intraclast fragments of similar cements suggest that erosion and deposition have occurred many times *within* the

porous sediment body and that more than half of the rock volume may be occupied by cavities cement linings and supposed vadose sediment masses.

In contrast to these horizontally extensive caves and their deposits, there are also vertical solution pipes in the limestones, extending below sealevel but otherwise identical to those forming subaerially at the present time. Most of the phosphorite in these is in the form of disorientated blocks of oolite, described below, but there are some small, fine-grained masses adhering to walls and, on the southeastern shore of Esprit, phosphate deposits found in pipes contain moulds of marine bivalves (particularly *Scutarcopagia*), gastropods and corals. Disorientated bioclasts have been coated with laminated colloform phosphate, which extends, stalagmite-like, into large interparticle pores. Following solution, most fossils are now represented by moulds with thin phosphatic linings, but lumps of coral have been replaced *in situ* by granular phosphate or by coarsely crystalline calcite in which inclusions define septa and corallite walls.

The precipitated phosphorites that cover these fossils resemble crusts lining smaller cavities within the Esprit Limestones (figure 3, plate 1). These are selectively distributed. In the higher limestones they line only primary interparticle pores: mouldic porosity is either vacant or filled with coarsely crystalline calcite. At lower levels, although generally less common, phosphatic crusts line both primary and secondary pores.

The second major group of phosphorites is exposed principally on the shore at the eastern tip of Esprit. Sediments again rest on a pinnacled limestone surface and isolated columns of limestone project upwards through them (figure 4, plate 1). Further west they occur at low levels in the solution pipes noted above. The sediments are banked in crude 'alluvial fans', 2–3 m high and extending up to 5 m above sealevel, usually in channel-like depressions.

The deposits are dominantly red–brown (5YR 4/4–5/6, U.S.G.S. Munsell rock colour chart) and are often very porous. They are essentially unbedded and include jumbled, angular

---

Description of plate 1

Figure 2. High-level bedded phosphorites on the summit of Esprit, resting on the eroded surface of the Esprit Limestones. Contact indicated by arrow. Scale given by 35 cm hammer handle.

Figure 3. Phosphatic crusts (arrowed) in cavities within the Esprit Limestones. Bar scale 15 cm.

Figure 4. Low-level conglomeratic phosphorites resting against pinnacle of Esprit Limestone on southeastern shore of Esprit. Scale given by 35 cm hammer handle.

Figure 5. General view of oolitic phosphorite (10B31A). Ordinary light. Bar scale 1 mm.

Figure 6. Detail of concentric oolith (10A16). Ordinary light. Bar scale 0.25 mm.

Figure 7. Internal (vadose) sediment trapped above tight pore throats (10C26). Ordinary light. Bar scale 1 mm.

Description of plate 2

Figure 8. Phosphatic oolitic mudstone (10A14). Ordinary light. Bar scale 1 mm.

Figure 9. 'Micritic' lithoclasts (4D15). Ordinary light. Bar scale 1 mm.

Figure 10. Limestone lithoclasts bound by phosphatic cement (10B22). Negative print. Bar scale 5 mm.

Figure 11. Lithoclasts of multilayer phosphatic cement (10B25). Negative print. Bar scale 5 mm.

Figure 12. Poorly ordered, soil-like fabric (10B19). Negative print. Bar scale 5 mm.

Figure 13. Fabric resulting from granular replacement of phosphatic mud (10A30). Ordinary light. Bar scale 1 mm.

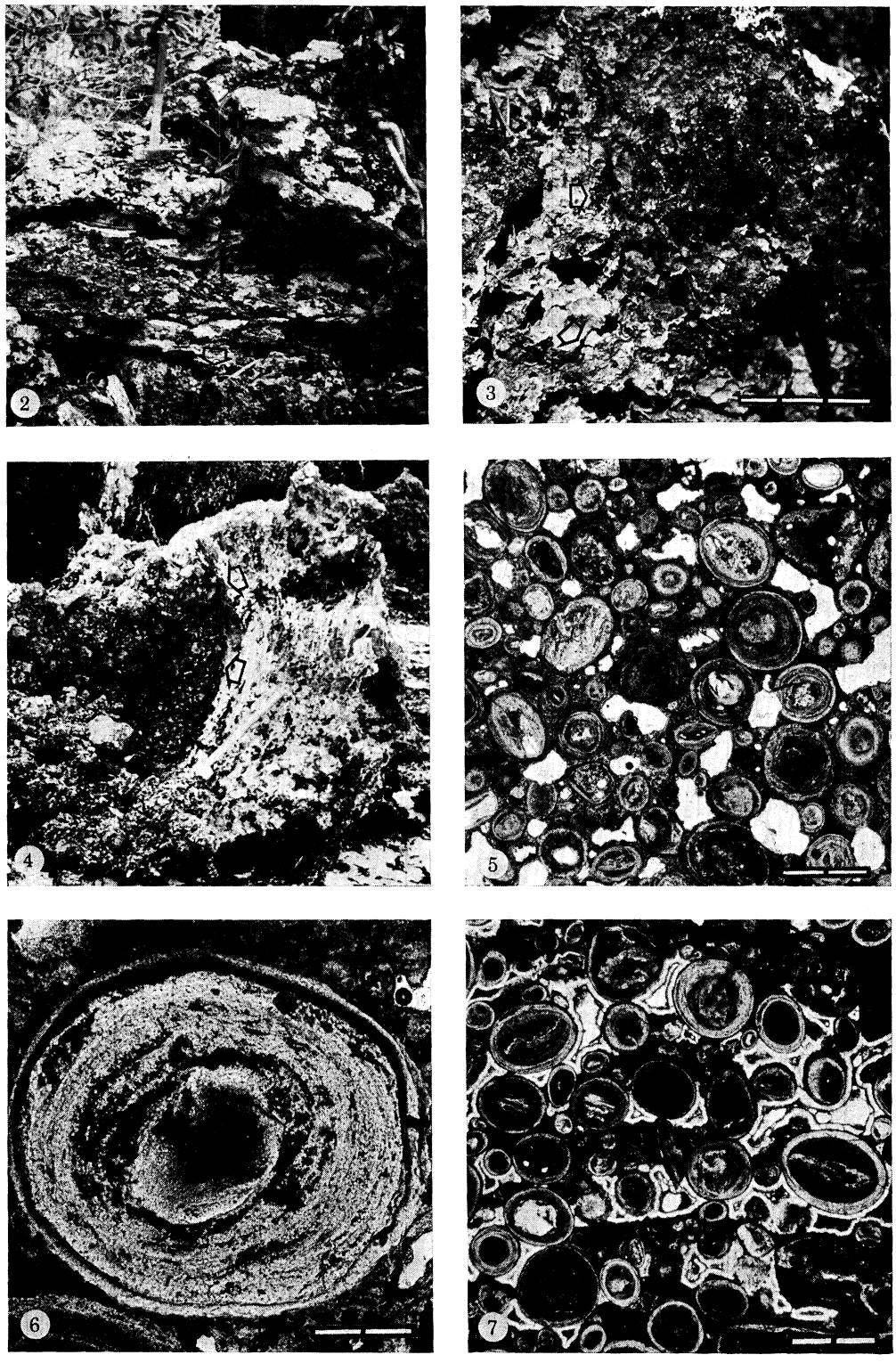

FIGURES 2–7. For description see opposite.

(*Facing p.* 514)

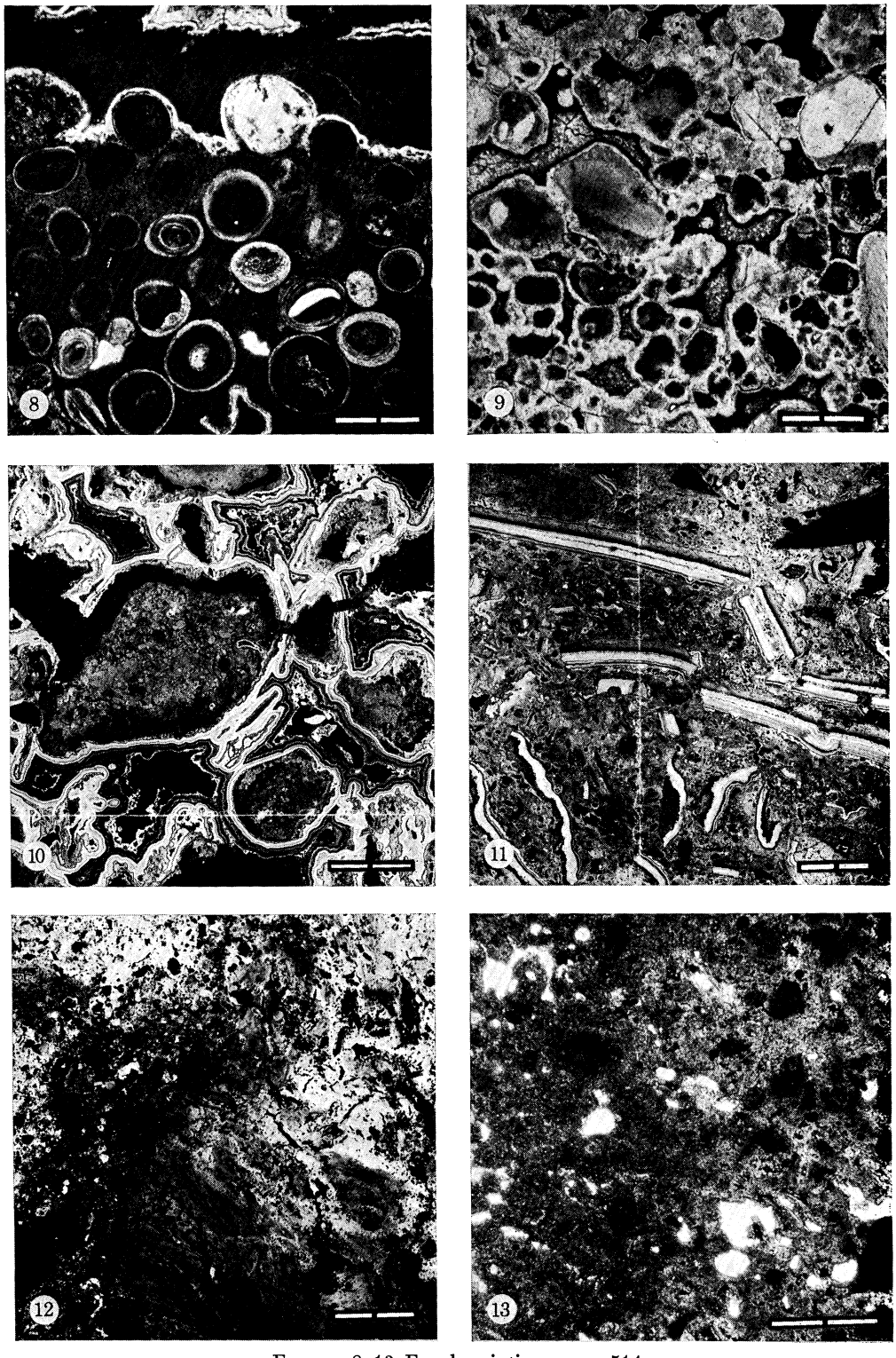

FIGURES 8–13. For description see p. 514.

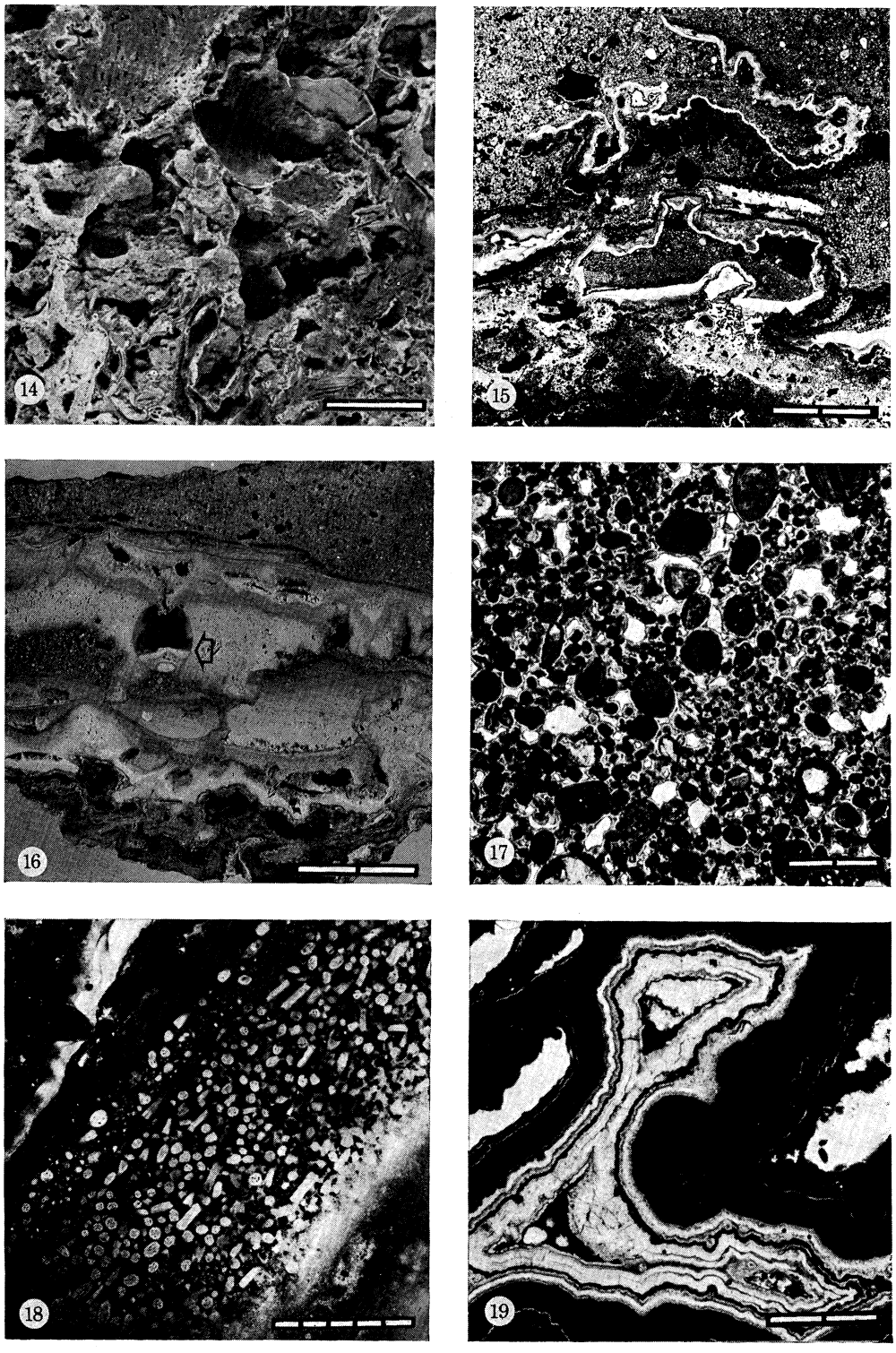

FIGURES 14–19. For description see p. 515.

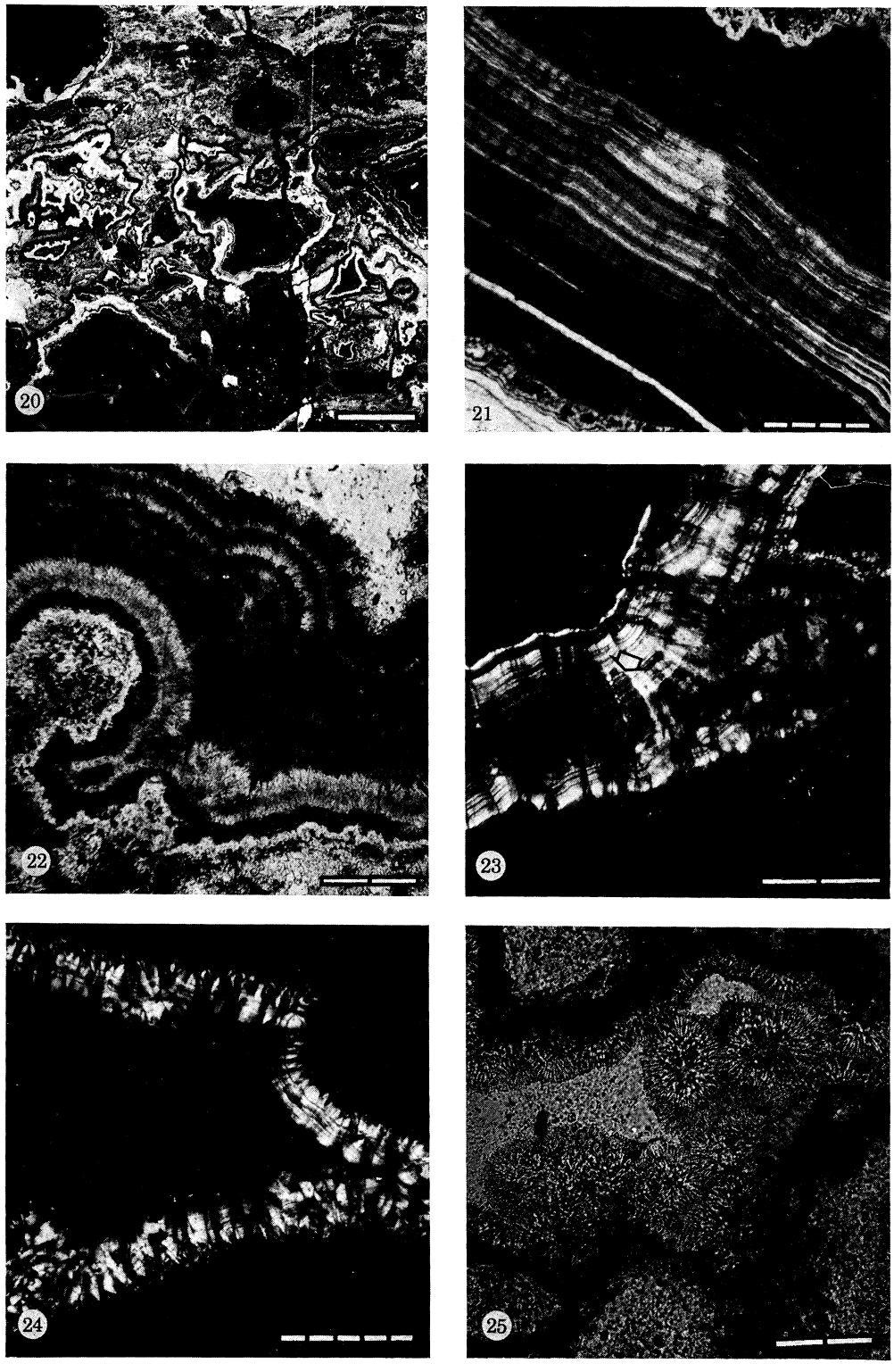

FIGURES 20–25. For description see opposite.

blocks of a wide range of sizes up to metre dimensions. Most blocks are oolitic and some are of well bedded sediments. Much of the matrix is also oolitic, with individual ooliths up to 2 mm diameter accompanied by angular fragments of laminated cements and other lithoclasts. Such features suggest that these deposits have been formed by erosion of phosphorites similar to those exposed along the ridge.

Braithwaite *et al.* (1973) noted that pebbles of oolitic phosphorite and isolated phosphate ooliths occur in the Picard Calcarenites northeast of Esprit, and have taken this as evidence that the deposition of the lower phosphorite series was contemporary. Unfortunately, no absolute age dates are available. Comparison with the data of Mesolella *et al.* (1969) suggests that the Esprit Limestones might represent deposition in a period between 170 and 230 ka B.P., but uncertainty concerning both possible sealevel changes during phosphorite deposition and low-level stands since make this no more than speculation.

The highest sealevel to which the phosphatic sediments can be related was 7–8 m above the present position. Although the high-level phosphorites rest in solution cavities that were presumably subaerial, they contain marine bioclasts and cannot, therefore, have been far above sealevel. In contrast, the extension of phosphatic linings into cavities well below the principal deposits suggests a relief of as much, or more than, the present 8 m. These small-scale fillings are perhaps related to deposition within the deep solution pipes formed subaerially when the sea stood *below* its present level. However, the presence of marine fossils, including *Scutarcopagia* and corals, in the phosphorites lining such cavities suggests that the sea had been *higher* before falling perhaps 1–2 m to about its present position. If the suggested correlation of the low-level phosphorites with derived phosphatic pebbles in the Picard Calcarenites is valid, then it follows that erosion of the high-level group had begun at a time when sealevel was 1–2 m higher than it is now.

In each of these cases the lack of phosphatization of the Esprit Limestones is taken to imply a non-marine and non-pervasive mode of emplacement.

Description of plate 3

Figure 14. Hand specimen showing bioclasts of coral (arrowed) and molluscs coated with phosphate (10B17). Bar scale 25 mm.

Figure 15. Internal sediments in lined secondary cavities (10A4). Negative print. Bar scale 30 mm.

Figure 16. Hand specimen showing internal sediments within cavities. Note cone of debris (arrowed) derived from small hole in roof (10A5). Bar scale 20 mm.

Figure 17. Structureless pellets (10A4). Ordinary light. Bar scale 1 mm.

Figure 18. *Favreina* pellets in internal sediment (10A7). Negative print. Bar scale 5 mm.

Figure 19. Multilayer phosphatic cements (10B22). Ordinary light. Bar scale 1 mm.

Description of plate 4

Figure 20. Intricate cavity system showing multilayer phosphatic cements (10A12). Negative print. Bar scale 5 mm.

Figure 21. Multilaminar phosphate cement morphotype (10A13). Ordinary light. Bar scale 250 μm.

Figure 22. Fibrous phosphate cement morphotype (10A3). Ordinary light. Bar scale 100 μm.

Figure 23. Replacement of high- by low-birefringence phosphate. Contact arrowed (10A1). Crossed polars. Bar scale 500 μm.

Figure 24. Spherular bundles in phosphate cement (10A12). Crossed polars. Bar scale 400 μm.

Figure 25. Acicular phosphate cement morphotype (10A15). Ordinary light. Bar scale 100 μm.

Petrographic groups

The field classification of these phosphorite deposits into primary, high-level, and secondary low-level series is only paralleled in a general way by petrography and, since many textures have been recorded only in detached blocks, groupings are based on a simple petrographic division. Sediments are referred to five basic types: (1) oolitic phosphorites, (2) lithoclast rocks, (3) fine-grained phosphorites, (4) bioclastic deposits, and (5) internal sediments.

Separate sections will be devoted to particular features of cements, including crystal morphology, and to cement stratigraphy in relation to internal sediments. The descriptions that follow are in general of thin sections. Numbers in parenthesis of the style (10B31A) refer to samples in the author's collection.

(1) *Oolitic phosphorites*

A wide variety of oolitic sediments is represented in these rocks, ranging in colour from moderate to light brown (5YR 4/4–5/6), with ooliths 0.2–2.0 mm in diameter (figure 5, plate 1). Some sediments are well sorted, while others may show a wide size variation or a biomodal size distribution (10A16). Three kinds of nuclei can be identified.

(*a*) *Lithoclasts*

Fragments of earlier multilayer phosphate cements, irregular fragments of older phosphatic rocks, including oolites and lumps of phosphatized limestone (10A14).

(*b*) *Bioclasts*

Phosphatized carbonate bioclasts are rare and identification is usually uncertain. Rounded bone fragments are common, although no bones large enough for identification have been recovered.

(*c*) *Mud fragments*

In limestones these nuclei might be referred to as pellets. They are ovoid or spherical, consisting of yellowish, transparent or opaque, clay-size material. Relative transparency is probably a result of alteration. Regularly shaped 'pellets' may have been of faecal origin (10A4)

Nuclei are 0.1–2 mm in diameter. The largest, with only superficial oolithic coats, resemble other allochems in the rock, but uniform coats of 0.5 mm or more are common. Some ooliths are essentially isotropic but others show a low birefringence and the black extinction cross characteristic of an orientated fabric. Individual fibres or crystals cannot be resolved but appear to lie with their long axes tangential to the surface of the ooid (figure 6, plate 1) and to be length-fast. Laminae taper laterally and show convergences and truncations that suggest micro-unconformities. There is thus substantive evidence that they have formed by accretion. S.e.m. photomicrographs, unfortunately, reveal only flat fracture surfaces and do not discriminate between internal structures.

Sediments range from clean-washed, well sorted, materials in which intergranular porosity is lined with multilayer colloform cements (to be discussed), to those in which ooliths are dispersed in a matrix of clay-size particles (10B20). In some the matrix occurs as irregular masses lying within a grain-supported fabric (10C26). It occurs above tight pore throats, bounded by meniscus-like surfaces (figure 7, plate 1) and beneath grain arches and 'umbrellas' sheltering

areas of high residual porosity. These features suggest a vadose origin, with fine sediment emplaced by infiltration. A few pipe-like masses of pale, fine-grained, sparsely oolitic sediments occur within grain-supported oolites. These probably formed by upward-stoping of ooliths washed into cavities produced at lower levels, and were filled by infiltration (10B31B). This may be the explanation for other irregular masses of sparsely oolitic clay-size sediment, but these might also be considered as the residue of a matrix that has been washed through. The stripping of matrix material by percolating waters would improve apparent sorting, but would only be possible where the sediment overlay a high-porosity, grain-supported zone into which smaller particles could be displaced. The erosion of oolitic rock is indicated by the presence of irregular channels with ooliths truncated against their margins (10B20).

Mud-supported oolithic sediments with a finely granular matrix (figure 8, plate 2) are common. Some matrix grains in these are opaque while others are translucent in shades of yellow–brown, but are mostly isotropic. The matrix often occurs in irregular masses that define the margins of numerous 'birdseyes', giving a porous, soil-like, aggregated texture. Sparsely oolithic sediments are transitional with phosphate muds (discussed below).

These ooliths appear similar in texture to marine and other ooliths and the evidence of intervals of erosion interrupting accretion is in keeping with the active, free-rolling origin commonly assumed for such bodies. Those intermixed with finer sediments can be supposed to have been transported to accumulate away from sites of generation. However, as Braithwaite (1975) and others have pointed out, concentrically zoned bodies may form in several different environments. There are analogies with cave pearls, described by Hess (1929), Davidson & McKinstry (1931), and Baker & Frostick (1947, 1951), and structures described by Braithwaite (1979), but there are also important differences. Phosphatic ooliths are made up of tangential rather than radial crystal elements. Loreau & Purser (1973) indicate that such differences might reflect a relation between the rate of accretion or growth of crystals and the amount of attrition to which they are subjected. Surface accretion is involved here, although there are also resemblances both to Brewer's (1964) photographs of concentric sesquioxide glaebules and to phosphate bodies described by Emigh (1958), which are supposed to have grown without agitation.

Three questions present themselves:

(i) Is the phosphate primary?

(ii) If it is, what is the mechanism of accretion?

(iii) Where did growth take place?

It seems that these must be answered in the light of a more general discussion of associated sediments.

(2) *Lithoclast rocks*

Folk (1962) differentiated grains formed by the erosion of weakly consolidated carbonate sediments within an area of deposition (intraclasts) and fragments of older lithified limestone (lithoclasts). In the present phosphatic sediments there are numerous angular fragments, some of centimetre dimensions, that fulfil the criterion of having been locally derived from recently deposited sediment. However, many of these are fragments of cemented rock and, in the absence of any objective means of dividing them, all will be referred to as lithoclasts.

These phosphorites consist of loosely packed, angular or well rounded (10B21) fragments 0.2 mm to more than 10 mm in diameter (4D15, figure 9, plate 2). The clay or silt-size sediments of which these are made up are structureless, opaque or pale greyish or brownish in

colour and isotropic, suggesting that they are poorly crystalline. They may be products of alteration or have been a finely granular, detrital phosphate. Clasts resemble some angular blocks of altered limestone (figure 10, plate 2), such as biopelsparites and sparse biomicrites (mudstones). Bioclasts in these include *Amphiroa* foraminifera (possible miliolids and *Heterostegina*), bivalves and gastropods (*Cerithium*). All of the lithologies found can be related to textural variants within the Esprit Limestones. In one sample (10B22) lithoclasts are of calcite showing patchy neomorphic replacement and a marginal alteration to phosphate, the latter resulting in a loss of structure. In all other samples, however, lithoclasts are wholly phosphatic and reveal only traces of a limestone origin. In several sediments they bear minute borings of algal or possibly fungal origin on their surfaces, suggesting a relatively long history of derivation (10B21).

Other lithoclasts consist of fragments formed by the erosion of rocks that were originally phosphatic (10C28). These are identified by the presence of multilaminar phosphate cements and include dense, fine-grained sediments, fragments resembling laminated and glaebular soils (Braithwaite 1975), oolithic phosphorites and older lithoclast rocks. Lithoclasts of all types may be associated with rounded pellets of clay-size phosphate, ooliths, including superficial ooliths with lithoclast nuclei, small bone fragments and, in one case, fragments of wood. One sample (10B25) contains large numbers of centimetre-sized flake-like fragments of multilayer phosphatic cements (figure 11, plate 2). These only loosely parallel bedding and were presumably supported by the matrix at the time of deposition, which indicates that they were a product of the same depositional event. The matrix is fine-grained, clay-size sediment and includes pellets or lithoclasts, which, since they are of similar sediment, are hard to differentiate. Irregular masses of fine-grained phosphate commonly adhere to larger grains, producing a porous soil-like texture with numerous cavities formed both by aggregation of clay-size grains and by irregular packing. These are generally lined with a single layer of colourless, radially fibrous phosphatic cement.

Aggregated, clay-size, opaque or isotropic phosphates are common among lithoclast-bearing rocks, which, as a group, are notably heterogeneous. In a few samples the matrix is organized into ovoid, possibly faecal, pellets. Vague masses in others resemble the disorganized textures and rootlet channels described by Braithwaite (1975) in Aldabra palaeosols. Elsewhere, fine-grained sediments resting against pore throats suggest that the matrix has been emplaced by infiltration. These rocks form a group transitional to those in which no matrix is present and centimetre-size angular lithoclasts are bound by a multilayer, colloform phosphate cement, eaving a high residual porosity. In coarser sediments this may be reduced by the deposition of later internal sediments.

One example of a porous, lithoclast-bearing sediment is of particular interest since it contains two generations of carbonate cements; the earlier of these, a fibrous layer, is of microstalagmitic origin (c.f. Purser 1969). These will be discussed in greater detail in the section on cements.

It is probable that some lithoclasts have been derived by mechanical erosion of the Esprit Limestones. Contemporary weathering of these is almost entirely solutional but forms a minutely fretted and pinnacled surface. Continued solution could detach angular masses of limestone which could be incorporated in surface-wash deposits. However, limestone clasts are far outnumbered by fragments that were phosphatic at the time of derivation. It seems an inescapable conclusion that most of these sediments were formed from the mechanical breakdown of pre-existing phosphorites. This has already been suggested, by field relations, for the

low-level sediments. In the high-level deposits, one can only suppose that sediments were reworked soon after deposition and that there were many erosional and depositional events in the history of the sedimentary unit.

(3) *Fine-grained phosphorites*

In addition to fine-grained phosphate sediments forming matrices to oolitic or lithoclastic granular aggregates, there are a number of rocks that in carbonate terms would be described as micrites or microsparites. These are of clay-size materials and are usually light-coloured in outcrop (10YR 8/2). Scattered coarser allochems may show a distribution that suggests possible burrowing. In some rocks the micrite forms porous aggregate masses with an open, soil-like texture (figure 12, plate 2). Shrinkage fractures and dark, poorly defined, glaebules 0.3–0.4 mm diameter were recorded in one sample, while another showed stalagmite-like banding of the mud, with laminae defined by zones of opaque granules. Larger grains present include phosphate lithoclasts and ooliths, but bone fragments, bivalves (*?Scutarcopagia*), gastropods (*?Conus*) and foraminifera (principally miliolids) have all been recognized (10A3).

The sediment is of two kinds, buff-coloured and translucent, or opaque. The translucent materials are isotropic and may therefore be non-crystalline, while opaque grains might be carbonaceous. In most examples these two components show patchy alteration, a slight increase in grain size to about 5 μm and a general 'clearing' (a loss of, or change in, the opaque particles). The new granular material has a low but distinct birefringence and is thus crystalline (figure 13, plate 2). Vague outlines of bioclasts, including foraminifera, can sometimes be recognized within it, but these are less distinct than in the original sediment (in which they are, in any case, represented largely by moulds).

Many fine-grained sediments contain large irregular cavities which may simply be lined with laminated phosphatic cements, or may be filled with internal sediments (discussed below) or, in some samples, may contain fragments apparently eroded from their own walls.

Nearly all of these rocks occur among the high-level bedded phosphorites. They *do not* appear to represent replacements of Esprit Limestone. They show, in cavity formation and internal sediment deposition, the same kind of evidence of rapid erosion and redeposition shown by other rock groups. Their fossil content, however sparse and poorly preserved, is important since it suggests that areas of deposition had access to an open marine system.

(4) *Bioclastic sediments*

Bioclasts are widely distributed but do not normally form significant volumes. Frequently, because of diagenetic alteration, it is impossible to differentiate between 'fresh' bioclasts and those contained in lithoclasts. There are a few sediments for which there is less doubt. These are found occupying the floors of roughly cylindrical solution pits close to sealevel, on the eastern shore of Esprit. They consist (10B17) largely of shells of gastropods and bivalves, resembling *Scutarcopagia* and *Fragrum*, accompanied by fragments of coral (perhaps a faviid) 10 cm in diameter (figure 14, plate 3). The large mollusc shells are represented only by moulds lined with laminate phosphatic cements, while the coral is replaced by granular phosphate. The phosphatic matrix is finely granular, either of low birefringence or opaque, but within it are microgastropods, *Marginopora*, *Heterostegina*(?) and *Halimeda*. These are important since they suggest an addition of fresh marine-derived sediment. The rock mass is cavernous and

there have been several periods of cement deposition, some of which have followed dissolution of the shells.

Although this deposit might represent altered lithoclastic debris it is believed to be a primary sediment. That being so, sealevel at the time of deposition is unlikely to have been lower than it is now and was probably slightly (1–2 m) higher. Vertebrate remains are not common in these sediments, but Fryer (1911) recorded bones of *Testudo* as well as teeth of *Carcharias*, *Ciodon* and *Scarus* in phosphorites that he found on Picard, which are probably equated with the low-level unit described here.

(5) *Internal sediments*

This is a large and diverse group of phosphate deposits. The cavities in which they rest range from primary interparticle porosity to vugs of centimetre dimensions. Relatively large caverns are visible in the field, but the present discussion is limited to structures visible in hand specimen and thin section. These are irregularly shaped although their greatest dimensions tend to be horizontal. Repeated erosion and redeposition has reduced some rocks to a porous mass in which internal sediments and crustose cements occupy the total volume of the solid material present (figure 15, plate 3). In a few samples (10A2) smooth, symmetrical walls suggest the work of boring organisms. Whatever their origin, it is common to find within cavities associations of several different sediments, separated by erosional or non-depositional surfaces or by precipitated colloform phosphate cements. The floors of cavities, covered by internal sediments, are generally horizontal with bedding draped only slightly from the margins. This apparent horizontality is, however, related to the particular conditions of deposition. In some samples (10A5) steep-sided mounds have formed by the discharge of sediment from a small hole in the roof of a cavity (figure 16, plate 3). In more extensive systems a sloping spiral floor may be generated as sediment spills to successively lower levels. Roofs are extremely irregular, but most become coated with stalactite-like masses of colloform cement, which may interleave with sediments forming the floor. Small amounts of clay-size materials, sometimes in the form of pellets, may be found adhering to side walls, interposed between cement sequences.

The mechanical movement of sediment in cavities is limited by its ability to pass pore throats of critical sizes. Thus, although there may be a broad correlation between the sediment types found in adjacent systems, particular sequences may lack the younger additions as their access to the source of supply became blocked. The effect of pore size is also seen in the grading of some deposits, fining-upwards sequences reflecting a progressive pore throat occlusion. Streams of sediment were sometimes of very limited distribution and only reached cavities within a restricted volume. There is, therefore, no overall internal sediment or cement stratigraphy that would allow correlation between samples. Virtually all of the samples in which extensive internal sediments occur are from the upper *in situ* bedded phosphorites.

Most internal sediments are fine-grained clay- or silt-size materials that locally become coarser and more crystalline. There is some variation in colour and translucency. Some of these sediments contain large numbers of opaque granules, which seem to fill an intergranular porosity, while others are wholly transparent. Of the latter most are isotropic or of very low birefringence, presumably reflecting poor crystallinity. These fine-grained phosphates are locally organized into irregular crumb-like aggregates, giving a loose porous texture that commonly shows a gradation, progressive compaction yielding, within a few millimetres, a dense mud. In some cases it is difficult to separate such sediments from those in which an irregular system of vugs has been produced by post-depositional processes.

The origin of these aggregates is not known, but it seems unlikely that they 'aggregated' in their present positions. They may represent lithoclasts formed by the erosion and relocation of sediment first deposited at higher levels within the cavity system. Some were soft (and show compaction), but many cavities contain obvious lithoclasts, including fragments (2–3 mm in diameter) of multilayer cements and older sediments. In one example lithoclasts overlie the eroded surface of a sediment with exactly the same texture (10A14). Selective solution of lithoclasts has locally produced an extensive system of secondary cavities (10A11).

Fine-grained phosphates are also seen in the form of pellets. These typically show a range of sizes (30–70 μm) and are of rounded or ovoid form with structureless interiors (figure 17, plate 3). They are sharply contrasted with cylindrical pellets, up to 1 mm greatest diameter, that have a symmetrical series of tubes running along their axes (10A7). These compare closely with published figures of *Favreina* pellets (Horowitz & Potter 1971) and with pellets ascribed to *Callianassa* (Pryor 1975) and are probably faecal (figure 18, plate 3). Reason suggests that there are practical limits on the distance of transport of such bodies, which, unless the organism was a cave dweller, are strong evidence for the proximity of the cavity to and its connection with an open surface. In some samples pellets rest in a structureless, fine-grain matrix, but in others they represent a clean-washed deposit, 3–4 mm thick, presumably laid down in the absence of any alternative contemporary sediment.

In addition to these well defined types, phosphatic internal sediments include poorly sorted materials. These are dominantly fine-grained. Some have disordered, soil-like textures and, in one case, these are modified by irregular shrinkage cracks and include dark, poorly defined glaebules, 0.3–0.4 mm in diameter.

Many internal sediments contain ooliths (see above). These are up to 2 mm diameter, and include both superficial and thickly coated forms, associated with lithoclasts and bone chips. Sediments vary from well sorted grainstones to phosphate mudstones containing only scattered ooliths. It is likely that the matrix in some grain-supported sediments has been introduced by infiltration.

Finally, in a few samples, scattered bioclasts, principally moulds of bivalve shells, lie within internal sediment and cement sequences. These may be lithoclasts but it seems more likely that they provide additional evidence of the near-surface location of these depositional systems.

Many of the textures and relations shown by internal sediments resemble those described by Deelman & de Coo (1976). The depositional processes are probably also analogous. The idea of repeated introduction of fresh sediment from above reinforces the interpretation of these rocks as near-surface deposits.

Cement morphology

The analysis of the cements in these sediments is hampered by two attributes.

(1) There is a diverse cement morphology, which is not reflected in identifiable compositional variation.

(2) Precipitation varied in adjacent cavities and deposition may appear markedly different within the same cavity, where quantities of internal sediment are interposed.

Accepting both of these facts, the only easily understood way to describe cements is to examine morphology in isolation, to give a limited number of examples of cement stratigraphy and to discuss the significance of variation.

Most phosphate cements are colloform; they form mammilated or botryoidal crusts with a banded structure lining cavities (figures 19, plate 3, and 20, plate 4). They fall into two groups:

(1) Transparent, colourless or pale yellow to dark brown phosphate made up of numerous closely spaced microlaminae that are presumably growth increments (figure 21, plate 4). Colour zones are distinct and are believed to reflect compositional differences.

(2) This group is also yellow–brown but includes some cements that are so darkly stained as to be virtually opaque. They are also zoned, but bands are relatively widely spaced and consist of fibres the long axes of which lie normal to the accreting surface (figure 22, plate 4).

Both groups show a range of optical properties. Normally they are weakly birefringent, showing first order white and greys consistent with apatite. Some colourless cements are isotropic and the degree of optical anistropy probably reflects the degree of crystallinity. Precipitation, in some cases, may initially have been in a poorly ordered form that has been neomorphically replaced. Cements of both structure varieties may be found showing high birefringence, which is usually masked by strong body colour but resembles that of carbonates. However, no carbonates are recorded on X-ray diffraction traces (see 'Mineralogy'). Relations (figure 23, plate 4) suggest that the low-birefringence material is formed at the expense of the high-, but with the methods available no detailed identification could be made. Colourless, translucent, cements sometimes replace coloured varieties; the fibrous structure and layering are less distinct and birefringence is low. S.e.m. photomicrographs of fracture surfaces fail to reveal details of fibre morphology.

All of the cements so far described, even colourless, microlaminate materials, show a marked radial fibrous structure under crossed polars. Fibres are optically continuous from zone to zone and waves of extinction move normal to depositional surfaces. In a few cases, bundles of fibres form spherular masses within zones. In these, crystallization took place radially from point nuclei rather than along the whole depositional surface (figure 24, plate 4). Zones of discrete fibrous spherules, not forming a continuous colloform sheet, are present in some sections.

Both microlaminar and fibrous cements may occur within the same sequence. There is a tendency for laminar cements to be earlier, as in the phosphorites on Remire (Braithwaite 1968), but either may occur first or they may alternate in sequence, separated by thin layers of internal sediment. Multilaminar crusts may exceed 150 μm thickness with 20–30 separate laminae of 5–6 μm (10A11B), while fibrous zones are somewhat thicker. Cements may be millimetres thick but crusts consisting of one or two zones only are common although entirely absent from some cavities.

Groups of colourless acicular crystals (10A15) may be related to banded fibrous cements. Crystals are of low birefringence and lie with their long axes normal to depositional surfaces (figure 25, plate 4). Layers thus resemble fibrous cements but differ in that the crystals are larger (26–70 μm long) and terminations project as a ragged fringe into free cavities. Such crusts may be divided into subzones with fibres optically continuous from layer to layer. Similar colourless needle crystals occur in loosely aggregated groups, sheaf-like bundles and well defined spherules (figure 26, plate 5). Their composition is not known (see 'Mineralogy'). A few spherular bundles of crystals have been replaced by finely granular phosphate.

Granular cements, 120 μm thick and consisting of grains or crystals 7–10 μm in diameter, are present. These are usually of a light, golden brown colour, and are either isotropic or show very low birefringence. They were assumed to be wholly phosphate until terminations against open cavities in some samples were seen to be cubic crystals of 10–12 μm diameter (figure 27, plate 5). Layers of crystals bounding cavities, or even patches of such layers, could be of a

different composition to those beneath, but there are no obvious differences. Cubic pseudomorphs, 80 μm in diameter, observed in other sections (figures 28 and 29, plate 5) have a thin, colourless, presumably phosphatic, coat over a granular and partly opaque interior. These crystals have not been identified, but fluorite, which frequently shows weak anomalous birefringence, could be precipitated from solutions, released by replacement of fluorine-bearing carbonatian apatites (see 'Mineralogy').

Randomly orientated rhombohedral crystals, 0.2 mm maximum diameter, and ghostly remnants of prismatic crystals (see below) have been found associated with brown, cloudy, granular cements. Some granular horizons contain large numbers of opaque granules and, as has been noted, layers of opaque dust appear between some cement laminae. Most of these 'dusts' are probably detrital, but some may have been precipitated.

In addition to these widespread cements, several sections contain larger crystals, commonly confined to one cavity within a specimen and frequently pseudomorphed so that they cannot be identified. Bundles of blunt-ended prismatic crystals, which are square or rhomboid in section, sometimes form crude stellate (spherular) masses (figure 30, plate 5). They are usually colourless and transparent, but some are completely opaque, either through the presence of numerous inclusions or by replacement. Crystals 150 μm long with similar general form but with acute scalenohedral (?) terminations have also been noted and, in two samples, were associated with hexagonal cross sections. In one of these the crystals themselves had dissolved and their shape was outlined by a pale phosphatic cement. Such crystals resemble some carbonate cements described below, but in all other examples transparent crystals show a low birefringence and are clearly not carbonates. Cook (1972) records well formed apatite crystals, but in the present examples undulose extinction is common and suggests that many are pseudomorphs. Examples of crystal morphologies are seen in figures 31–36, plates 5 and 6.

The last group of 'phosphatic' crystals are of bladed form (figure 37, plate 6). In one section they are 1–2 mm long with well defined asymmetric terminations, resembling those of gypsum, and are, therefore, probably monoclinic. Zones of opaque, possibly carbonaceous, inclusions are present in the outer margins of the crystals. The inner portions lack inclusions and are golden brown in colour and transparent. They show low birefringence with a biaxial positive interference figure. However, extinction is undulose and some crystals are made up of a series of subgrains and so are probably pseudomorphs. The outer zones of the same crystals are dark brown and, although the colour has a strong masking effect, appear to have a relatively high birefringence.

In a few samples banded, fibrous, crystalline masses resemble stalagmitic deposits. These may originally have been carbonate and may be lithoclasts, but structures and relations are never clear. Undoubted carbonate cements are rare. In the Esprit Limestone, banded phosphatic cements coat unaltered, coarse, prismatic calcite cements (figure 38, plate 7); elsewhere carbonates overlie phosphates (figure 39, plate 7). Three carbonate morphologies are represented. Elongate (150 μm in length) prismatic crystals and fibrous needles (up to 200 μm in length) are present within the same rock, binding phosphatic lithoclasts and separated by a solution-erosion surface. The fibrous zone is the most significant since the orientation and distribution of the fibre bundles strongly suggest deposition in microstalagmites similar to those described by Purser (1969). They are therefore evidence of precipitation within the vadose zone (figure 40, plate 7). In addition to these, granular calcite has been recorded locally overlying banded phosphate cement.

In conclusion, there is evidence that some phosphatic cements formed as alteration products, although the nature of the original precipitate is not known. It might be thought that carbonates are likely precursors. There is evidence here and elsewhere (Braithwaite 1968; Trueman 1965; Weber & White 1973; Roy 1976) that phosphates are able to replace carbonates while preserving original structures. However, the close association of phosphates and unaltered carbonates seen in many samples (figure 41, plate 7) implies either a highly selective alteration or the primary deposition of the cements in a non-carbonate form. Possible minerals are discussed under 'Mineralogy'.

Cement stratigraphy

The variation in cement morphology described is fully expressed in detailed cement sequences. In some samples cements display a common stratigraphy, while in others adjacent cavities show substantial differences, which become more marked as cavities become larger. Two processes are in operation. First, internal sediments are often locally distributed and are derived from particular infiltration streams. Their presence or absence has significance only in relation to the passage of such a stream. Secondly, the precipitation or crystallization of cements ceased in some cavities, although the lumen was not closed, while it continued elsewhere. Thicker and more diverse sequences of sediments and cements are seen in cavities that remained connected to transport paths for longer periods. This is taken as evidence of the occlusion of pore throats, either by cement growth or by physical blocking by relatively large particles, suggesting, perhaps, that some solutions were colloidal. Restrictions are particularly evident in some Esprit Limestone samples where the phosphatic cements, which commonly overlie unaltered prismatic calcite, are absent from smaller cavities. Thicker cements occur on the roofs of cavities, where successive generations are not separated by the internal sediments that characterize floors.

The most common cements are the simplest, being monolayers or having one or two changes. It seems necessary to describe other, more complex, sequences in detail, to demonstrate both their overall character and the range of morphologies involved.

Five examples have been selected. Numbers in bold type indicate the supposed order of deposition of zones and can be related to figure 44. All thicknesses are approximate.

Description of plate 5

Figure 26. Spherular bundles of fibres, partly pseudomorphed, in phosphate cement (10A1). Ordinary light. Bar scale 500 μm.

Figure 27. Cubic terminations on granular phosphatic cement (10B17). Ordinary light. Bar scale 100 μm.

Figure 28. Cubic phosphatic pseudomorphs in cement (10A12). Ordinary light. Bar scale 100 μm.

Figure 29. Cubic phosphatic pseudomorphs associated with vadose sediment in cement (10A1). Ordinary light. Bar scale 250 μm.

Figure 30. Stellate clusters of prismatic phosphate crystals in cement (10A12). Ordinary light. Bar scale 250 μm

Figure 31. Minute prismatic crystals of (?)apatite in microcavity (10B21). Ordinary light. Bar scale 150 μm.

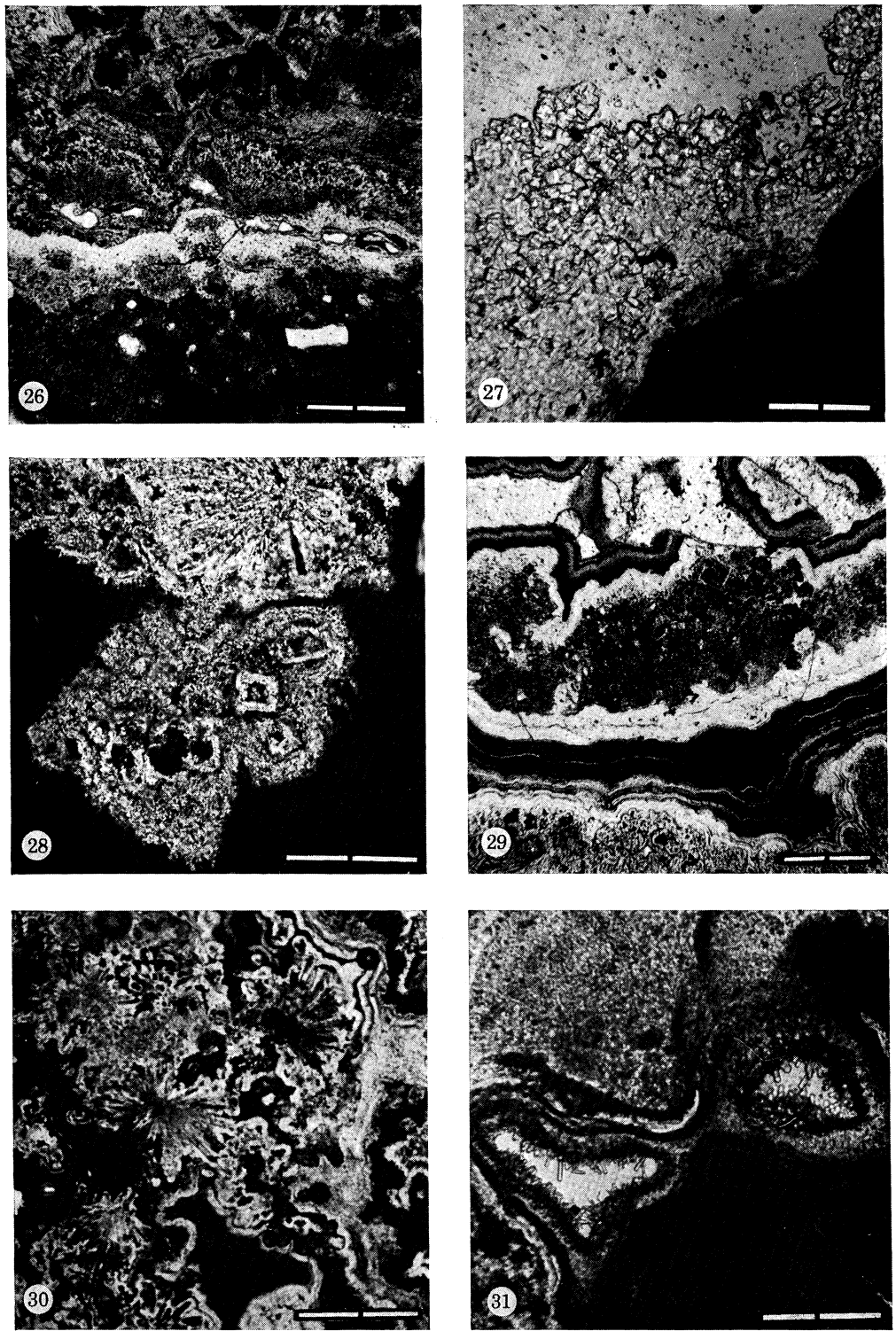

FIGURES 26–31. For description see opposite.

(*Facing p.* 524)

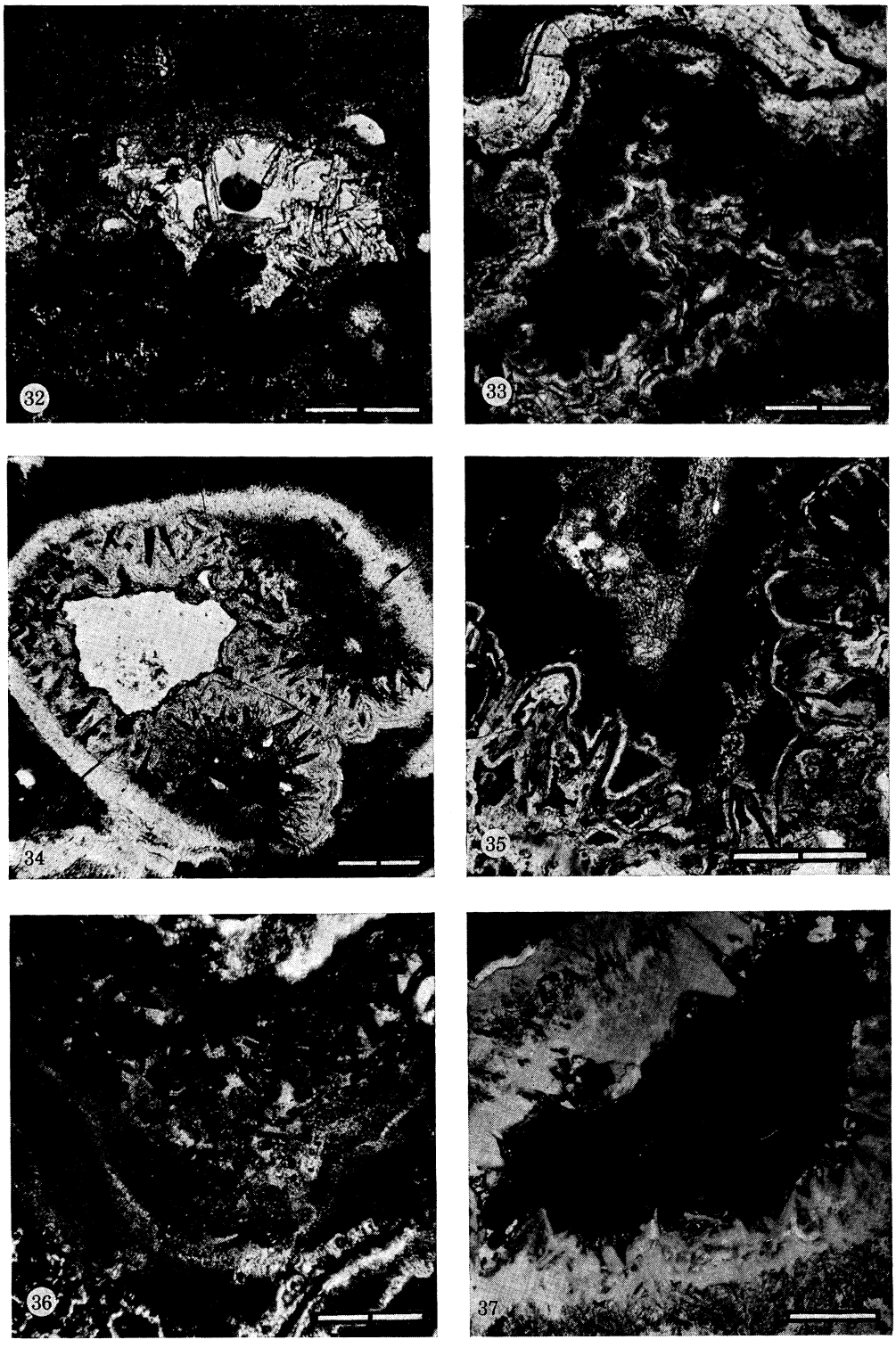

FIGURES 32–37. For description see opposite.

Description of plate 6

Figure 32. Square-ended prismatic crystals lining cavity (10C27). Ordinary light. Bar scale 250 μm.

Figure 33. Hexagonal prismatic crystals lining cavity and coated with phosphate (10A5A). Ordinary light. Bar scale 250 μm.

Figure 34. Scalenohedral terminations to crystals in cement contained in lithoclast (10A14A). Ordinary light. Bar scale 250 μm.

Figure 35. Pseudomorphs of large prismatic (? hexagonal) crystals with rhombohedral terminations lining cavity and overlain by phosphate. (10A4). Ordinary light. Bar scale 300 μm.

Figure 36. Pseudomorphs of rectangular and rhombic crystal sections in cavity fill (10A2). Ordinary light. Bar scale 300 μm.

Figure 37. Large monoclinic (?) crystals (pseudomorphs) lining cavity (10A13). Negative print. Bar scale 1 mm.

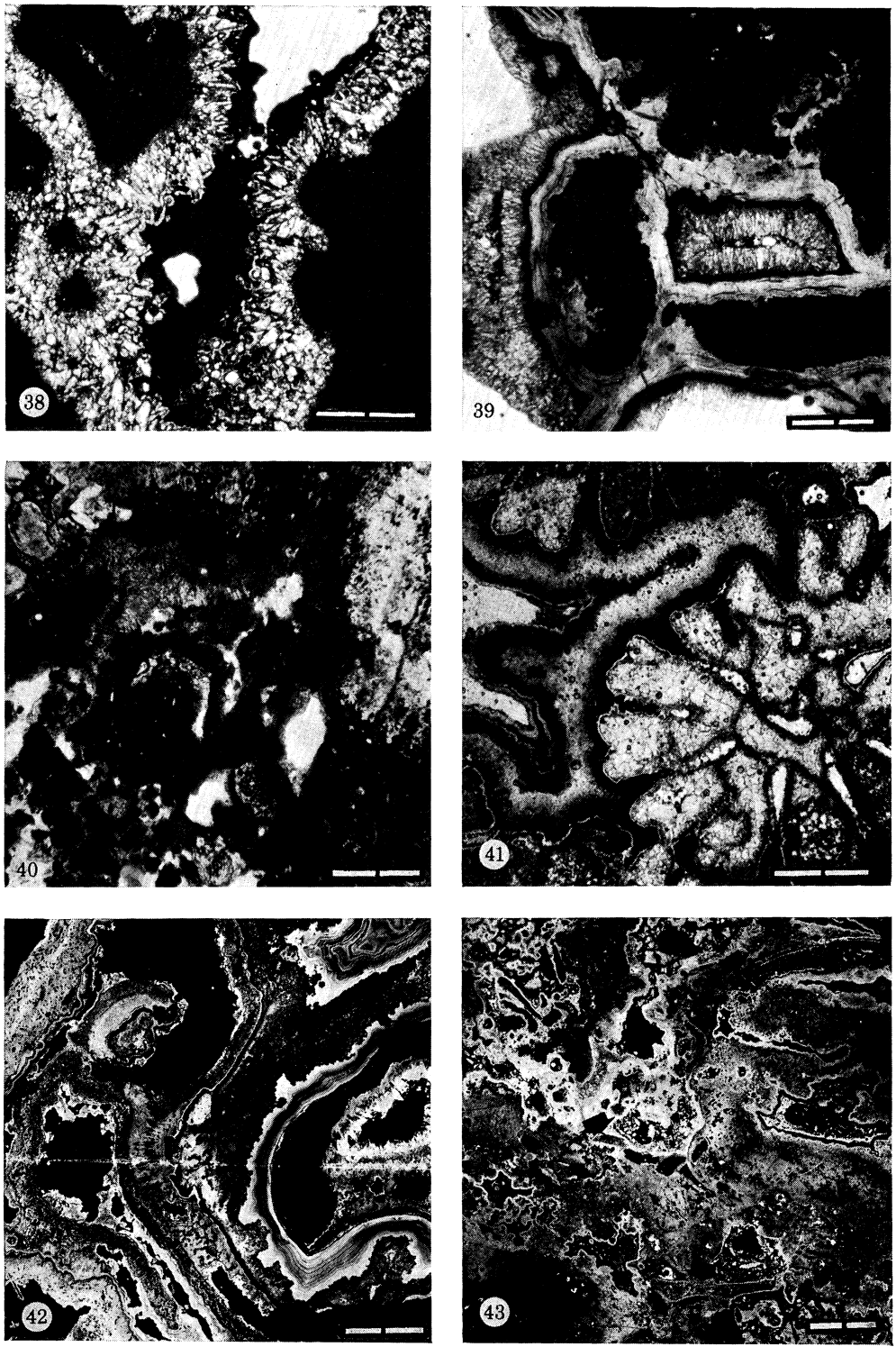

FIGURES 38–43. For description see opposite.

(*a*) *10A1*

The first sample forms part of the *in situ* bedded phosphorites on the summit of Esprit. In it, a tenuous framework of old phosphatic cements defines large (greater than 5 cm), irregular cavities floored with internal sediments in which several phases of deposition can be recognized.

The presumed oldest material is a mottled, fine-grained sediment (**1**) in which non-opaque grains are virtually isotropic. Numerous 'birdseye' cavities are present but many, significantly, contain no cement. This phosphate mud was eroded to define a new system of irregular cavities, which have been lined by a thin (40 μm) colourless, colloform, multilaminar cement crust (**2**), which is radially fibrous under crossed polars. In some large cavities this is overlain in turn by a partly opaque, multilaminar crust (**3**), locally more than 150 μm thick and including more than thirty depositional increments. There is a well defined fibrous structure and the mineral is generally highly birefringent, although it is locally replaced by low birefringence phosphate.

In one cavity a brownish multilayer cement, resembling **3** but with at least 24 microlaminae, is overlain by 100 μm of colourless phosphate. This consists (**4**) of two major sublayers, each with about six minor divisions, but is isotropic. It is overlain by a finely granular zone (**6**) containing cubic pseudomorphs outlined in phosphate. The crystals surrounding these are of very low birefringence and contain irregular opaque masses. The whole zone thins rapidly and is absent on adjacent walls. There are three layers above it: first (**7**), a pale yellow, transparent, low-birefringence phosphate with a radial structure under crossed polars; secondly (**8**), a fibrous zone with dark inner and pale outer subzones that has a high birefringence (masked by the body colour); and finally (**9**), a thin, completely colourless horizon consisting of minute (8 μm), irregular, isotropic granules.

Elsewhere in the section, zone **3** is absent and its position is occupied by scattered spherular sheafs of crystals pseudomorphed by granular phosphate. These are surrounded by a finely granular material (?**6**) that was deposited irregularly on cavity walls but has since been partly removed by solution. The resultant cavities are lined with a colourless, colloform phosphate (?**7**), but this must post-date the multilayer (at least seven sublayers) clear cement (?**4**) that overlies the sediment.

This sequence, culminating in a multilayer cement, is overlain by irregular lumps, 0.1–1 mm in diameter, of fine-grained, earthy sediment (**5**). These are virtually isotropic, but vague outlines of foraminifera and bivalves suggest that some may represent replaced limestone fragments. Three cement generations bind them. The earliest (?**7**) is colourless, 50 μm thick, with four subzones; it has low birefringence and a radial fibrous structure (under crossed polars). It is overlain by a further multilayer zone (**8**), which is locally also fibrous but has a

---

DESCRIPTION OF PLATE 7

FIGURE 38. Phosphate coating prismatic calcite crystals (10A29). Ordinary light. Bar scale 1 mm.

FIGURE 39. Calcite cement coating early phosphate (10C28). Ordinary light. Bar scale 250 μm.

FIGURE 40. Fibrous stalagmitic carbonate cement (top left) (10C28). Ordinary light. Bar scale 250 μm.

FIGURE 41. Phosphate cement coating unaltered carbonate (10B23). Ordinary light. Bar scale 1 mm.

FIGURE 42. Tenuous framework formed by repeated phases of phosphate cement deposition (10A13). Negative print. Bar scale 5 mm.

FIGURE 43. Phosphatized carbonate showing replacement of mollusc, *Halimeda* and *Marginopora* fragments (arrowed) (10B17). Negative print. Bar scale 5 mm.

strong brownish colour (sometimes almost opaque) that masks high birefringence. The outermost zone (**9**) is colourless. Cavities formed by the solution of clasts are also lined with a colourless, low-birefringence cement, but it is not clear whether this represents the earliest or the latest of the above three zones.

The main inference drawn from this sequence is that the rock has had an unusually complex history which, if we ignore incremental bands within cement zones, has included at least nine depositional events. Some of these may originally have involved non-phosphatic minerals.

(*b*) *10A5*

The second sample selected for illustration is also from the *in situ* bedded deposits on the summit of Esprit. The original sediment (**1**) appears to have been a fine-grained limestone. It is now partly opaque and partly a colourless or buff, low-birefringence, finely granular phosphate. Scattered pseudomorphs of foraminifera and arcuate, probably molluscan, shell fragments are present. The surface has been bored by organisms of the dimensions of *Lithophaga* and dissolved to form irregular cavities centimetres in diameter.

The eroded surface is overlain by a thinly bedded, fine-grained sediment (**2**), which covers the floors of cavities and blocks small pore throats. This is aggregated into small, irregular pellets bound by two cements. The earlier of these (**3**) is dark brown, prominently fibrous, and commonly (although not always) of high birefringence. The later (**4**) is colourless, and although laminate, locally shows a low-birefringence, radial fibrous structure. In some intergranular spaces this is overlain by colourless, isotropic, acicular crystals (**5**) with their axes normal to the depositional surface. The upper margin of this sediment (0.22 mm thick) contains only a colourless cement (?**4**) between grains. This also coats the sediment surface, where it is covered by a fine-grained, opaque internal sediment (**6**), which marks the beginning of a sequence shared by several of the larger cavities.

The first zone of this second series is a colourless, multilayer phosphatic cement, 150 μm thick (**7**). This is colloform but, although traces of a radial fibrous structure can be seen, the optical structure (under crossed polars) defines spherular accretion centres rather than precipitation over the entire surface. Parts of the zone are coloured (yellow–brown) and show higher birefringence.

This cement is overlain by a fine-grained, low-birefringence sediment (**8**), which, on its upper (outer) margin, is loosely aggregated and contains numerous, dark, fine-grained pellets of 50 μm diameter (**9**). In one cavity these are accompanied by larger *Favreina* pellets, but in the largest spaces a clean-washed oopelletal sediment (**10**) (including ooliths, superficial ooliths and pellets 0.1–1 mm in diameter and containing lithoclastic and other nuclei) occurs in their place. This is bound by a transparent microlaminate phosphatic cement (**11**) that has a low birefringence and an optically radial structure.

Within the oopelletal sediment one lithoclast, of 4 mm greatest diameter, is of special interest since it consists of a cement sequence that includes well formed crystals. A colourless, multilayered cement, 150–200 μm thick (fibrous under crossed polars) is overlain by a partly spherular zone, of varied thickness, that has a strong (buff) body colour masking high birefringence. The third zone is colourless with low birefringence. It has a gradational relation with a pale buff, generally isotropic (sometimes opaque), granular layer that has been partly eroded. The surface of the cavity is lined with prismatic crystals with hexagonal cross sections and rhombohedral terminations. The largest of these are 100–150 μm in length but, un-

fortunately, those not charged with inclusions (opaque) are isotropic and all are now pseudomorphs. The final cement in this series is a multilayer, colourless to pale yellow, low-birefringence phosphate, 75 μm thick, with at least eleven subzones.

This sample again shows the range of morphological variation possible within one cement series, but also demonstrates the relation between internal sediments and cements. There were at least eleven changes in the depositional milieu.

(*c*) *10A7*

The third sequence to be examined is once more from the summit of Esprit, but is dominated by internal sediments. The earliest (**1**) consists of fragments of older banded phosphatic cements, up to 1 mm in diameter, accompanied by fine-grained, cylindrical pellets, of 25 μm cross-sectional diameter, and dense, fine-grained lithoclasts. These are all bound by a colourless, faintly fibrous, low-birefringence, multilayer phosphatic cement, 50 μm thick (**2**), with six subzones. In some cavities this is the final deposit, elsewhere it is overlain by a fine-grained sediment (**3**) that varies from a light brownish, isotropic, to opaque. The outer 300 μm of this consists of irregular, detached masses coated with a thin (20 μm), colourless, low-birefringence cement (**4**) that, with the fragments, defines an intricate colloform surface. Even small particles are coated, so that the outer margin of this zone is generally colourless and appears minutely granular under crossed polars.

Surface irregularies are dramatically smoothed by a colourless multilayer cement (**5**) 140 μm thick, including at least 25 sublayers. There are traces of a fibrous structure, but fibres form spherular packets that link laterally into a colloform sheet. In some cavities this cement sequence rests directly on the earlier one (**2**) without any intervening sediment. It also lines larger cavities within the internal sediment mass.

The sediment overlying **6** is fine-grained but includes fragments of cement (up to 1 mm in length) and dark, structureless pellets. In many cavities it is no more than 2 mm thick, giving way to a layer (less than 1 mm thick) of angular fragments of mud. Scattered *Favreina* pellets also appear, but there is a layer, greater than 2–3 mm thick, consisting almost exclusively of them (**7**). They have an average cross-sectional diameter of 300 μm and are loosely bound by flocculent masses of brown mud retaining a high residual porosity. Most of the sediment is isotropic, but pores have a thin, birefringent, lining suggesting that a tenuous cement is present. There is an abrupt transition from this pelletal deposit to a dark to light brown sediment consisting of transparent (isotropic) to opaque, irregular granules, 15 μm in diameter, separated by an opaque pore filling (**8**). This is followed by 2 mm of fine-grain, flocculent aggregates (**9**) with intergranular pores lined with a thin, colourless, low-birefringence phosphate cement (**10**).

The irregular surface of these early deposits is overlain by a distinctive sediment (**11**) that closely resembles some Aldabra palaeosols (Braithwaite 1975). This consists of well rounded bodies of a wide size range, some of them with thick, oolithic (concentrically laminated) coats. Nuclei include fine-grained sediment, fragments of phosphatic cements, and other lithoclasts. These bodies rest in a muddy matrix that forms aggregated masses, with a high residual porosity, lined with a thin (15 μm), colourless, low-birefringence phosphate (?**13**). The sediment is overlain by a colourless, almost isotropic granular (grains 6 μm in diameter) cement (?**13**) (greater than 150 μm thick), which fills some residual cavities.

Elsewhere in the sample, ooliths and glaebules are more tightly packed and lack the mud matrix (**11**). In smaller pores no obvious cement is present but in the larger there are two

distinct zones, each 40 μm thick. The earlier (**12**) is almost opaque, but has some dark brownish areas with high birefringence. The later (**13**) is colourless and includes about twenty subzones. It has a generally low birefringence, but some laminae, which are brownish in ordinary light, show more colour. Additional zones are present in the largest cavities. In one, colourless, fibrous crystals, 60 μm long (**14**), have a range of birefringence along their axes.

In addition to these variations the glaebular sediment (**11**) in some sections occupies much larger cavities. These are eroded principally in a fine-grained sediment (**8**), which forms lithoclasts among the glaebules, and their margins have a zone of alteration, 20 μm thick, in which the opaque 'pore filling' is absent.

In the above example seven sediments are separated by a minimum of seven cement increments. Erosional events have been of major importance in the formation of the cavity systems into which successive deposits were emplaced.

(*d*) *10A13*

The fourth and last sequence in this group was collected as a loose block, but was probably derived from the high-level bedded deposits. It is remarkable in consisting almost entirely of convoluted multilaminate cement sheets (figure 42, plate 7). Cavities are of centimetre dimentions. Little of the original sedimentary frame (**1**) can be recognized. It seems to have been fine-grained with scattered bivalves and foraminifera, the former represented by moulds, the latter by pseudomorphs of granular phosphate. The matrix is now finely granular with opaque grains intermixed with buff-coloured, low-birefringence phosphate. Lighter coloured areas are more birefringent and probably represent a later stage in a prolonged alteration process.

The first cement in many small solution cavities is a colourless, low birefringence, fibrous phosphate, typically with 4 or 5 prominent sublayers (**2**). This zone may be thin or absent, but in major cavities it is 50 μm thick and is commonly isotropic. It is overlain by a thick (locally more than 2 mm thick) cement (**3**) containing at least fifty subzones. This has a pronounced fibrous structure but is sometimes so deeply coloured as to be opaque. Lighter, brownish, areas show high birefringence, with patchy alteration to a colourless, low-birefringence product. In some cavities the whole zone is brownish, containing over 140 subzones. It is overlain locally by a thin (20 μm), colourless, isotropic zone (**4**) followed by a dark, finely granular deposit, 0–150 μm thick (**5**), associated with angular, opaque granules, 40 μm in diameter, forming a layer 100 μm thick (**6**). These last two zones together define a new irregular surface on which is deposited 300 μm of colourless to pale brown, laminar cement (**7**). Most of this has low birefringence, but some laminae appear to have higher.

The sequence of cements is coated by an irregular layer of angular, opaque masses (**8**) surrounded by colourless, fibrous, low-birefringence phosphate, 30 μm thick (**9**). In some cases this outlines cubic crystals and the whole layer may originally have been of cubes of 100–150 μm in diameter. Interiors that are not opaque consist of low-birefringence granules. Relations suggest that this zone may once have been thicker, perhaps more than 3 mm thick. Cavities within it are again coated with colourless cement, but it is difficult to judge the relative positions of this and the two remaining increments. The first of these (**10**) is a pale yellowish, multilayer cement, which also lines interior cavities and is 140 μm thick. It has low birefringence and a radial, undulose extinction, but some parts of it, particularly the outer margins, have a strong, brown colour and high birefringence. Irregular masses of fine-grained sediment locally included

within this zone form volumes with a high porosity. The second and final cement (**11**) is a colourless, isotropic layer, 15 μm thick.

All of the cements that appear to overlie the cubic crystals (**8**) may also post-date a series of very large crystals that line one major cavity. These are 1–2 mm in length, with monoclinic terminations paralleled by zones of opaque inclusions. They are overlain by a thin, colourless, low-birefringence layer.

Eleven major diagenetic events are recorded in this sequence. However, cavities of equal size may lack the early, brown, multilaminate zone or other zones, and relative thicknesses vary. The cubic pseudomorphs form a useful reference. These crystallized from a solution that removed most of the original rock mass from the framework provided by resistant early cements. The difficulty of placing in sequence cements following deposition of the cubic mineral shows that this solution event was not unique.

(*e*) *10B22*

In concentrating on the more elaborate cement/sediment sequences, we have so far avoided reference to the low-level, derived phosphorites. In these, cements are very much simpler, consisting, in general, of only a few layers. As an example, a coarse lithoclastic rock (10B22) with carbonate fragments of 1 cm diameter (**1**) contains seven separate cements. The earliest (**2**) is a colourless, laminate zone, 30 μm thick, with weakly birefringent bundles of radial fibres. It is overlain by a zone (**3**), 224 μm thick, with four poorly defined, radially fibrous subzones. These are generally opaque, but the outermost edge, 28 μm thick, is colourless and has low birefringence.

The third major cement (**4**) is 100 μm thick and has a marked fibrous structure, but is again virtually opaque. It is followed by another colourless zone (**5**), 140 μm thick, with four weakly birefringent, radially fibrous, subzones, the edges of each of which, in some cavities, have a finely granular structure. The fifth zone, 400 μm thick (**6**), is also generally colourless but sometimes has brownish, highly birefringent patches and traces of fibrous structure. It contrasts sharply with the overlying cement, a colourless to pale yellow, isotropic, multilaminate zone, 55 μm thick (**7**).

In some cavities a final, thin (40 μm), colourless, low-birefringence zone with a coarse prismatic structure is present (**8**). This is overlain locally by a dense, fine-grained, pelletal sediment (**9**) that includes fragments of older cements.

The main variations seen in low-level sequences lie in changes in total numbers and thicknesses of zones of a particular morphology. Cements are sometimes greater than 2 mm thick but are less commonly associated with internal sediments than in the high-level group. Such sediments are present, showing evidence of infiltration, damming up against tight pore throats and forming geopetal layers within cavities. Cements, apart from vadose carbonate in one specimen, are a late introduction to the sediment. Solution effects are much less common.

(*f*) *10A29*

The last group of samples for discussion are those in which phosphate has been emplaced in a dominantly carbonate rock. Cavities in the Esprit Limestones, some metres below the main contact with the high-level phosphorites, have phosphatic linings. In a random example (10A29) the limestone contains cavities formed by the solution of both aragonitic bioclasts and biomicrite matrix. Two calcite cements are present, an early, slightly brownish phase, which pre-dates a period of fracturing, and a later phase filling fractures. In large cavities the later

cement has a coarse, prismatic habit with scalenohedral terminations. These crystals are overlain directly by a colourless, laminate phosphate cement, 30 μm thick, followed by zones of brownish-opaque and of colourless phosphate. In another sample (10A18) three phosphatic cements total 130 μm in thickness, and, in one cavity, laminate phosphate is overlain by a thin coating of granular calcite.

The most significant feature here is the apparent lack of phosphatic cements from some small cavities. These are lined with dog-tooth calcite with clean terminations and their existence seems to pre-suppose, as in most of the phosphorites, pores that the phosphate-bearing solutions were unable to enter.

(*g*) *10B17*

Analogous to these deposits are samples collected from the floors of solution pits exposed near sealevel on the eastern shore of Esprit. These (10B17) consist of moulds of large bivalves resembling *Scutarcopagia* and *Fragrum* and of fragments of coral, 10 cm in diameter. A fine-grained internal sediment within and between shells, now wholly replaced by phosphate (figure 43, plate 7), but with a 'chalky' friable appearance, contains *Marginopora*, *Heterostegina*(?) and possibly *Halimeda*. Major cavities formed very early, shells were coated with phosphate before dissolution, and pores formed by their removal often do not contain additional cements.

There is considerable variation in the detail of cement sequences. Six depositional events can be recognized. The earliest layer (**2**) is 14 μm thick, colourless and isotropic. It is overlain by a 300 μm thick, brown, high-birefringence zone (**3**) with alternating near-opaque and translucent bands (seven dark bands) having a marked radially fibrous structure. This is overlain by a 120 μm thick, colourless and prominently granular zone with some cubes, 13 μm in diameter, formed on free surfaces (**4**). Small amounts of an opaque, brownish substance are associated with the boundaries of granules that are themselves weakly birefringent, even where they appear to be cubes.

The fourth zone (**5**), 0–160 μm thick, is completely colourless and shows traces of a laminar structure with vague, radial fibres. Two subzones are separated by a line of opaque, granular inclusions. The layer following (**6**) is 0–56 μm thick and radially fibrous, but is almost opaque on its inner margin while the outer is pale yellow and transparent. Birefringence is low, although the body colour gives the whites a distinctive tint. The final cement (**7**) is 14 μm thick and is also yellowish and transparent, but with a high birefringence. A few cavities contain small amounts of a fine-grained internal sediment (**8**).

In several samples a colourless cement zone resembling the earliest described above (**2**) overlies scalenohedral crystals full of opaque inclusions. Since similar crystals in one cavity are calcite, these are interpreted as pseudomorphs after an early carbonate cement.

(*h*) *Conclusions*

There are four conclusions relating to cement and internal sediment sequences.

(1) Sequences are often elaborate, reflecting a large number of depositional and erosional events.

(2) The lack of a uniform cement stratigraphy indicates that many such events modify only restricted volumes.

(3) The exclusion of widespread cements from some large cavities points to a lack of interconnection between pores, which may reflect some property of the transporting medium.

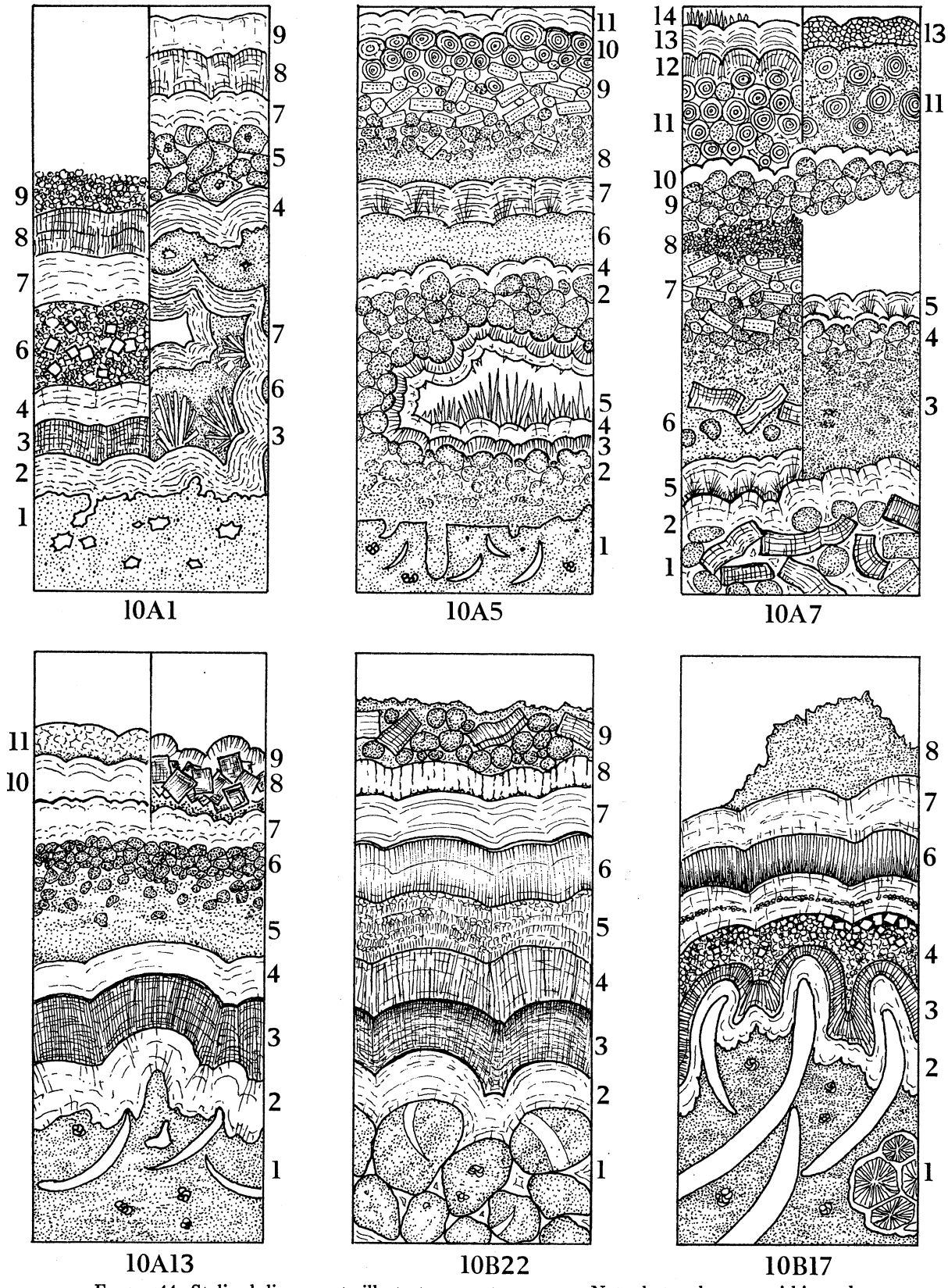

FIGURE 44. Stylized diagrams to illustrate cement sequences. Note that scales vary within and between illustrations, which are intended only as a guide to the text.

(4) The heterogeneity of patterns of distribution of cements seems impractical in a uniform groundwater system. The degree of independence of precipitating streams is possible only in the vadose zone.

Mineralogy

Some aspects of mineralogy have been indicated. Irrespective of morphological variation, samples are almost monomineralic and there is evidence that many minerals are represented entirely by pseudomorphs. The small size and erratic distribution of crystals makes individual identification impractical and the weight of evidence rests with X-ray diffraction of bulk rock samples.

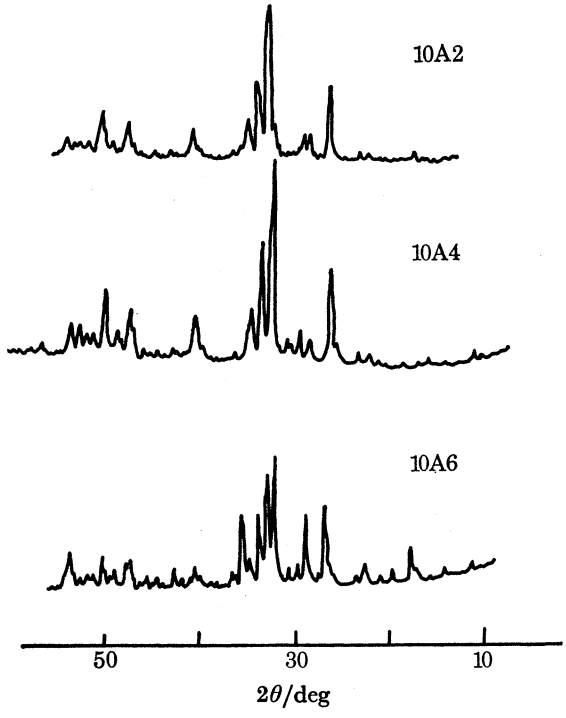

Figure 45. Selected X-ray diffraction traces of bulk samples. The scale, referring to all three curves, indicates intervals of degrees of 2θ.

Frondel (1943) noted from earlier work that most insular and continental phosphorites are minerals that fall into a well defined section of the apatite series. These can be described as carbonatian hydroxylfluorapatites, $Ca_5(P_{(1-x)}C_xO_{(4-x)}OH_x)_3$ (F,Cl,OH). Many contain little or no fluorine (less than 3%) and are properly classed as dahllite (McConnel 1958), while in others fluorine increases with age, sometimes to form francolite. There is a mutual substitution relation between Cl and OH, dominated by OH, but no simple hydroxylapatite from insular deposits has yet been reported and chlorapatites are extremely rare.

If mineralogy is so restricted, what explanations are there for the variety of crystal morphologies and optical properties observed? Chemical substitutions have an undoubted effect upon crystallography. McConnel (1952) and Trautz (1955) showed that the replacement of OH by F tends to shorten the *a*-axis, while replacement by Cl lengthens the *a*-axis but shortens the *c*-axis. In addition to these changes, substantial variations in the ratios of phosphate to carbonate may occur. Le Geros *et al.* (1967) suggested that the carbonate substitutes for phosphate in the

apatite lattice, although Elliot (1969), McConnel (1952) and others have pointed out that one carbonate ion could also substitute for two hydroxyl ions. Le Geros *et al.* (1967) believed that the total carbonate content is generally small. Their diagrams show the effect of increasing carbonate content in shortening the *a*-axis of the unit cell and in producing substantial shifts in *d*-spacing, and this work has been underlined by Cook (1972). Le Geros *et al.* (1967) also suggested that apatites richer in carbonate tend to form more equant crystals with a length : thickness ratio approaching unity. Such variations, and those associated with OH and F substitution, may help to account for the range of crystal form seen among the present cements.

TABLE 1. X-RAY DIFFRACTION OF BULK SAMPLES, FIGURES FOR *d* SPACING OF SAMPLES ILLUSTRATED IN FIGURE 45

sample					
10A2		10A4		10A6	
d/Å	*I*(%)	*d*/Å	*I*(%)	*d*/Å	*I*(%)
7.9642	5	8.0729	5	7.9428	10
5.1510	5	5.6395	3	6.3564	9
4.5483	5	5.5345	3	5.1214	33
4.0044	5	4.0368	6	4.6068	10
3.8225	7	3.8388	8	4.3244	5
3.3933	47	3.4767	9	4.0044	15
3.1399	17	3.4176	50	3.8470	5
3.0404	14	3.1563	13	3.4112	70
2.8324	19	3.0557	17	3.3055	8
2.7732	100	2.9615	4	3.1563	60
2.7444	60	2.9190	12	3.0639	15
2.6727	50	2.7817	100	2.9711	10
2.5974	27	2.7608	64	2.8464	100
2.5615	8	2.6882	60	2.7944	95
2.4960	5	2.6121	28	2.7692	80
2.2711	8	2.5047	5	2.7001	61
2.2386	19	2.2821	8	2.6158	26
2.2280	20	2.2467	22	2.5757	61
2.1567	2	2.2071	5	2.5094	11
2.1252	5	2.1348	6	2.4926	13
2.0473	5	2.0562	5	2.3779	6
1.9844	3	1.9918	5	2.2905	3
1.9239	22	1.9317	24	2.2547	8
1.9030	3	1.8797	14	2.2493	19
1.8710	10	1.8329	33	2.2360	20
1.8260	28	1.7924	14	2.1716	10
1.7843	9	1.7672	12	2.1425	18
1.7571	9	1.7446	15	2.0562	10
1.7369	8	1.7172	15	2.0364	5
1.7113	17	1.6353	5	2.0128	13
				1.9786	6
				1.9336	26
				1.9125	24
				1.8771	20
				1.8574	12
				1.8345	35
				1.7931	14
				1.7787	12
				1.7524	13
				1.7113	33
				1.6937	5
				1.6681	4

The more birefringent cements may offer corroborative evidence of carbonate content, since Trautz (1955) showed that increasing birefringence could be related to a higher carbonate content. However, he doubted whether this would be enough, except at abnormally high carbonate levels, to resemble that of calcite, as it appears to do in the present samples. Trautz (1955) also showed that the main structural result of the substitution of carbonate for phosphate in apatite is a shrinkage of cell dimensions.

TABLE 2. X-RAY FLUORESCENCE ANALYSES (MAJOR ELEMENTS) OF SELECTED SAMPLES

10A	1	2	3	4	6	12
SiO_2	0.21	0.12	0.18	0.15	0.27	0.16
Al_2O_3	2.44	1.89	2.42	5.54	2.37	1.82
Total Fe	0.06	0.05	0.07	0.11	0.11	0.06
MgO	0.71	0.97	0.63	0.67	1.29	1.11
CaO	47.90	47.41	47.11	44.84	46.52	46.71
Na_2O	0.75	0.86	0.74	0.65	0.69	0.76
K_2O	0.05	0.06	0.05	0.11	0.07	0.06
TiO_2	0.01	0.01	0.01	0.02	0.02	0.02
P_2O_5	37.42	38.10	37.40	37.10	38.36	38.97
F	2.53	2.06	2.28	2.90	1.63	1.48
Sr	0.18	0.16	0.14	0.38	0.11	0.14
H_2O†	4.03	3.85	4.22	4.85	3.34	4.09
CO_2‡	4.51	3.24	4.53	3.96	4.73	3.34
total	100.80	98.78	99.78	101.28	99.51	98.72

† Total water (loss on ignition).
‡ Determined gravimetrically.

The frequency of weakly birefringent or isotropic materials has been noted as probably reflecting a poorly crystalline, disordered state. However, Frondel (1943) suggested that optical isotropy in many of these deposits is due to aggregate polarization in a mass composed of submicroscopic crystallites, i.e. it is a function of the size of the units rather than a reflection of a lack of structural organization.

The X-ray diffraction traces obtained in the present study correspond generally to published (Powder Diffraction Standards) figures for *d*-spacings of apatite minerals (carbonatian hydroxyl-fluorapatites). There is some variation between samples, which can be explained by substitutions of the kind described above, but these are not on a scale that can be resolved with the apparatus available (see figure 45 and table 1). A few samples contain high percentages of a phase that is probably whitlockite $(Ca_3PO_4)_2$. Figures compare well with data for natural and synthetic whitlockite, but are slightly closer to De Wolf's (1974) figures for the synthetic mineral. These variations are also explained in terms of minor differences in chemistry. Some semiquantitative X-ray fluorescence analyses are shown in table 2. Qualitative surveys of the specimens revealed no other elements. The figures compare reasonably well with published data of Cook (1972), Braithwaite (1968) and others.

The changes in cement morphology may be partly a reflection of real changes in structural organization. However, Buckley (1951) and others have indicated that interaction with the depositing solution and with adsorbed impurities is important in habit modification. This kind of control assumes particular significance when there is little overall chemical variation in the mineral(s) precipitated. It is especially important if the deposits are derived from a single source and are a result of the progressive relocation of material that originally accumulated on a

surface some distance above them. Most cements, of colloform or laminated, radially fibrous structure are best described as dahllite or, where they are of very low birefringence or are isotropic, as collophane. The high-birefringence mineral that appears to be a precursor of these (if not itself the primary precipitate) also seems to be apatite. X-ray diffraction failed to identify any other mineral.

There are several examples of crystal forms that cannot be explained in terms of either 'apatite' or whitlockite. Notable among these are large, apparently monoclinic crystals. There is no X-ray diffraction evidence that these are other than carbonatian apatite, but morphology suggests that they may originally have been either brushite ($CaHPO_4.2H_2O$) or, possibly, gypsum, which is isostructural with brushite. The record, in one sample, of a biaxial positive figure would accord with either interpretation, although brushite seems the more likely. The variety of prismatic and rhombohedral hexagonal crystals might have been carbonates (calcite), but the carbonatian apatites are all also hexagonal, as is whitlockite. However, since many phosphates have rhombohedral or tabular forms, calcite remains a strong possibility. It certainly occurs as well formed unaltered crystals in a few samples, where it emphasizes the point that some phosphate-depositing solutions were unable to effect alteration. Dolomite is a possible precursor in a few cases, but well formed rhombic crystals are comparatively rare. Blunt-ended prismatic crystals with square or rhombohedral sections suggest an orthorhombic mineral. There are few orthorhombic phosphates with the kind of simple chemistry that present analyses suggest. Of these, the most likely are newberyite, a hydrated magnesium phosphate ($MgHPO_4.3H_2O$), and struvite, hydrated magnesium ammonium phosphate ($MgNH_4PO_4.$ 6H2O). There is insufficient evidence to confirm either of these suggestions. The same doubt surrounds the occurrences of colourless, acicular crystals. These are presumed to be a phosphate, but, in the absence of clear evidence of the crystal system, no more precise suggestion can be made.

Finally, the cubic pseudomorphs and cubic crystals recorded cannot have been phosphates. Two chemically similar minerals, halite and fluorite, could have been precipitated from available elements. Of these, fluorite is the more attractive, since its components could have been released by the replacement of fluorine-bearing carbonatian apatites.

Discussion and conclusions

There are two general areas that need to be explored in the discussion of these phosphorites: (1) the nature of the environment of deposition; (2) the origin and mode of emplacement of the sediments.

The field relations indicate two separate depositional episodes. The earlier sediments rest on a solution-eroded limestone surface and occupy the floors of small caves. It cannot be doubted that the process that formed this surface was subaerial. Petrographic evidence, with one exception, does not provide direct confirmation of a subaerial origin for the phosphatic rocks. There are, however, several indirect lines of reasoning. The deposits are extremely diverse and show localized distributions of both cements and internal sediments. In addition, many have been subject to repeated erosion and deposition. This order of change, temporally and spatially, both of rate and of style of deposition, particularly of the cements, is difficult to support in any other than the subaerial environment. The pattern of deposition often resembles that described by Deelman & de Coo (1976), and supports the suggestion that the sediments were

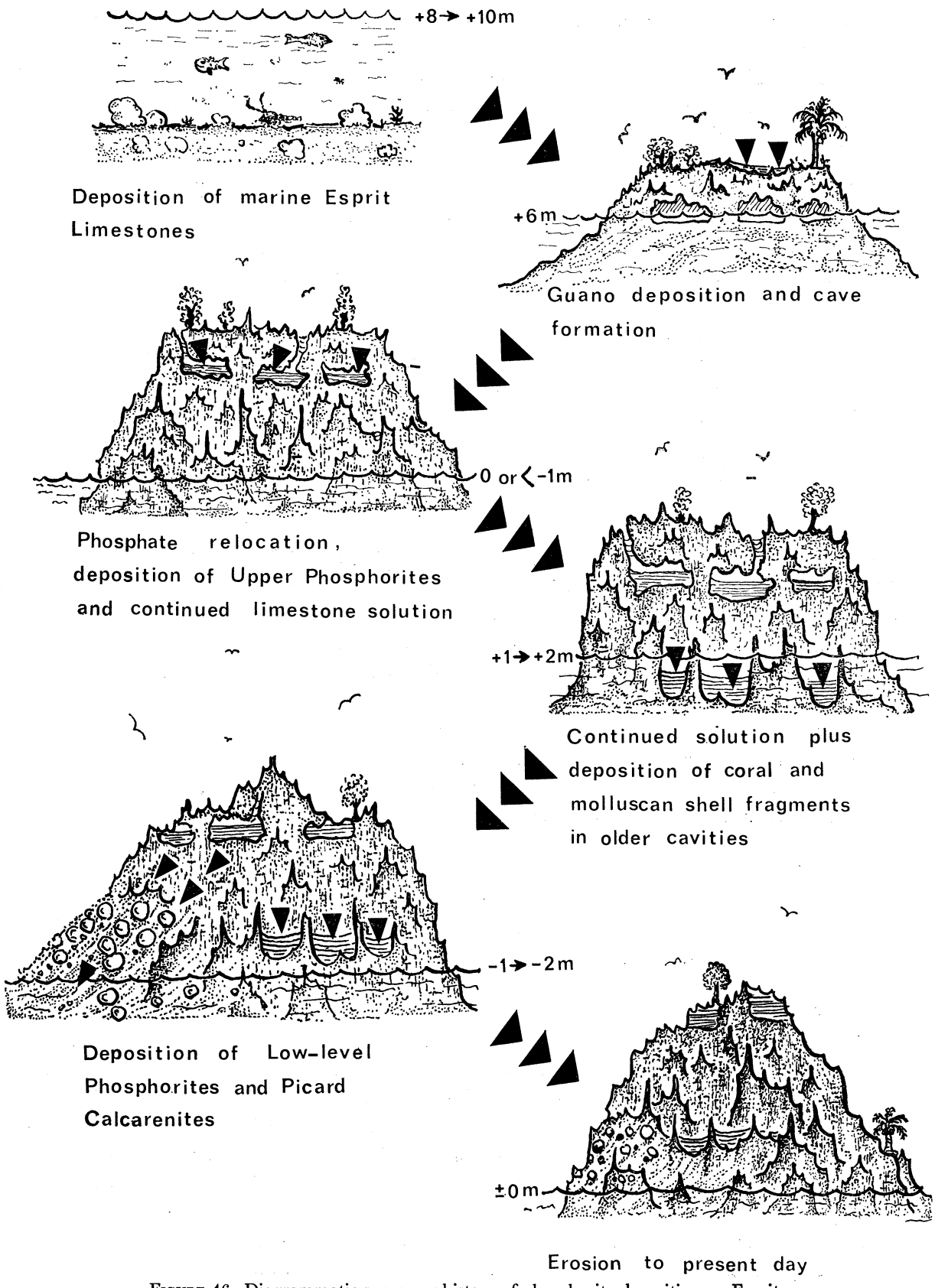

FIGURE 46. Diagrammatic summary history of phosphorite deposition on Esprit.

deposited in a series of caves. Solution repeatedly formed cavities within cave sediments and these became the sites of deposition of successive waves of infiltrating fine sediment.

This model is sufficient to explain most of the features of these deposits. Oolites from cave environments are recorded by several authors (Hess 1929; Davidson & McKinstry 1931; Baker & Frostick 1974). There is no evidence that the present examples have been replaced and they are assumed to have been primary phosphorite. The presence of lithoclasts also accords with a cave model, but it is more difficult to explain the occurrence of marine bioclasts. These could have been isolated from lithoclasts, but there is no indication that this was so and they are believed to have been primary. They rest on a subaerial erosion surface, but the relief on this is uncertain (see figure 46 and Braithwaite *et al.* 1973). However, deposition must have been related to a sealevel at least 6–7 m higher than at present. At this level, marine bioclasts could have been carried onto a land surface by storm overwash, and relocated in cavities.

A similar origin, by rain wash or gravity transport from an exposed surface, can be accepted for those 'primary' sediments the texture of which resembles that of Aldabra palaeosols. The occurrence within secondary cavities of supposed faecal pellets, particularly of the *Favreina* type also suggests a near-surface position. Pryor (1975) showed that *Callianassa* pellets are capable of surviving substantial transport and there is no evidence of widespread burrowing activity, and hence of habitation, in the cavities in which they are found. Moreover, the recognition of a *Favreina* horizon within a number of cavities argues strongly for their introduction as a result of some specific event. However, it is worth considering what kind of animal was responsible for their production. If it was a marine shrimp the presence of these bodies raises the possibility of an even higher sealevel during phosphorite deposition.

The low-level phosphorites are more easily interpreted. There can be little doubt that they were formed at a time when sealevel stood close to its present position. They were formed, perhaps entirely, of material derived from the erosion of the high-level group. This erosion was probably enhanced by a continued solution of the Esprit Limestone, and much of the sediment moved as a debris flow. Certain components of the earlier sediments, notably ooliths and fragments of banded cements, were more resistant. They are thus the dominant elements in these younger rocks. The processes of breakdown of the high-level deposits seem to have been able to produce and transport very large blocks, although these are not often bedded, as well as material down to the size of individual ooliths. Circumstantial evidence suggests that the time of erosion coincided with the time of deposition of the Picard Calcarenites in the Bassin Cabri area (Braithwaite *et al.* 1973). Pebbles of similar lithology and grains as small as single ooliths occur scattered within these calcarenites. There is no guarantee that they were not derived from the younger deposits but it seems reasonable to link the two erosion episodes.

There are two alternative origins for the phosphorites described. They may result from alteration of pre-existing deposits or they may be primary precipitates. Apart from the alteration of some banded cements there is little evidence of formation by replacement. Indeed, many sediments were emplaced as phosphates and available carbonates in contact with them have not been phosphatized. Low-level cavity fillings include moulds of aragonitic molluscs and corals that were coated *in situ* by a phosphatic cement precipitated from a solution incapable of reacting directly with this metastable mineral. Some authors, notably Ames (1959) and Gulbrandsen (1969), have suggested that carbonates in contact with phosphate-enriched seawater solutions will be replaced preferentially. Ames (1959) thought that this was the only way in which an apatite containing structural carbonate could be synthesized. However, there

is substantial evidence from other deposits that phosphates can form by primary precipitation provided that concentrations are high enough.

In a marine system the most likely source of phosphates is in nutrient-rich waters characterized by high organic productivity (Hutchinson 1950; Tankard, 1974). Such waters are commonly found at the sites of cold-water up-welling at the edges of areas such as the Chagos, Seychelles and Saya de Malha Banks. High marine productivity forms a food source for large populations of seabirds, which are present on some islands in the Indian Ocean, including Aldabra, and provides a means of transferring the phosphates from a marine to a terrestrial system. There are, however, no modern guano accumulations on Indian Ocean islands, perhaps as a result of a relatively high rainfall, and neither the present deposits, nor others in the area examined by the author, are themselves guano.

It is suggested that, as in the sediments described by Braithwaite (1968), high-phosphate residues from seabird rookeries accumulated on the surface of an island of which the cavernous limestones of Esprit formed the core. Solutions derived from these residues phosphatized some soils and superficial sediments containing marine bioclasts and lithoclasts, but had little effect on the underlying limestones. These surface deposits were transported downwards into a cave system that may be considered analogous to caves forming at the present day above the marine water table. At the time of deposition of the phosphates, however, the water table was probably lower, since the numerous reworking events are best explained as having occurred in a vadose environment. One way of reconciling these conflicting hypotheses is to suggest that the guano was deposited on low-lying islands in which caves were forming. As sealevel fell, towards the present position, the cavity system became available for the relocation of the surface deposits. This might be correlated with a period of high rainfall, producing erosion of superficial phosphatic deposits and further solution of the limestones. Surface induration of the limestones (by precipitation) would ensure that they were never saturated with water. Phosphate-rich solutions, probably moving in surface films, would have been responsible for the precipitation within cavities of crusts resembling stalagmitic coatings. More continuous flow encouraged the growth of phosphatic ooliths in a manner analogous to the formation of 'cave pearls', described by Hess (1929). Higher rainfall, giving more rapid flow, could carry the internal sediments, which reached their positions by infiltration. In addition, solutions passing rapidly through surface deposits might have contained relatively little phosphate. Being thus more aggressive they might locally have attacked previously deposited cements or sediment. Variations in concentrations of nitrates, urates or other super-soluble guano derivatives, or of organic acids, may be reflected in the varying morphology of phosphatic cements.

This major period of sediment relocation can be correlated with the principal interval of erosion of the Esprit Limestones. Other explanations are possible but are no less speculative. To complete erosion of the surface, sealevel must have fallen to at least 1–2 m below its present position, but must have risen to 1–2 m *above* it to deposit the shell and coral debris now seen flooring deep solution pipes. Continued solution had removed sufficient limestone to expose the upper phosphates to attack. Some solutions were able to penetrate small secondary cavities within the limestone mass and deposit thin phosphatic crusts, and phosphates were also precipitated to cement coral and shell debris lying in low-level cavities. However, most activity was centred upon the erosion and down-slope transport of the phosphoritic island cap. This debris accumulated in solution pits and hollows around the base of the island, but some entered the shelf sediments, to be carried northwestwards and be redeposited in the beaches of

the newly emerging proto-Picard sand cay (Bassin Cabri). The sequence is summarized in figure 46.

The relatively far-travelled pebbles of the Bassin Cabri area show evidence of more recent carbonate cement precipitation. These, however, are exceptional and, although Esprit has been submerged on at least two occasions, the last 125000 years ago, no evidence of more recent phosphatic deposits has yet been discovered.

It has been shown (Braithwaite *et al.* 1973) that the major high sealevel stand on Aldabra, represented by the Aldabra Limestone, can be dated at 125 ka B.P. Earlier high levels are reflected by the Takamaka Limestone and the Esprit Limestone. The data from the phosphorites, which post-date this latter unit, suggest a substantial period of subaerial erosion, although there is no indication of how low sealevel might have been. In the absence, therefore, of any more compelling evidence the phosphorites are regarded as having been deposited during a relatively warm period of an interglacial. Comparison with the temperature and sealevel curves of Emiliani (1970) and of Mesolella *et al.* (1969) suggests that this might have been between 170 and 230 ka B.P.

The work on Aldabra was made possible by the support of the Royal Society. The author would like to thank Dr J. D. Taylor for identification of molluscs, for assistance during field work and for helpful discussions. The X-ray fluorescence analyses are the work of Dr F. H. Hubbard and Mr R. J. McGill, to whom the author would also like to express his thanks. The present form of the text is due to the painstaking and constructive criticism of an unknown referee, whose help is also gratefully acknowledged.

References

Ames, L. L. 1959 The genesis of carbonate apatite. *Econ. Geol.* **54**, 829–841.

Baker, G. & Frostick, A. C. 1947 Pisoliths and ooliths from some Australian caves and mines. *J. sedim. Petrol.* **17**, 39–67.

Baker, G. & Frostick, A. C. 1951 Pisoliths, ooliths and calcareous growths in limestone caves at Port Campbell, Victoria, Australia. *J. sedim. Petrol.* **21**, 85–104.

Braithwaite, C. J. R. 1968 Diagenesis of phosphatic carbonate rocks on Remire, Amirantes, Indian Ocean. *J. sedim. Petrol.* **38**, 1194–1212.

Braithwaite, C. J. R. 1975 Petrology of palaeosols and other terrestrial sediments on Aldabra, Western Indian Ocean. *Phil. Trans. R. Soc. Lond.* B **273**, 1–32.

Braithwaite, C. J. R. 1979 Crystal textures of Recent fluvial pisolites and laminated crystalline crusts in Dyfed, South Wales. *J. sedim. Petrol.* **49**, 181–194.

Braithwaite, C. J. R., Taylor, J. D. & Kennedy, W. J. 1973 The evolution of an atoll: the depositional and erosional history of Aldabra. *Phil. Trans. R. Soc. Lond.* B **266**, 307–340.

Brewer, R. 1964 *Fabric and mineral analysis of soils*. New York: John Wiley.

Buckley, H. E. 1951 *Crystal growth*. New York: John Wiley & Sons.

Cook, P. J. 1972 Petrology and geochemistry of the phosphate deposits of northwest Queensland, Australia. *Econ. Geol.* **67**, 1193–1213.

Davidson, S. C. & McKinstry, H. E. 1931 Cave pearls, oolites, and isolated inclusions in veins. *Econ. Geol.* **26**, 289–294.

Deelman, J. C. & de Coo, J. C. M. 1976 Experimental analysis of floored interstices in clastic carbonate sediments. *Sediment. geol.* **16**, 1–13.

De Wolf 1974 *Selected powder diffraction data for minerals*, 9–169. Swarthmore, Pennsylvania: Joint Committee on Powder Diffraction Standards.

Elliott, J. C. 1969 Recent progress in the chemistry, crystal chemistry and structure of the apatites. *Calcif. Tissue Res.* **3**, 293–307.

Emigh, G. D. 1958 Petrography, mineralogy and origin of phosphate pellets in the Phosphoria Formation. *Idaho Bur. Mines Geol.*, pamph. 114, pp. 1–60.

Emiliani, C. 1970 Pleistocene palaeotemperatures. *Science N.Y.* **168**, 822–825.

Folk, R. L. 1962 Spectral subdivision of limestone types. *Am. Ass. Petrol. Geol. Mem.* 1 (ed. W. E. Ham), pp. 62–84.

Frondel, C. 1943 Mineralogy of the calcium phosphates in insular phosphate rock. *Am. Miner.* **28**, 215–232.

Fryer, J. C. F. 1911 The structure and formation of Aldabra and neighbouring islands—with notes on their flora and fauna. *Trans. Linn. Soc. Lond.* (*Zool.*) (2) **14**, 397–440.

Gulbrandsen, R. A. 1969 Physical and chemical factors in the formation of marine apatite. *Econ. Geol.* **64**, 365–382.

Hess, F. L. 1929 Oolites or cave pearls in the Carlsbad caverns. *Proc. U.S. natn. Mus.* **76**, 1–5.

Horowitz, A. S. & Potter, P. E. 1971 *Introductory petrography of fossils*. Berlin: Springer-Verlag.

Hutchison, G. E. 1950 Survey of existing knowledge of biochemistry: 3 The biogeochemistry of vertebrate excretion. *Bull. Am. Mus. nat. Hist.* **96**, 288–303 and 462–482.

Le Geros, R. Z., Trautz, O. R., Le Geros, J. P. & Klein, E. 1967 Apatite crystallites: Effects of carbonate on morphology. *Science, N.Y.* **155**, 1409–1411.

Loreau, J. P. & Purser, B. H. 1973 Distribution and ultrastructure of Holocene ooids in the Persian Gulf. In *The Persian Gulf* (ed. B. H. Purser), pp. 279–328. Berlin: Springer-Verlag.

Mesolella, K. J., Matthews, R. K., Broeker, W. S. & Thurber, D. L. 1969 The astronomical theory of climatic change: Barbados data. *J. Geol.* **77**, 250–274.

McConnel, D. 1952 The nature of rock phosphate, teeth and bones. *J. Wash. Acad. Sci.* **42**, 36–38.

McConnel, D. 1958 The apatite-like mineral in sediments. *Econ. Geol.* **53**, 110–111.

Pryor, W. A. 1975 Biogenic sedimentation and alteration of argillaceous sediments in shallow marine environments. *Bull. geol. Soc. Am.* **86**, 1244–1254.

Purser, B. H. 1969 Syn-sedimentary marine lithification of Middle Jurassic limestones in the Paris Basin. *Sedimentology* **12**, 205–230.

Roy, D. 1976 Bones from the laboratory. *New Scient.* **72**, 163–165.

Roy, K. T. 1970 Note on phosphate rock at Fanning Island. In *Fanning Island Expedition reports* (ed. K. E. Chave), pp. 193–199. University of Hawaii, Institute of Geophysics.

Tankard, A. J. 1974 Petrology and origin of the phosphorite and aluminium phosphate rock of the Langebaanweg-Saldanha area, south-western Cape Province. *Ann. S. Afr. Mus.* **65**, 217–249.

Trautz, O. R. 1955 X-ray diffraction of biological and synthetic apatites. *Ann. N.Y. Acad. Sci.* **60**, 696–712.

Trueman, N. A. 1965 The phosphate, volcanic and carbonate rocks of Christmas Island (Indian Ocean). *J. geol. Soc. Aust.* **12**, 261–283.

Weber, J. N. & White, E. W. 1973 Carbonate minerals as precursors of new ceramic, metal and polymer materials for biomedical applications. *Minerals Sci. Engng* **5**, 151–165.

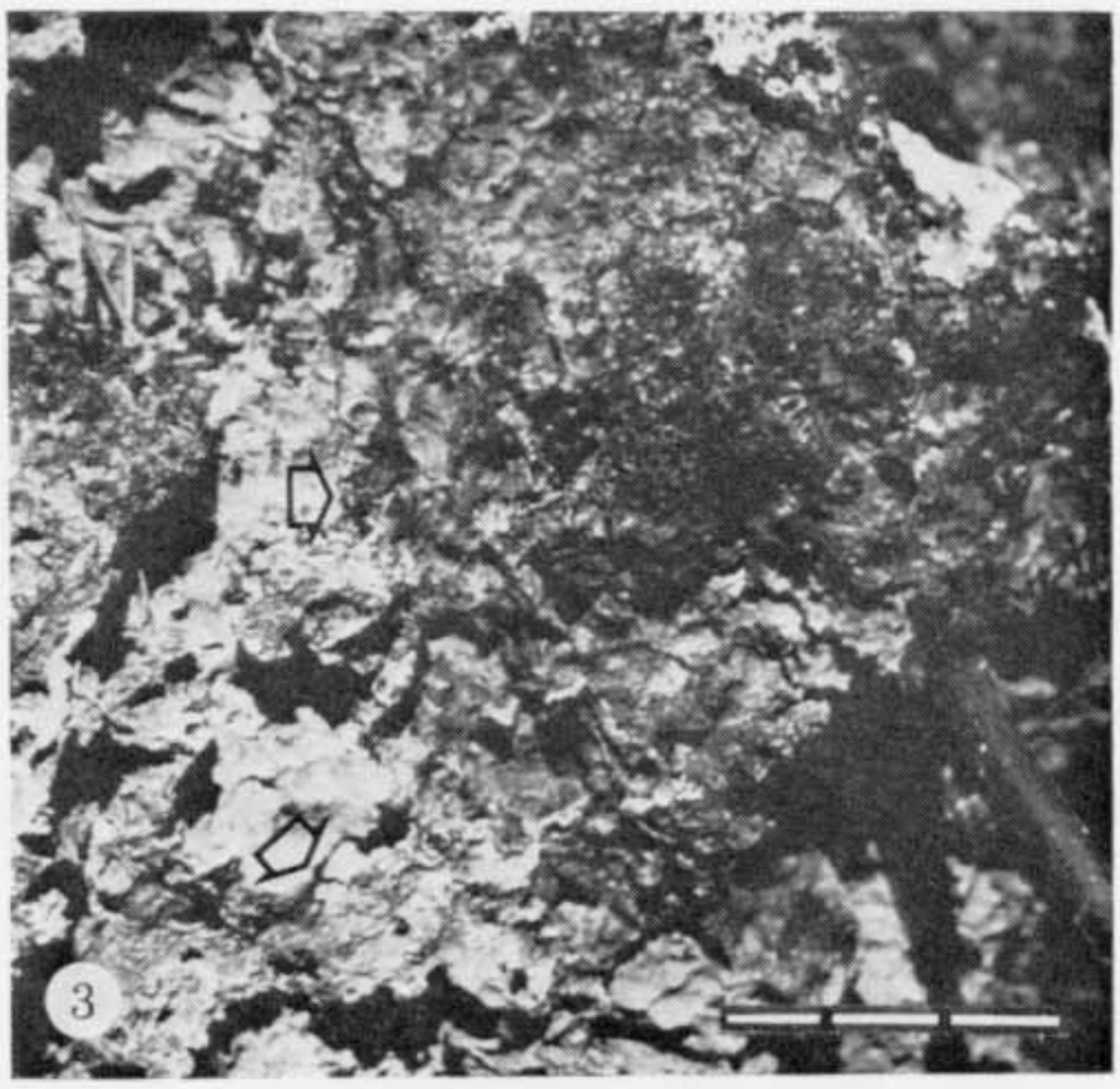

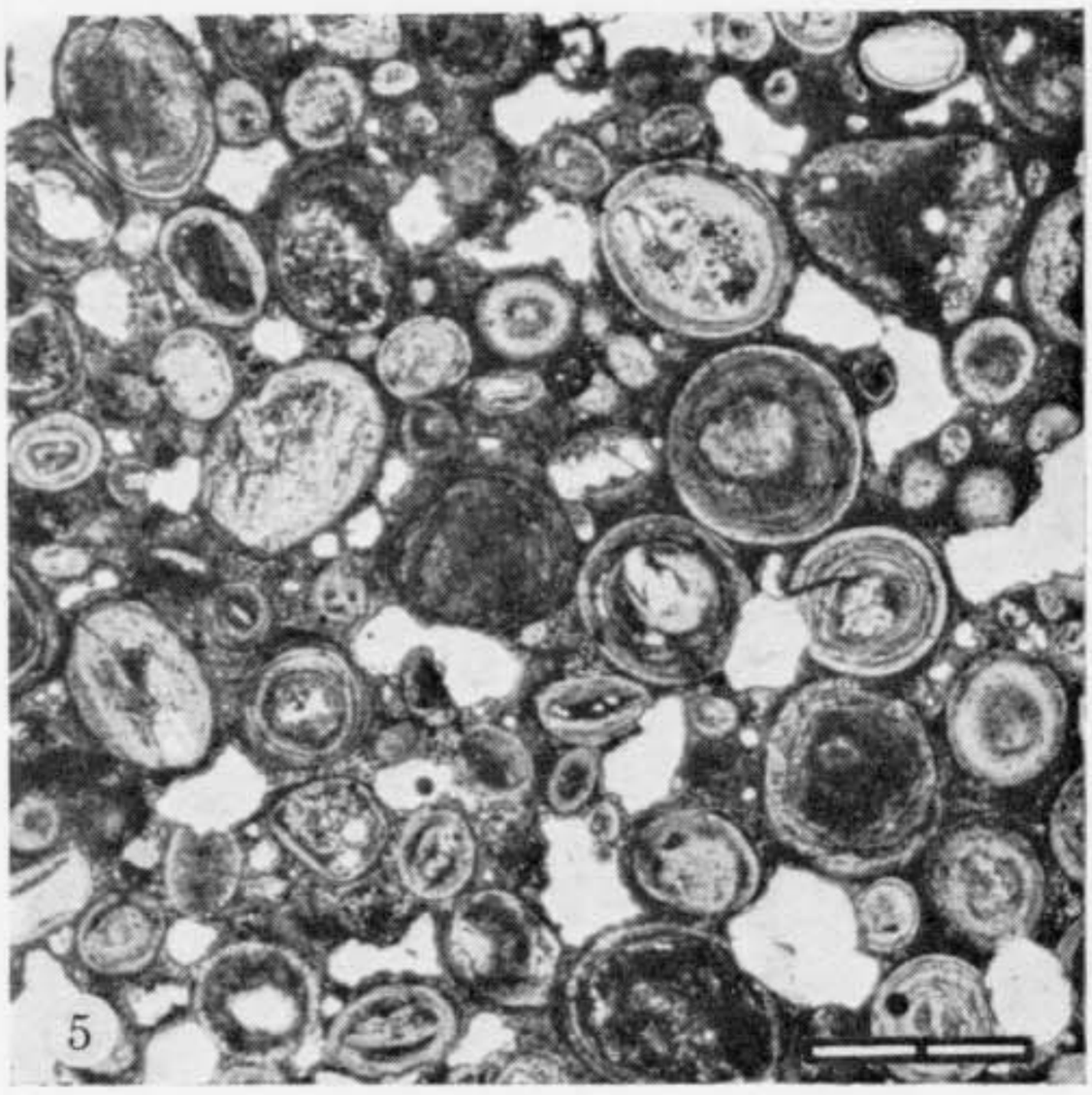

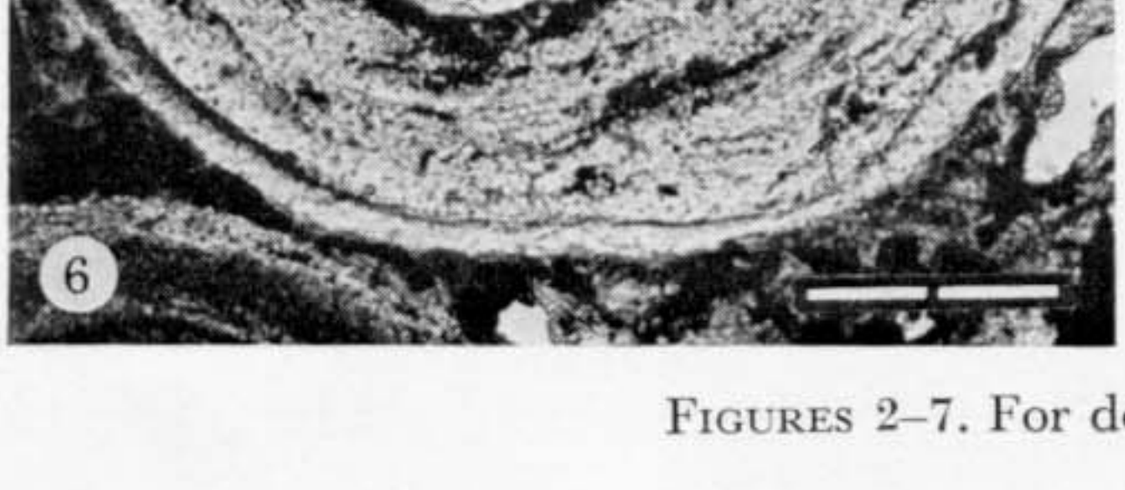

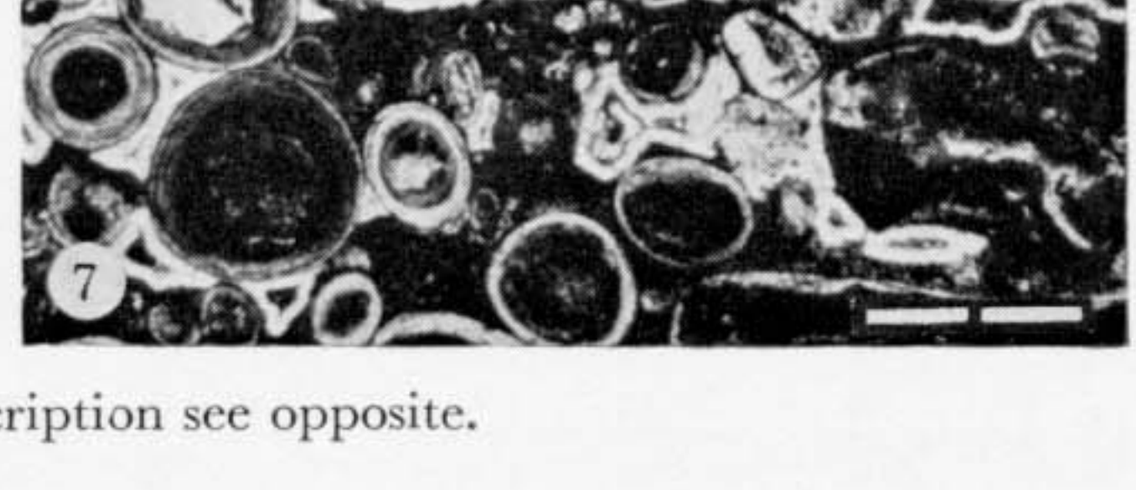

FIGURES 2–7. For description see opposite.

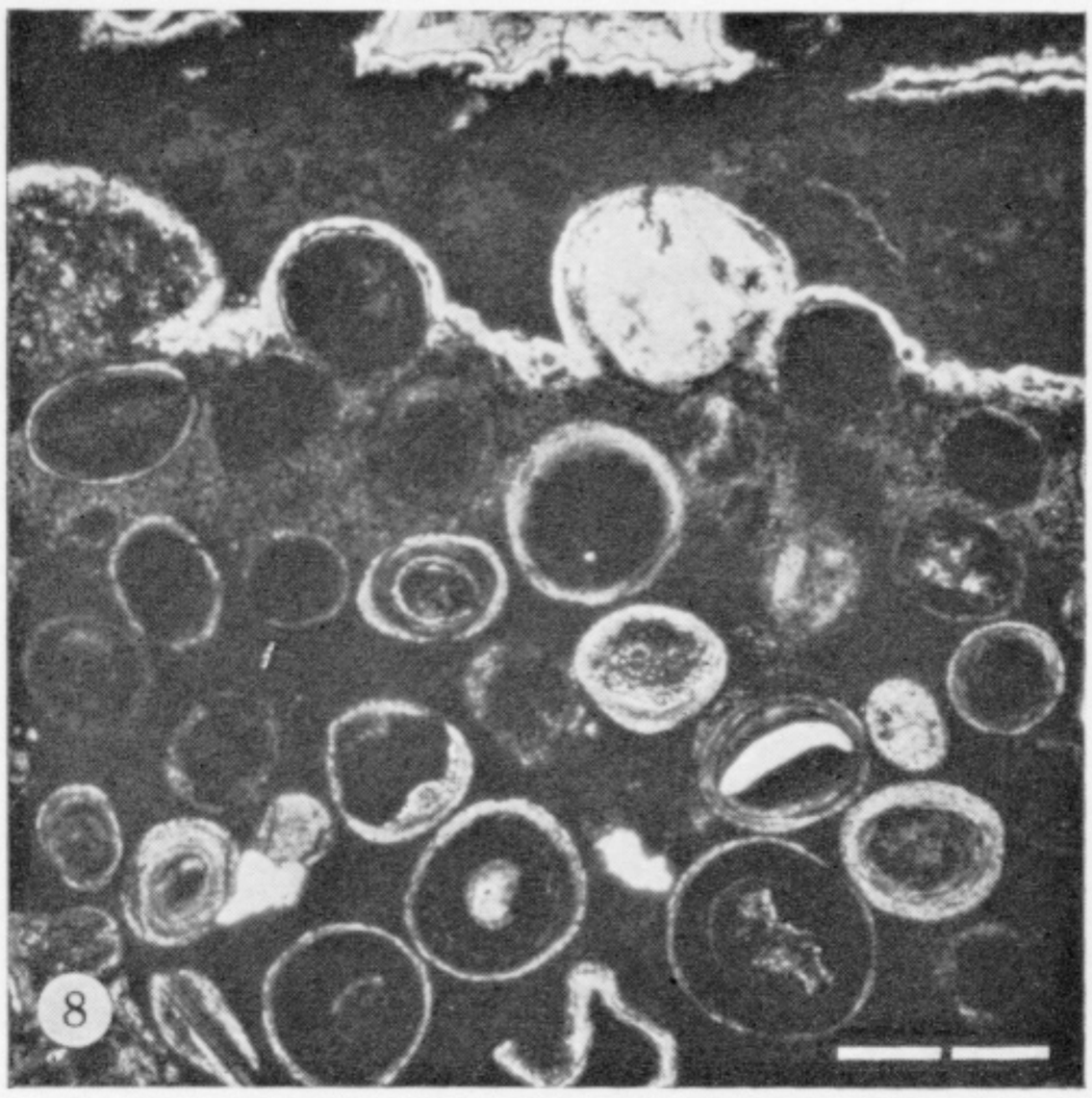
8

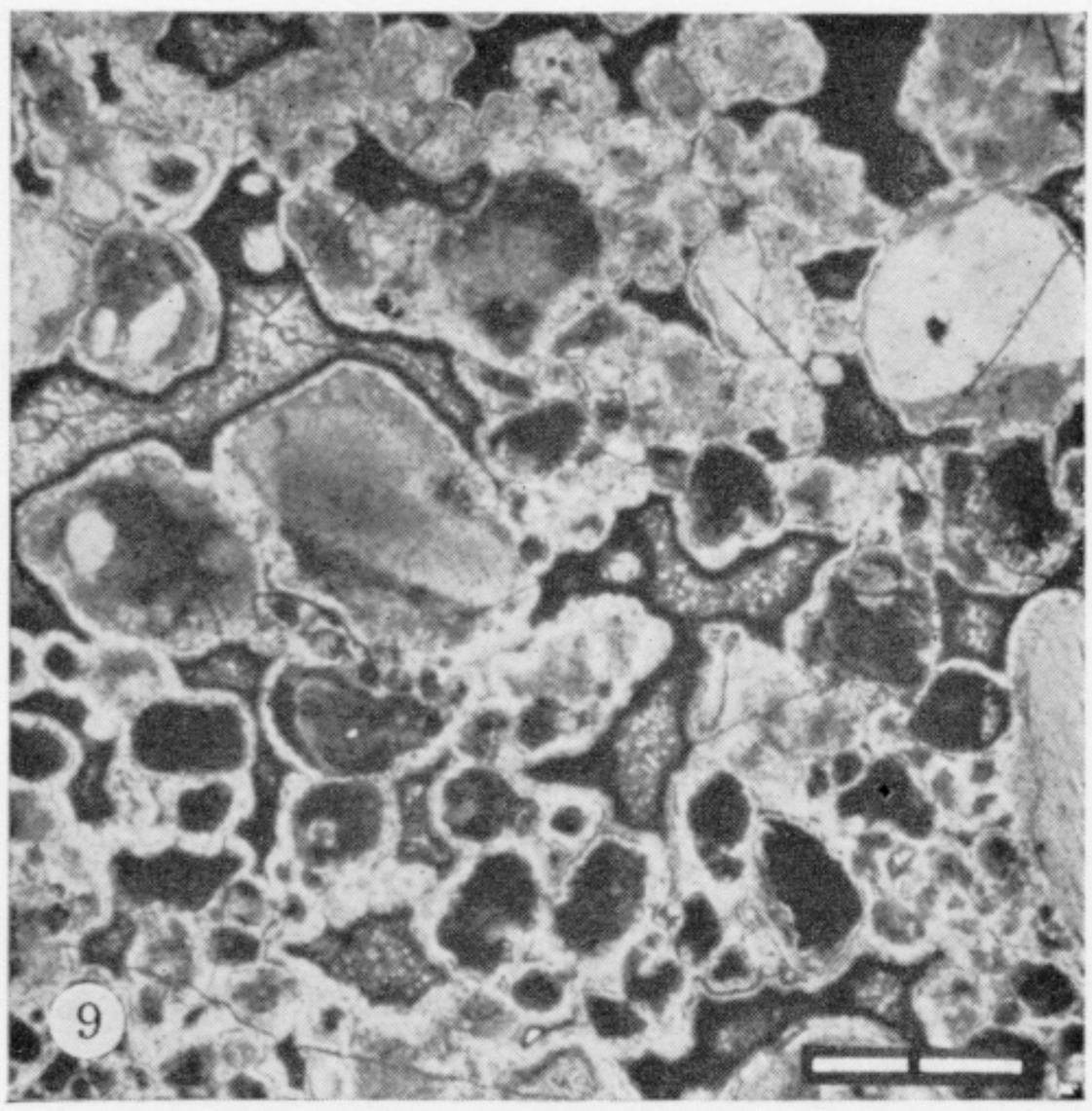
9

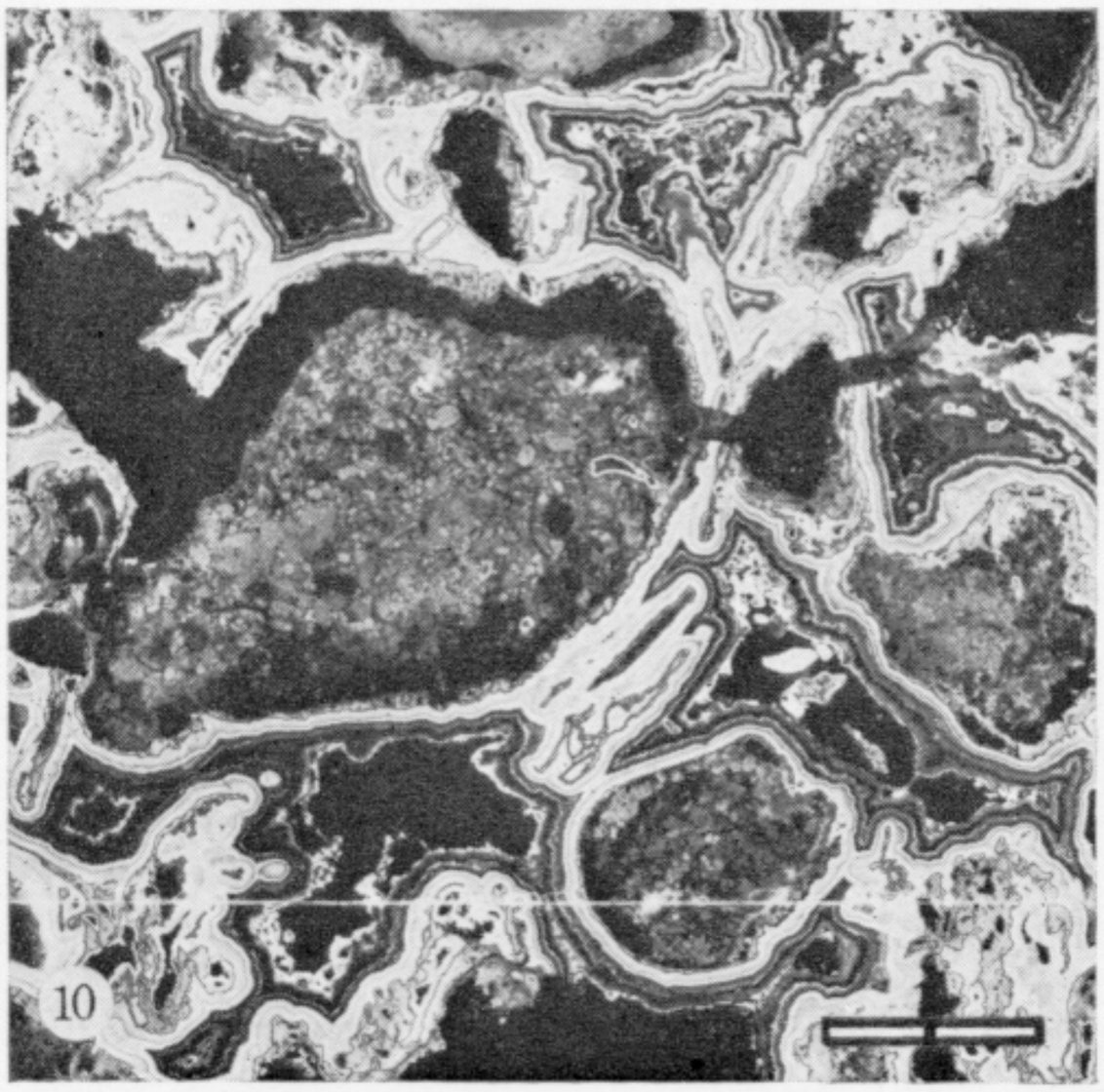
10


11

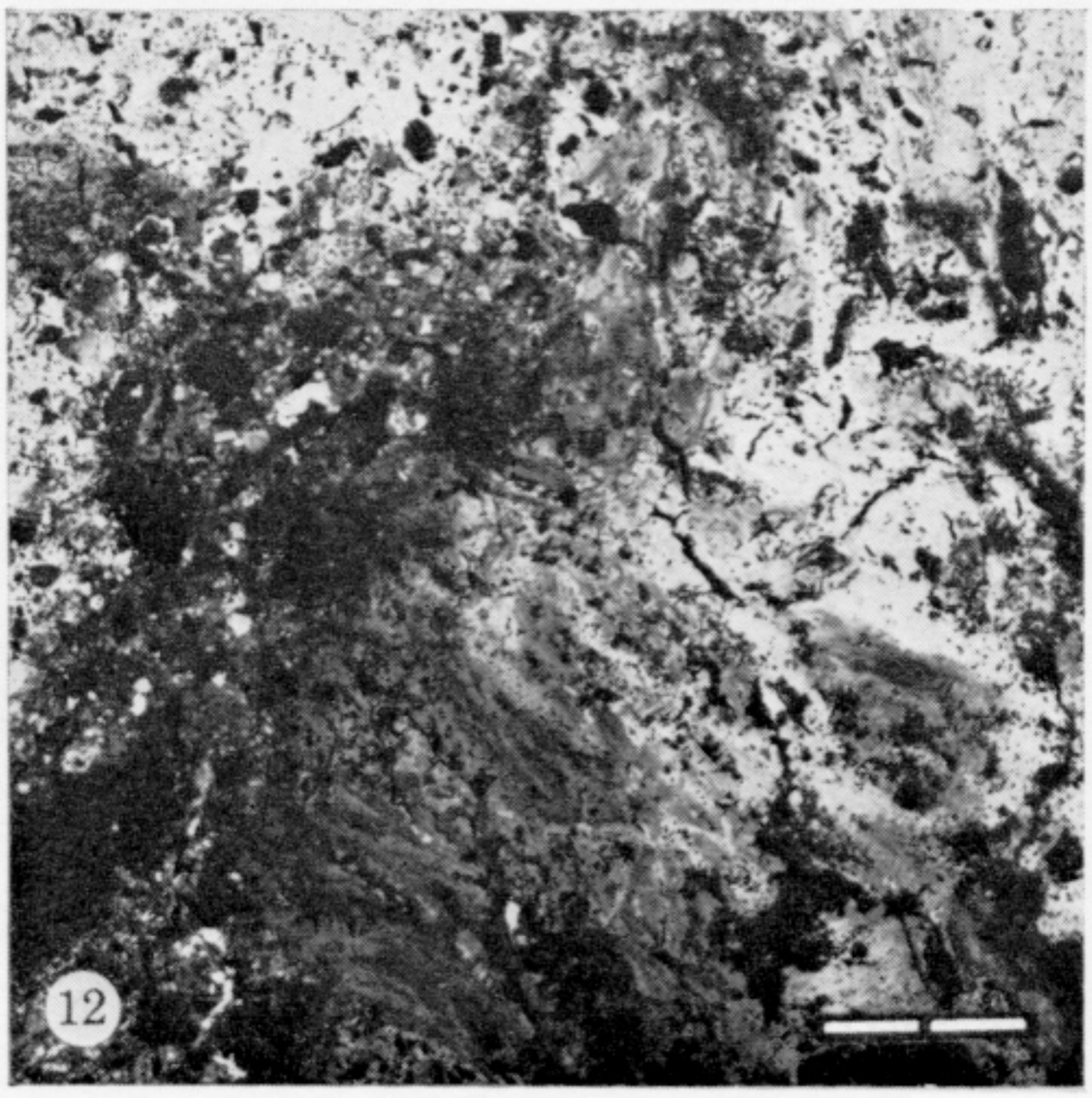
12

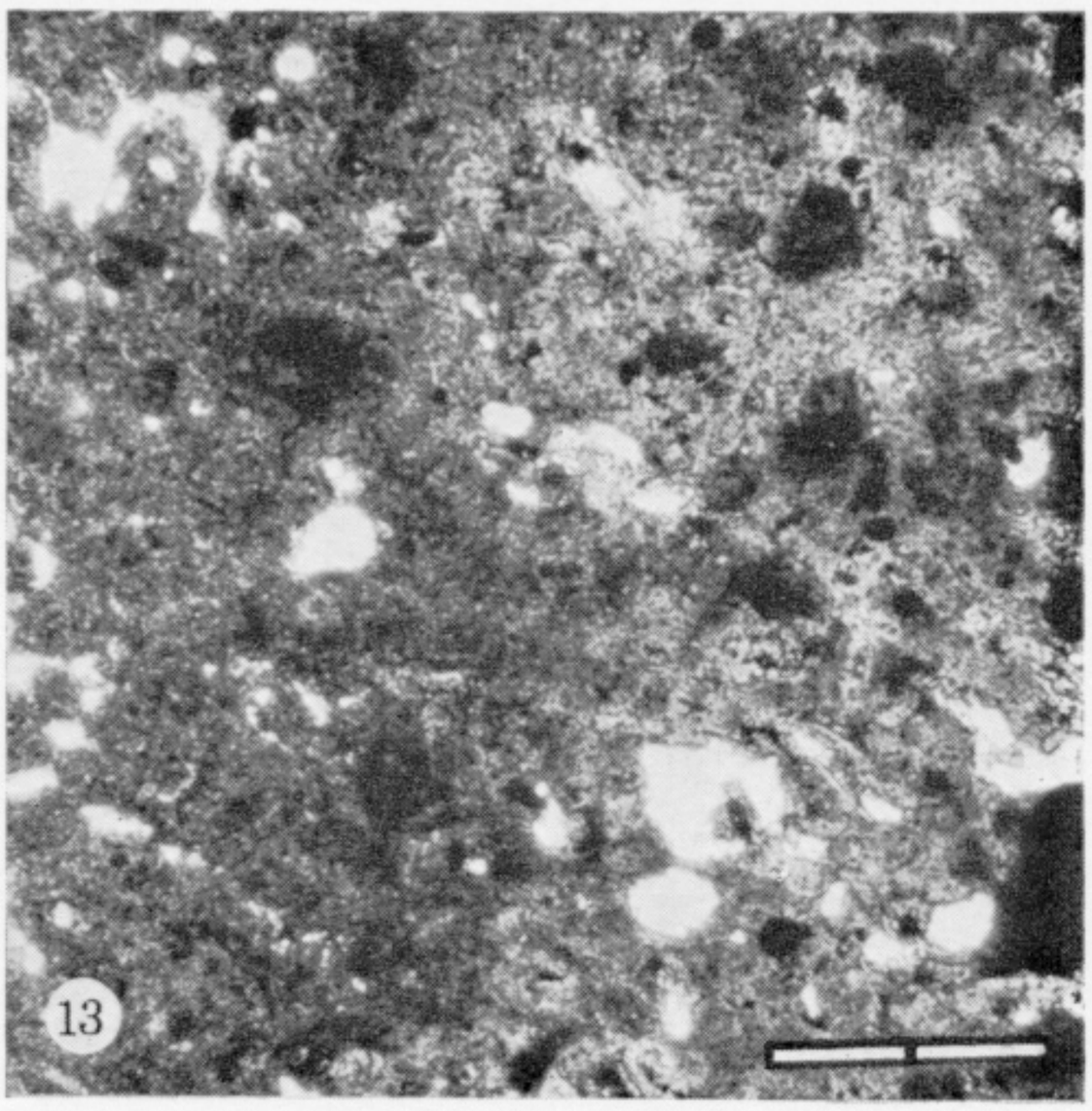
13

FIGURES 8–13. For description see p. 514.

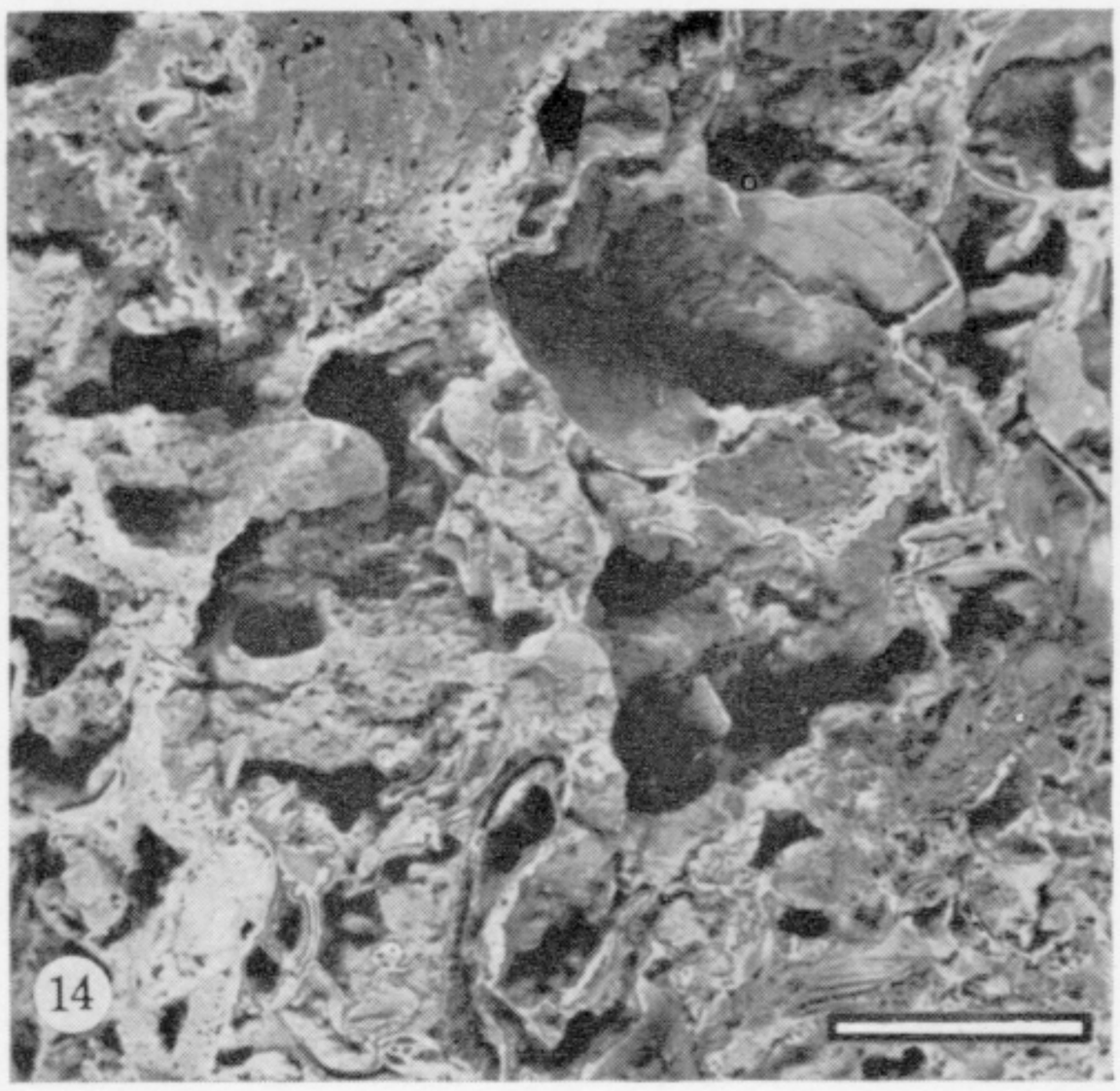

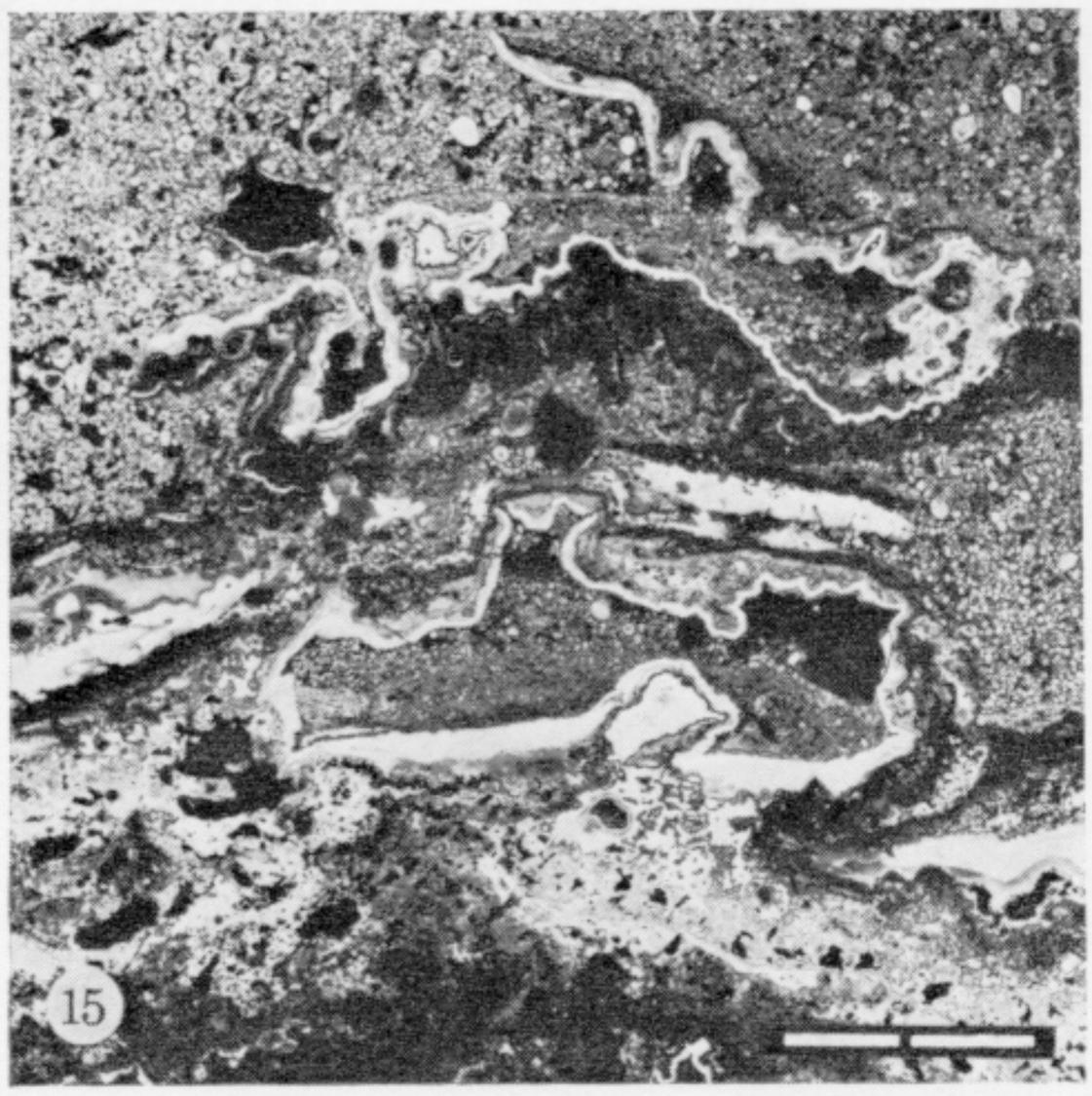

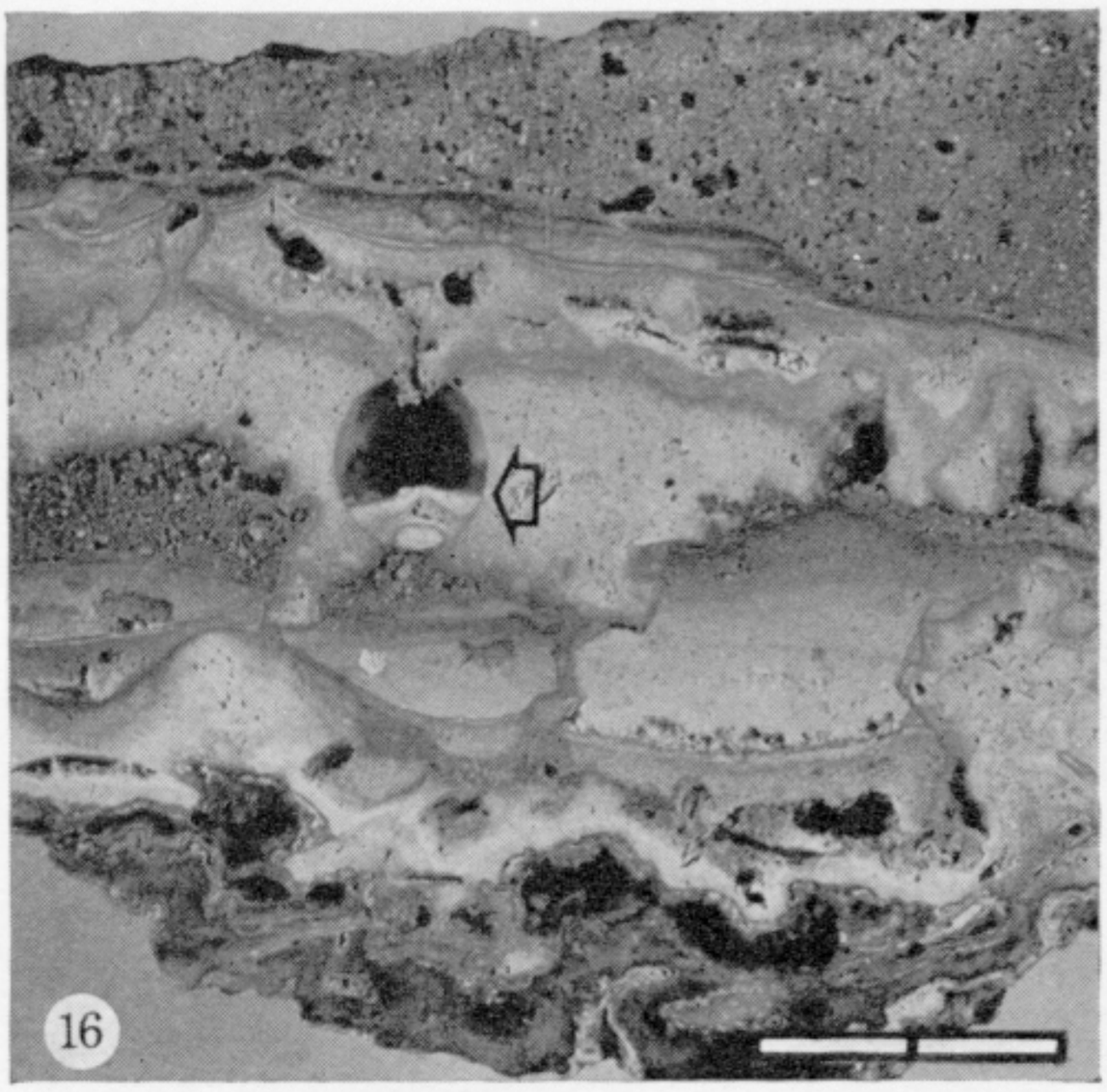

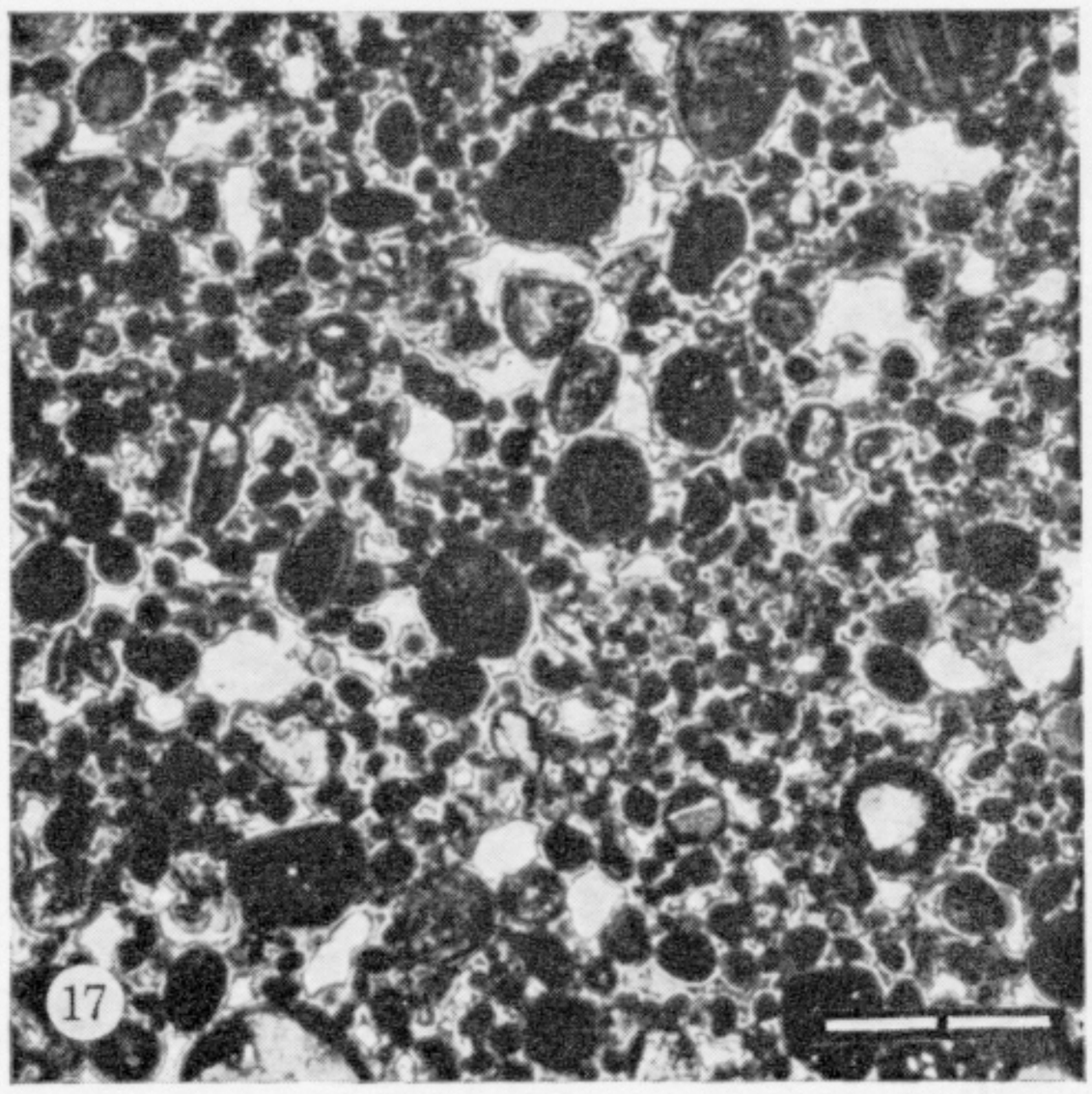

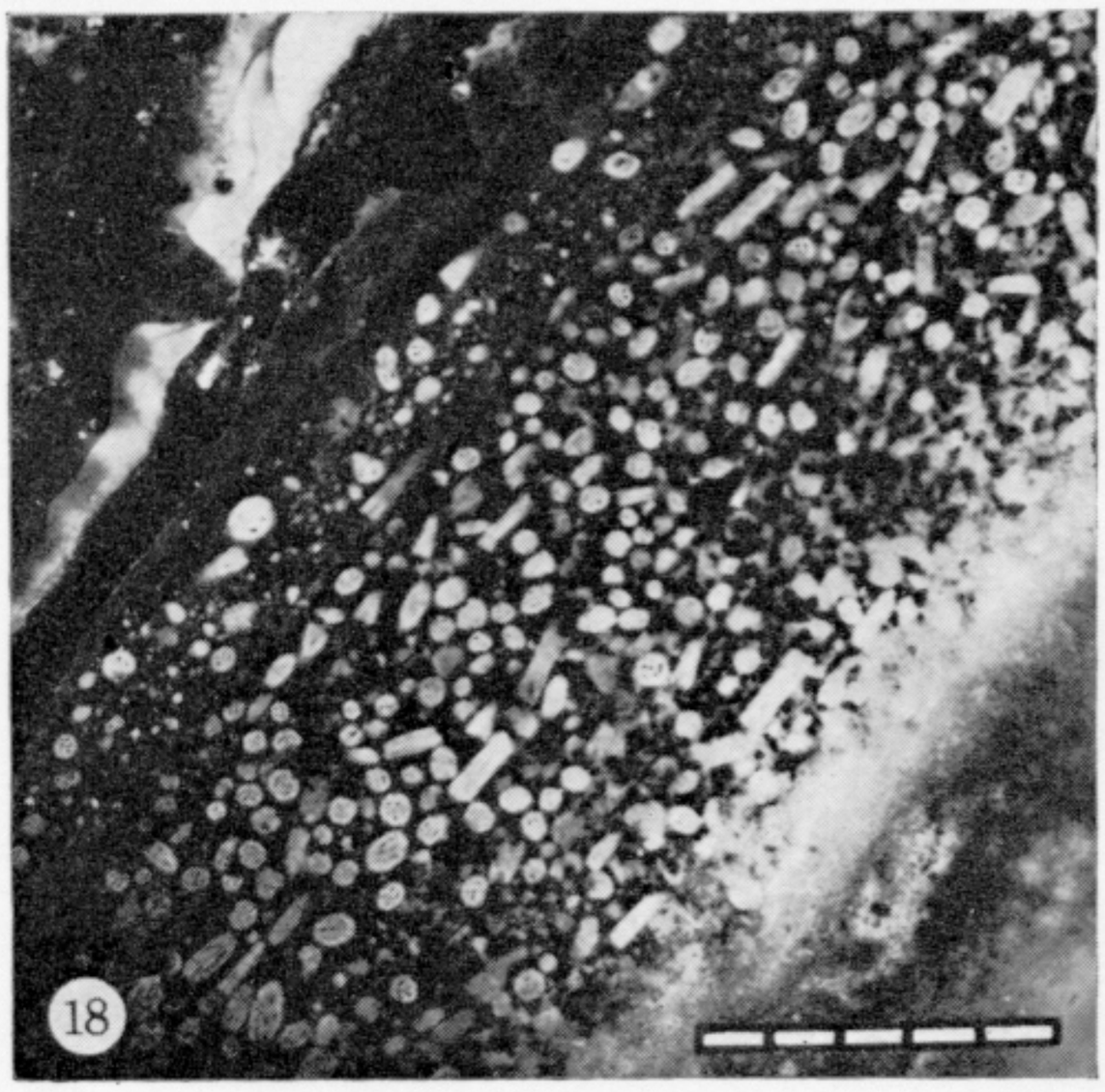

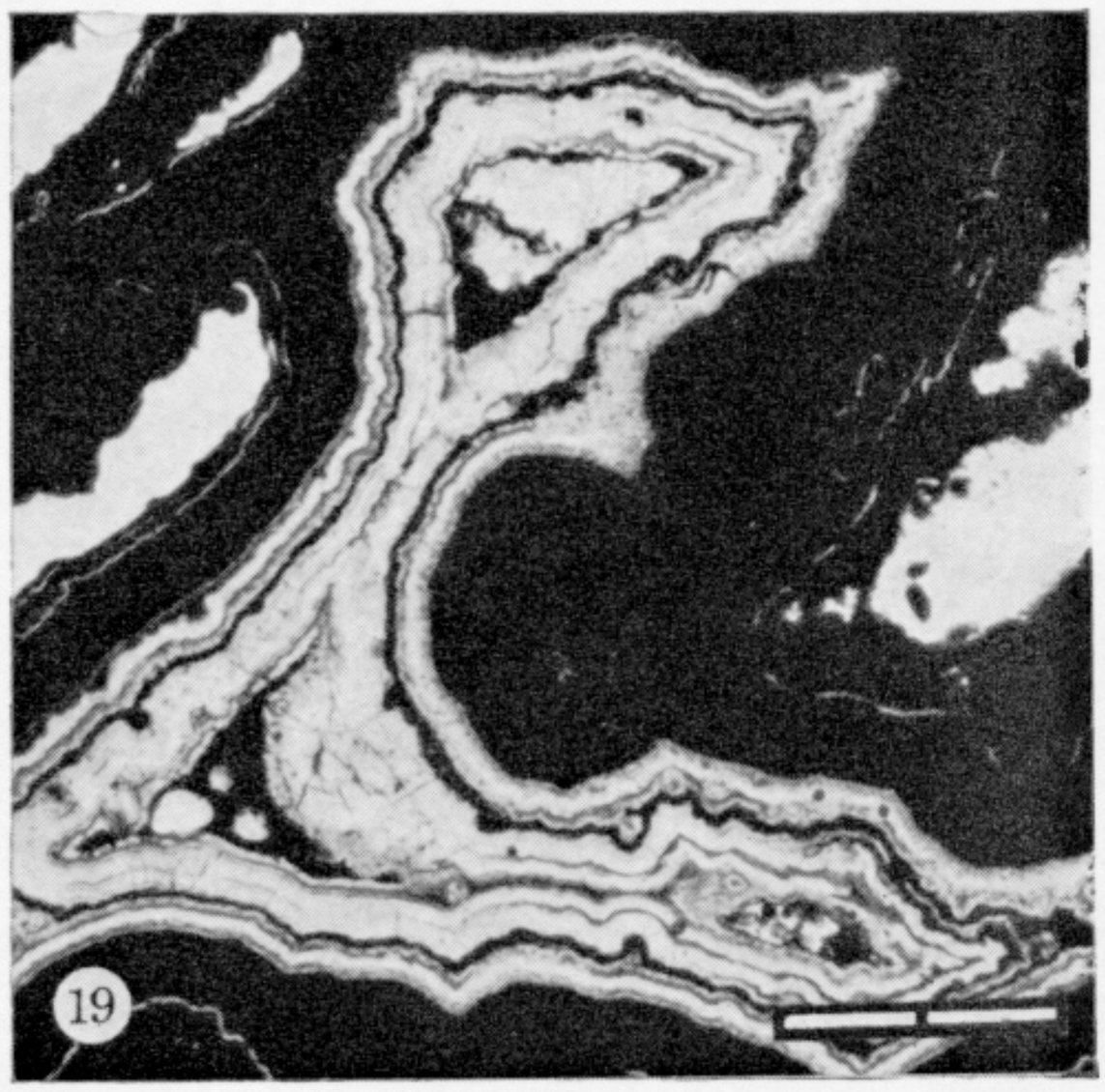

FIGURES 14–19. For description see p. 515.

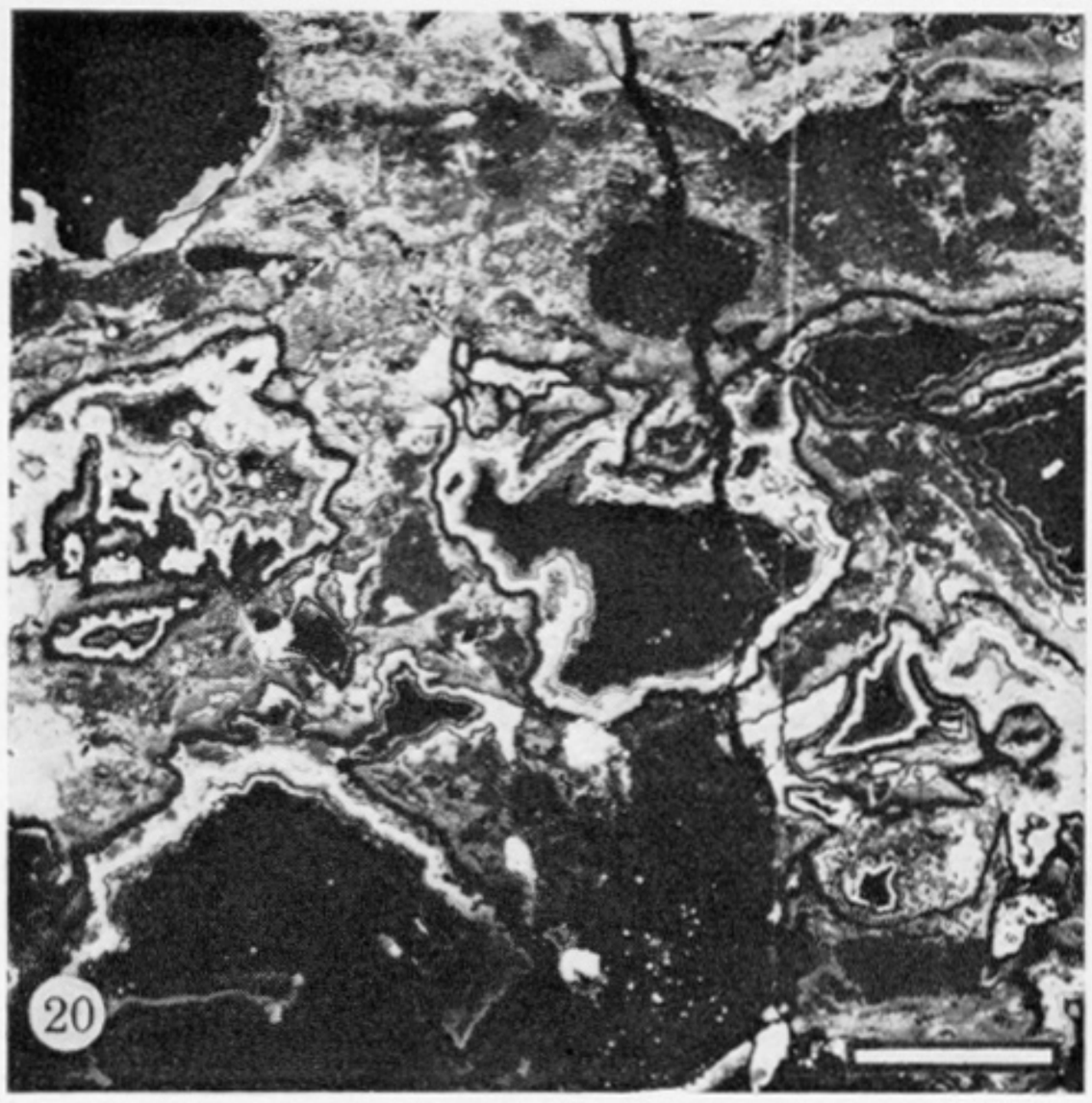

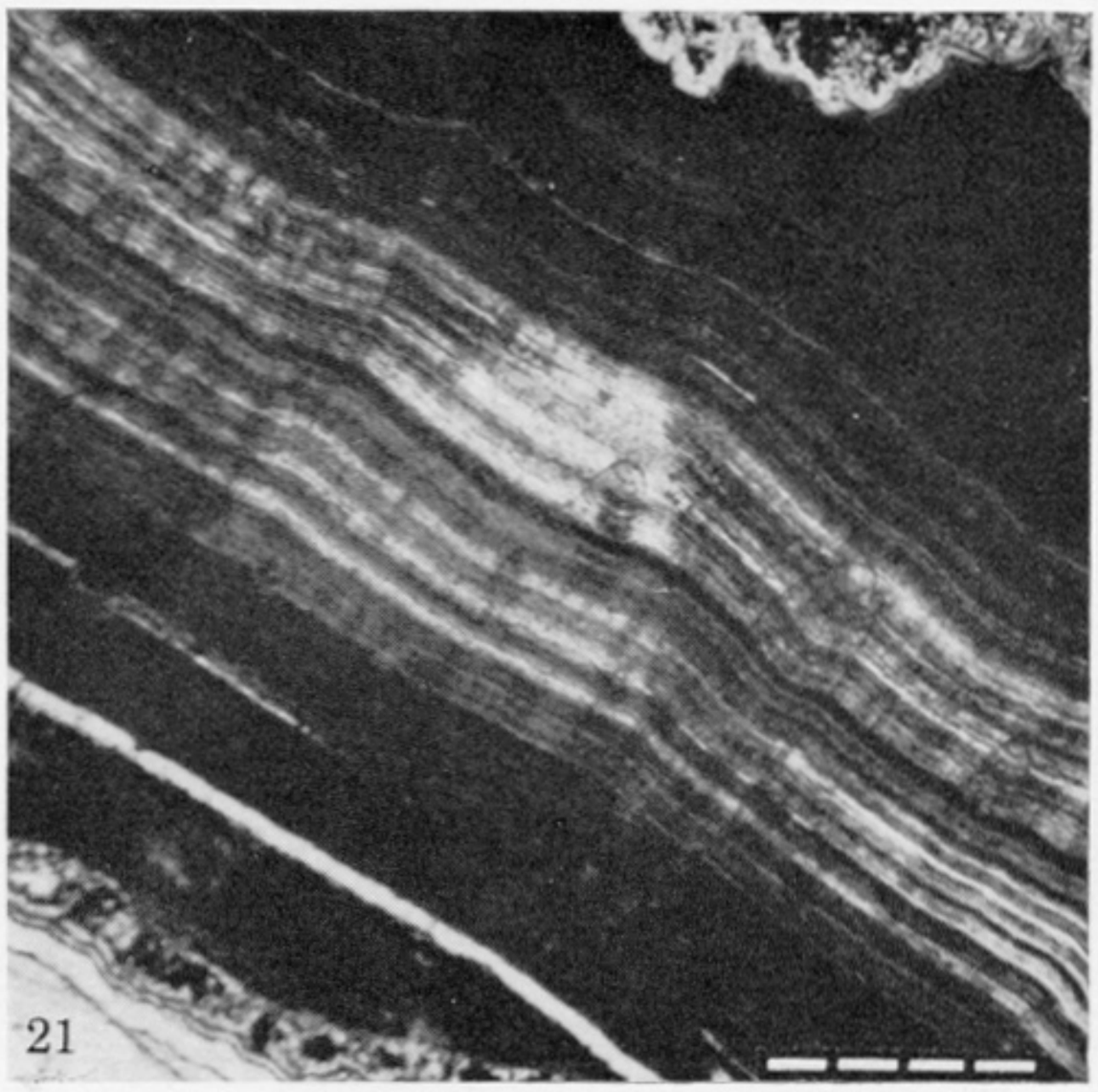

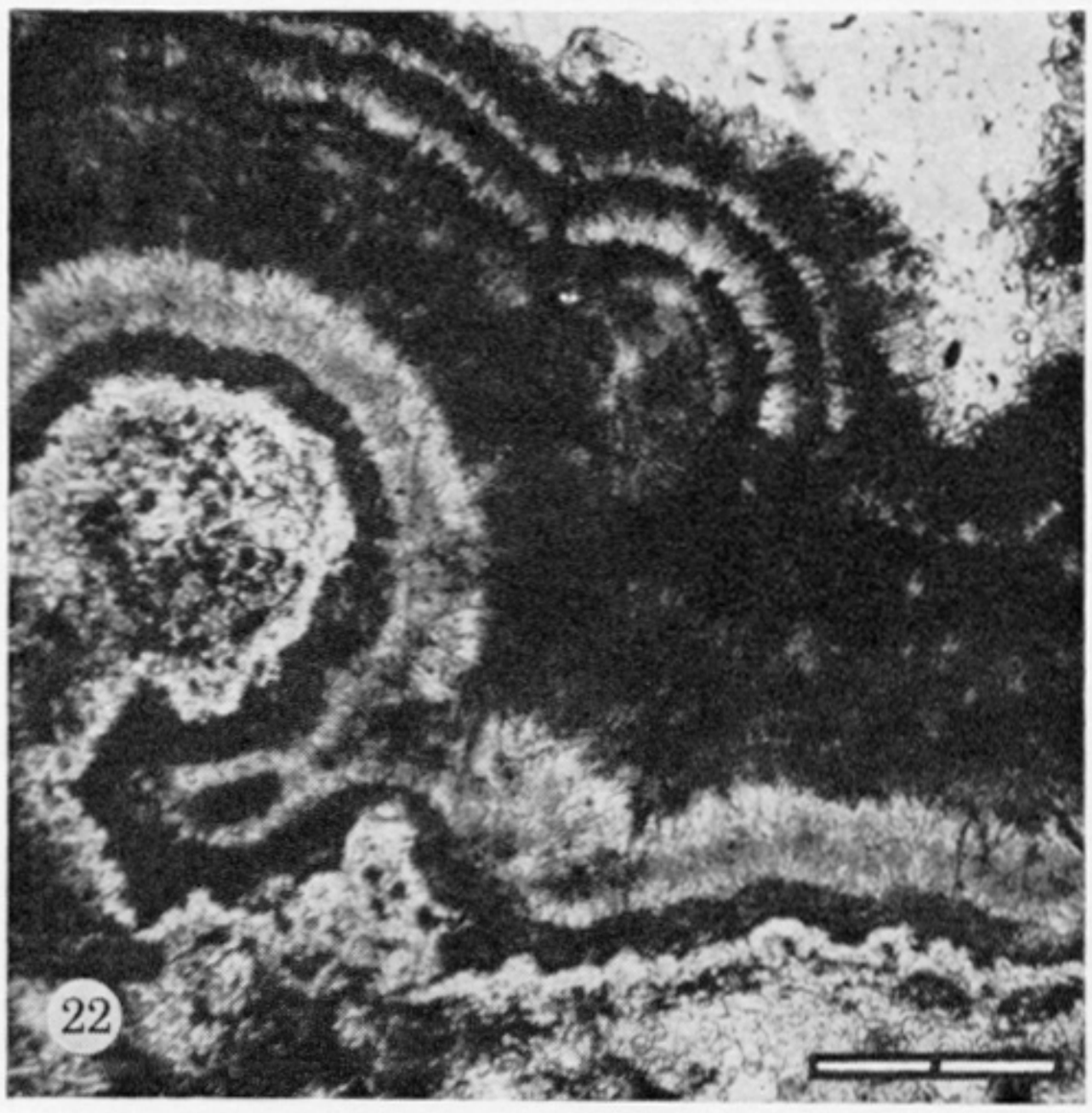

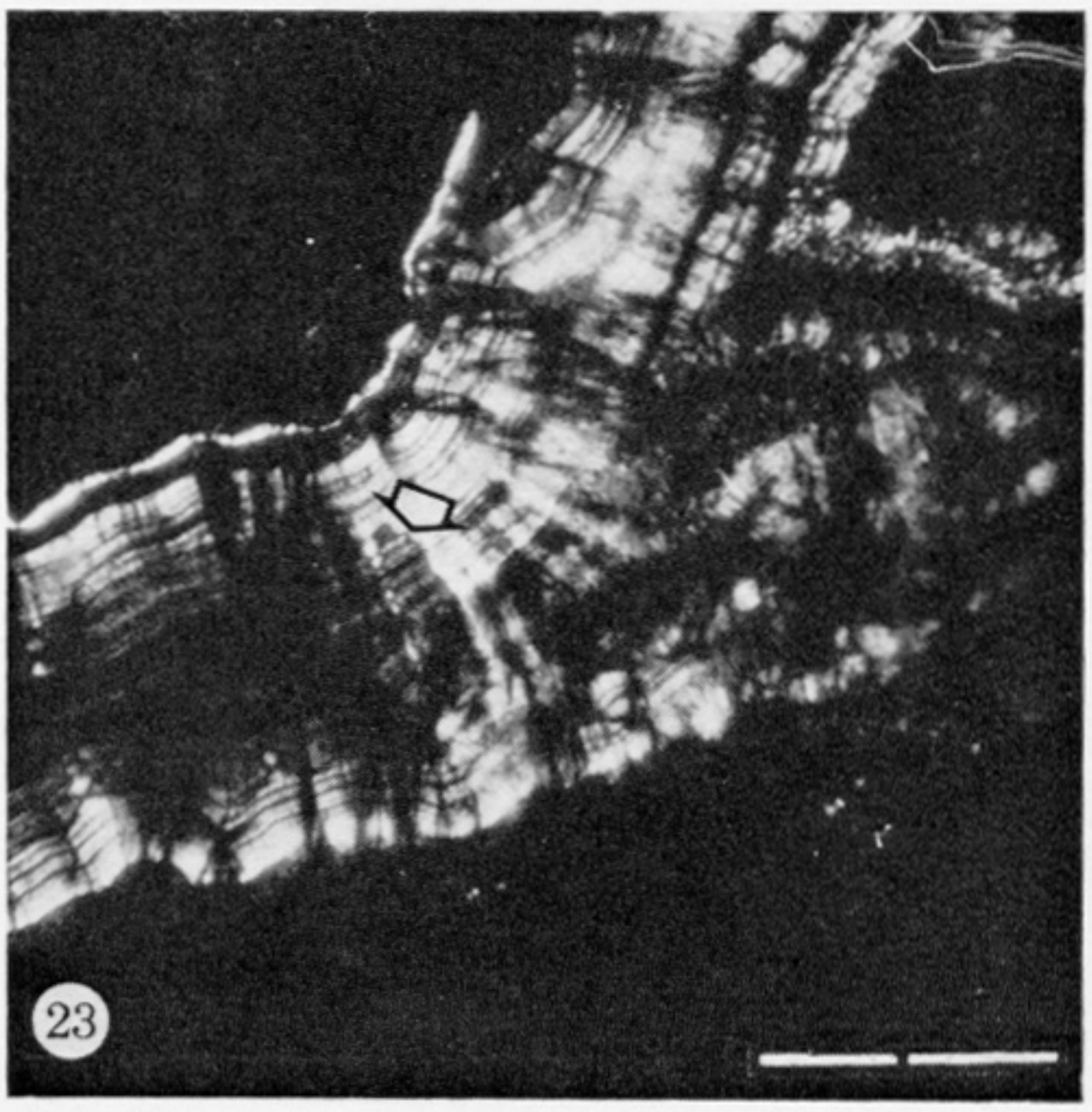

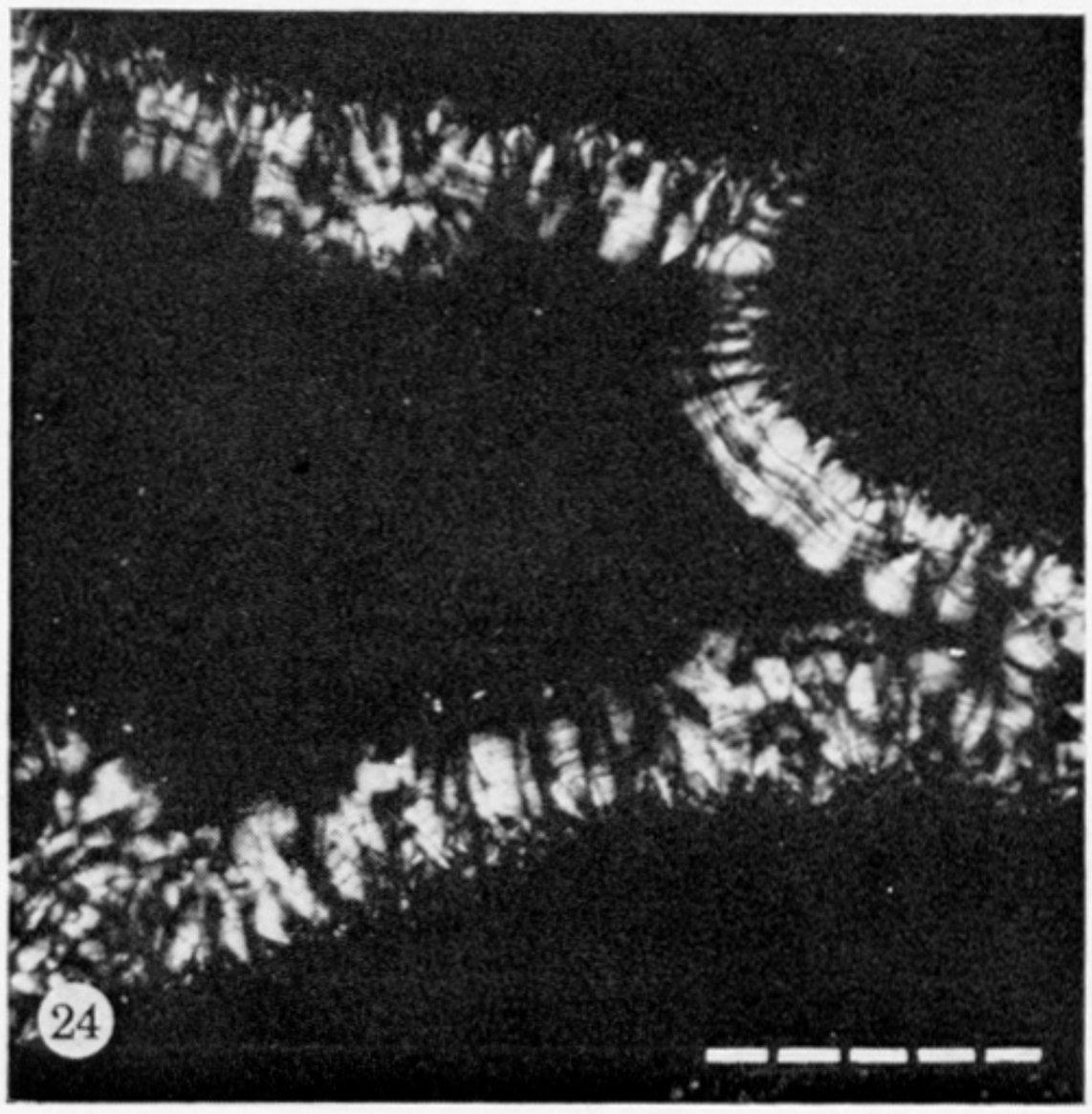

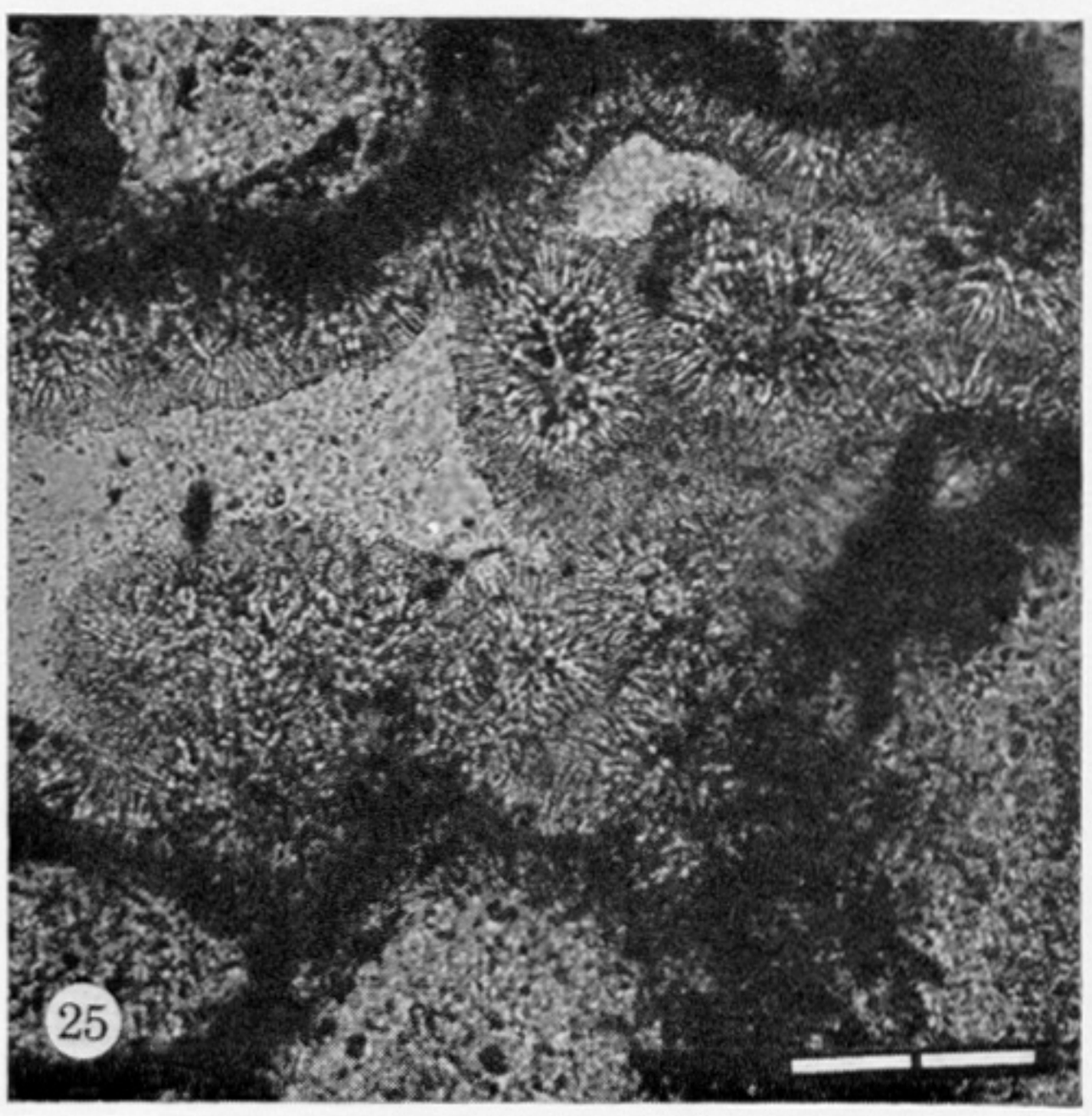

FIGURES 20–25. For description see opposite.

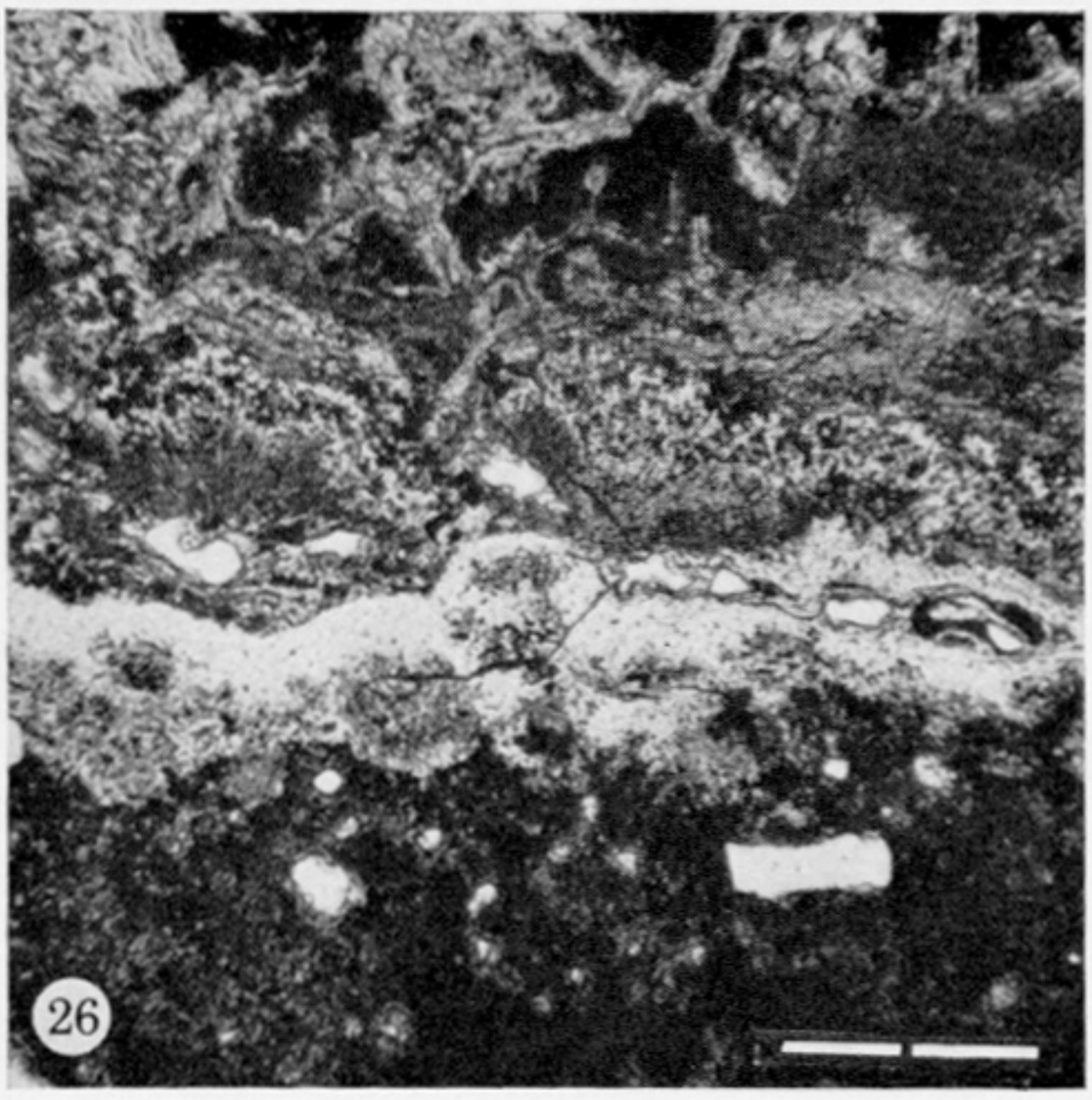

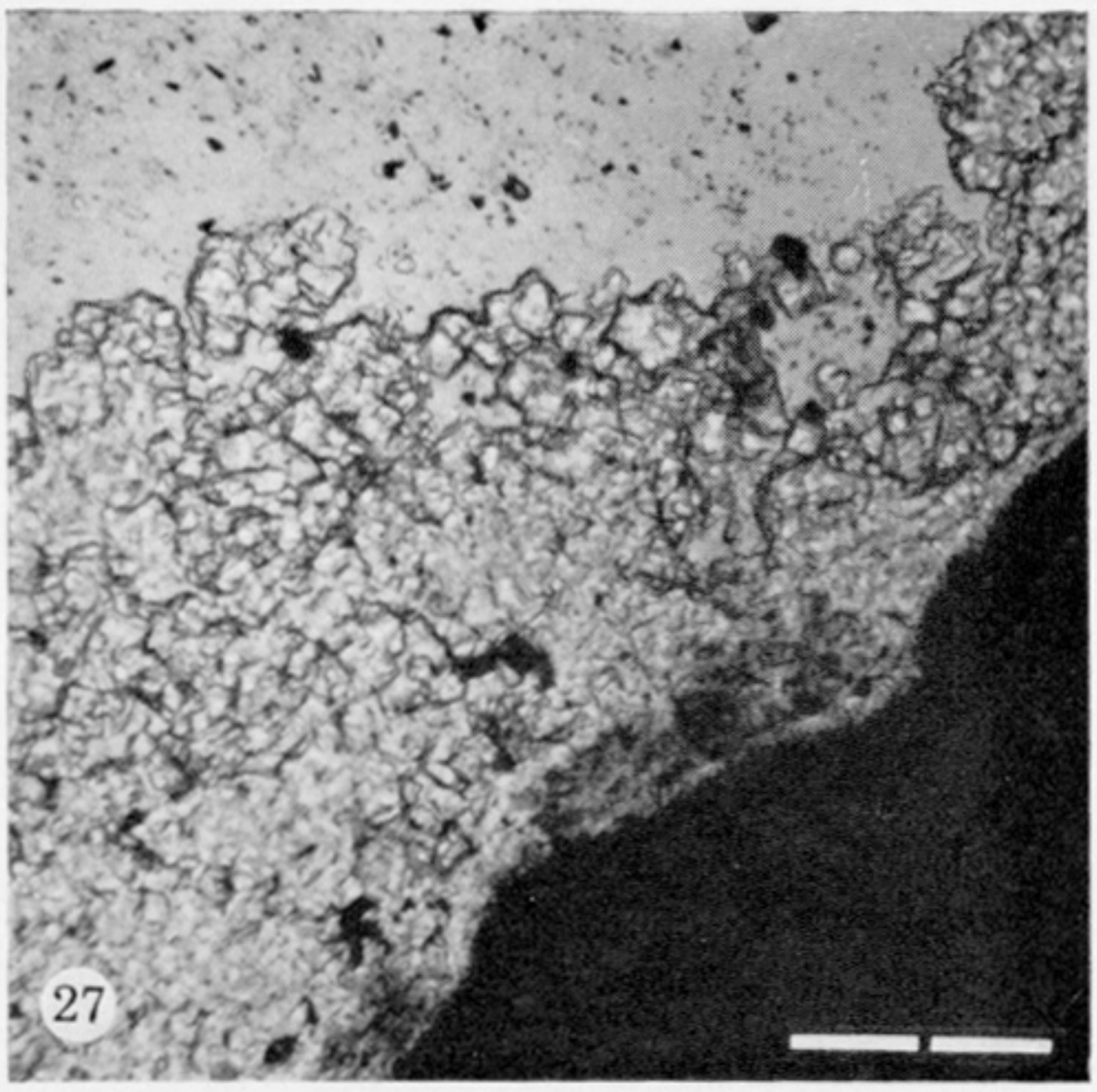

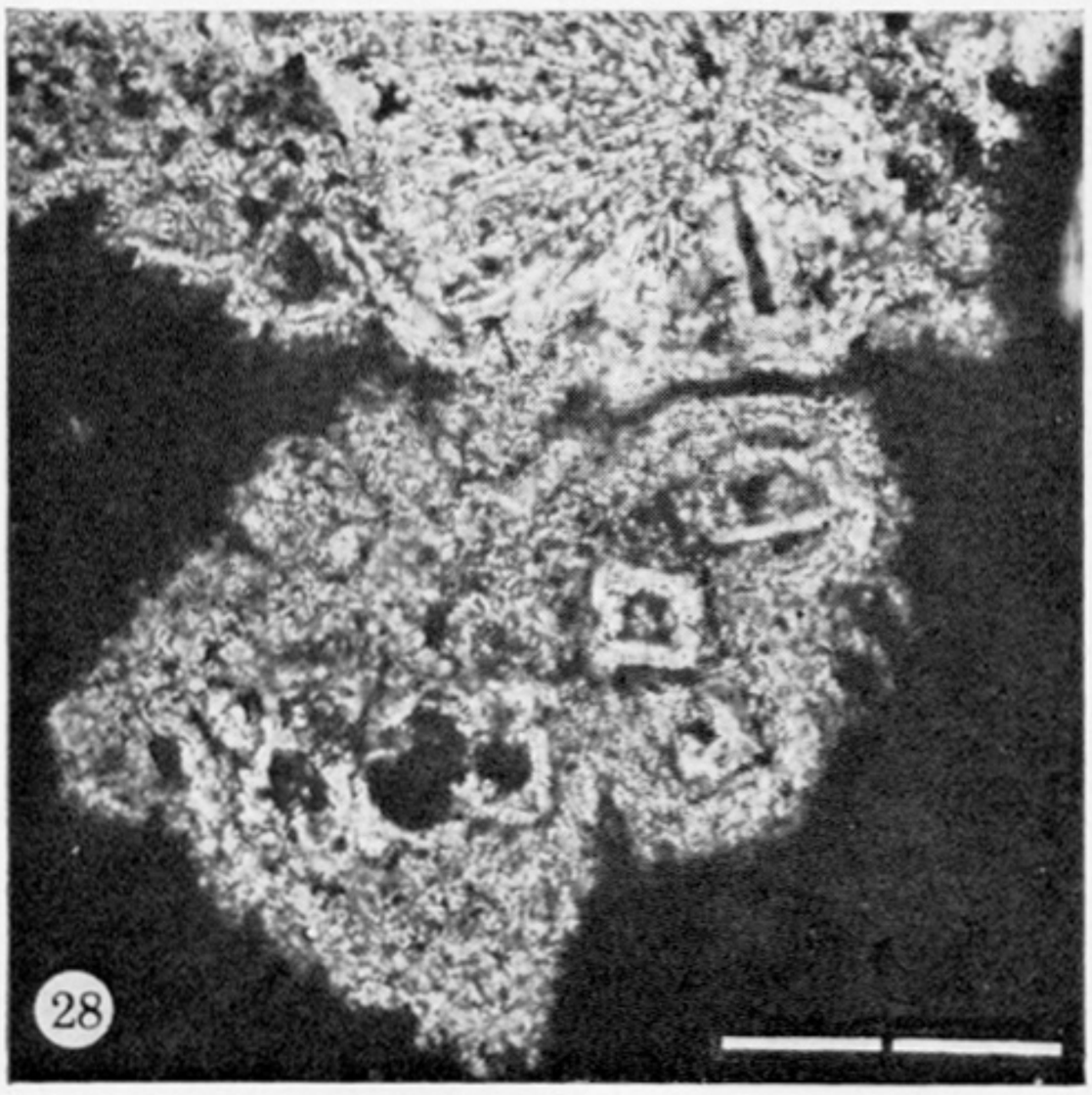

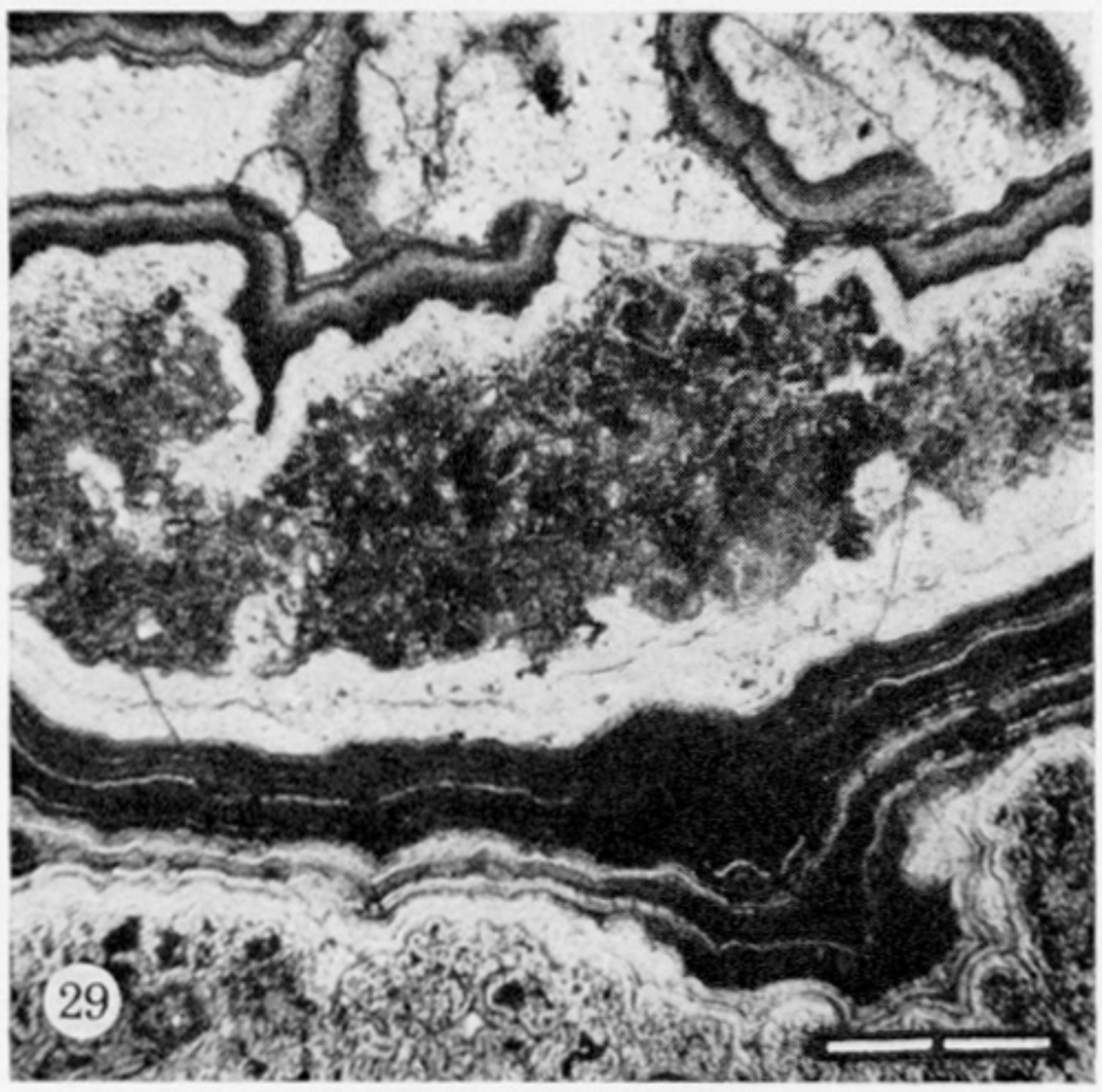

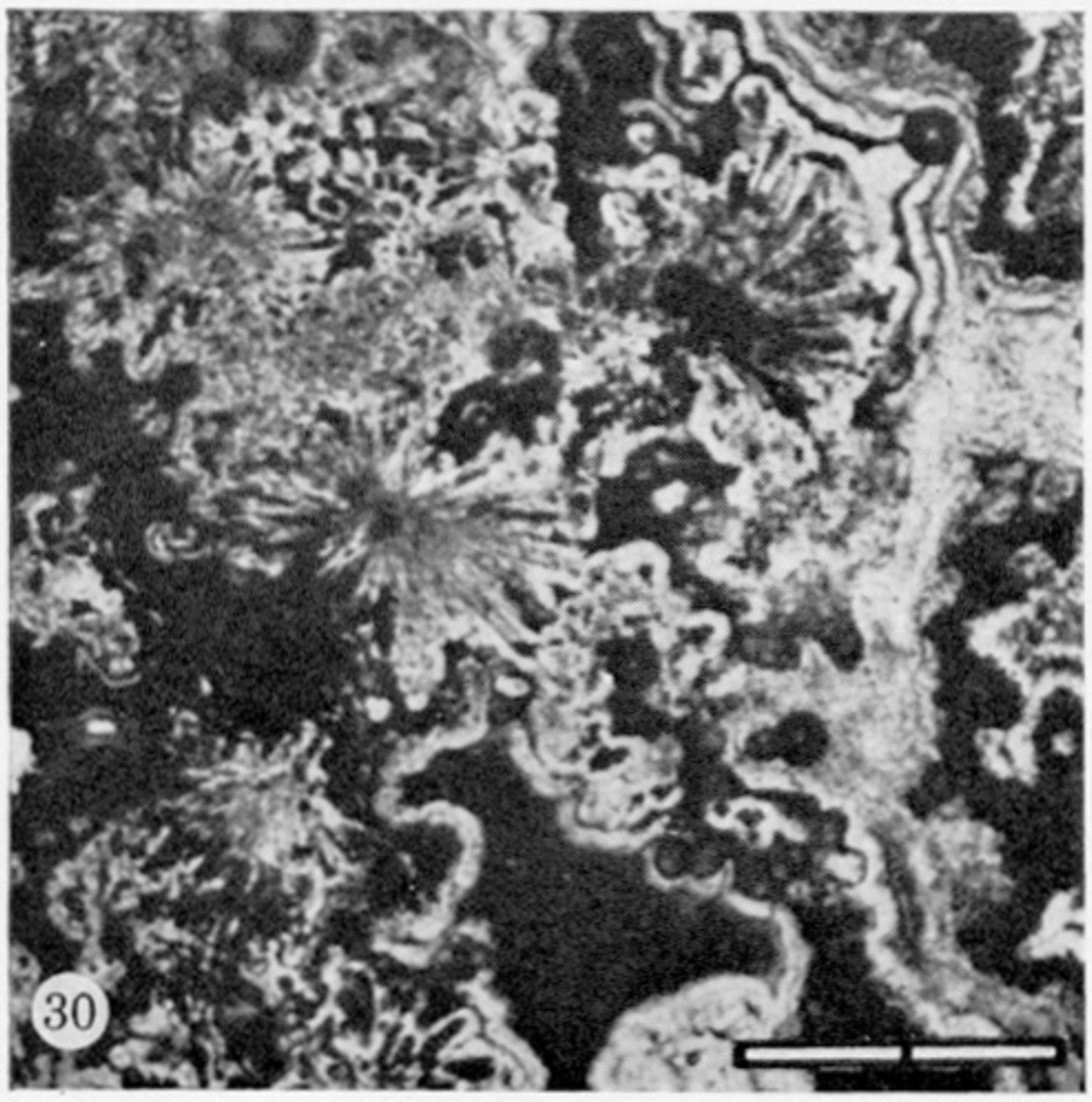

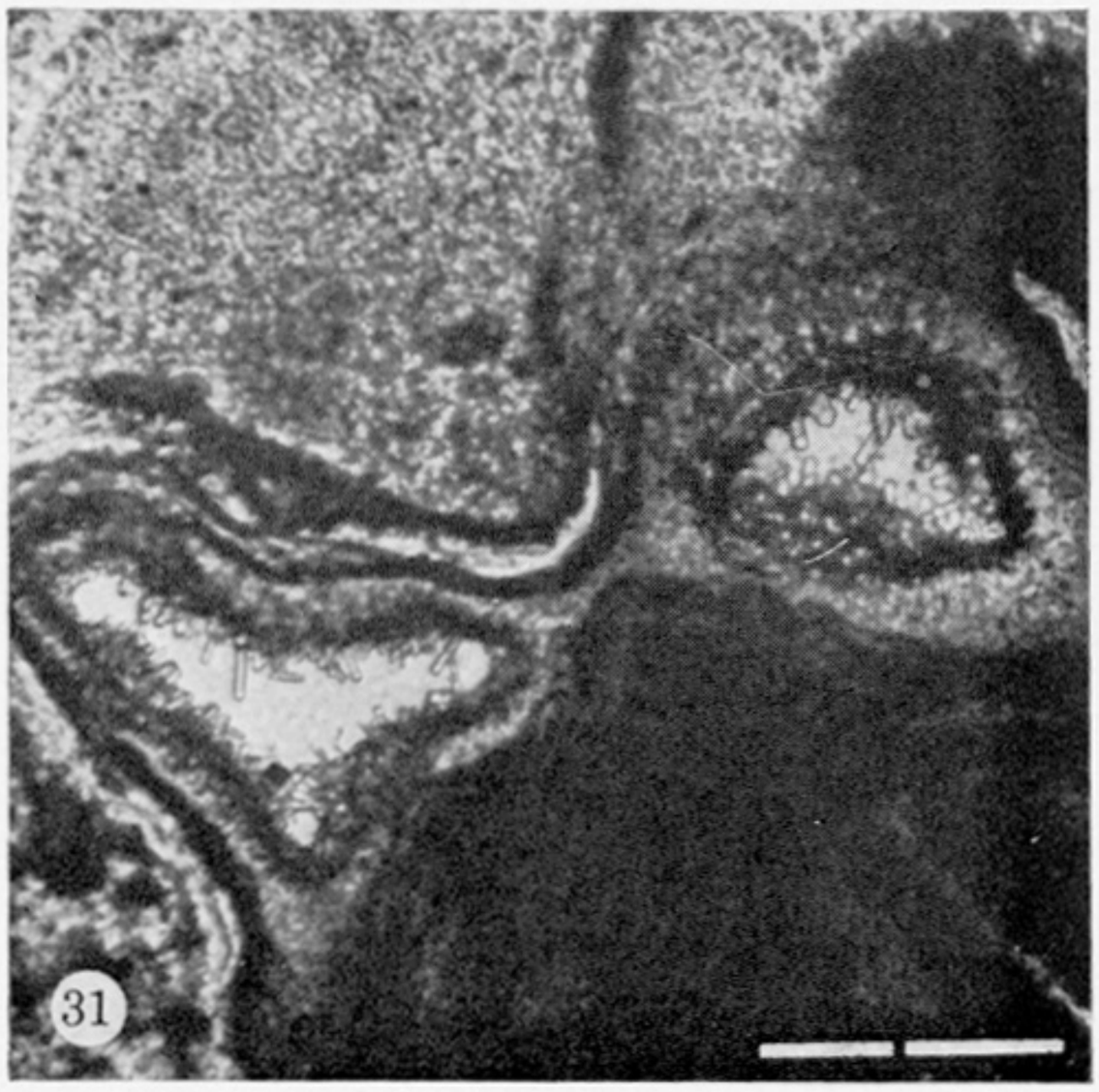

FIGURES 26–31. For description see opposite.

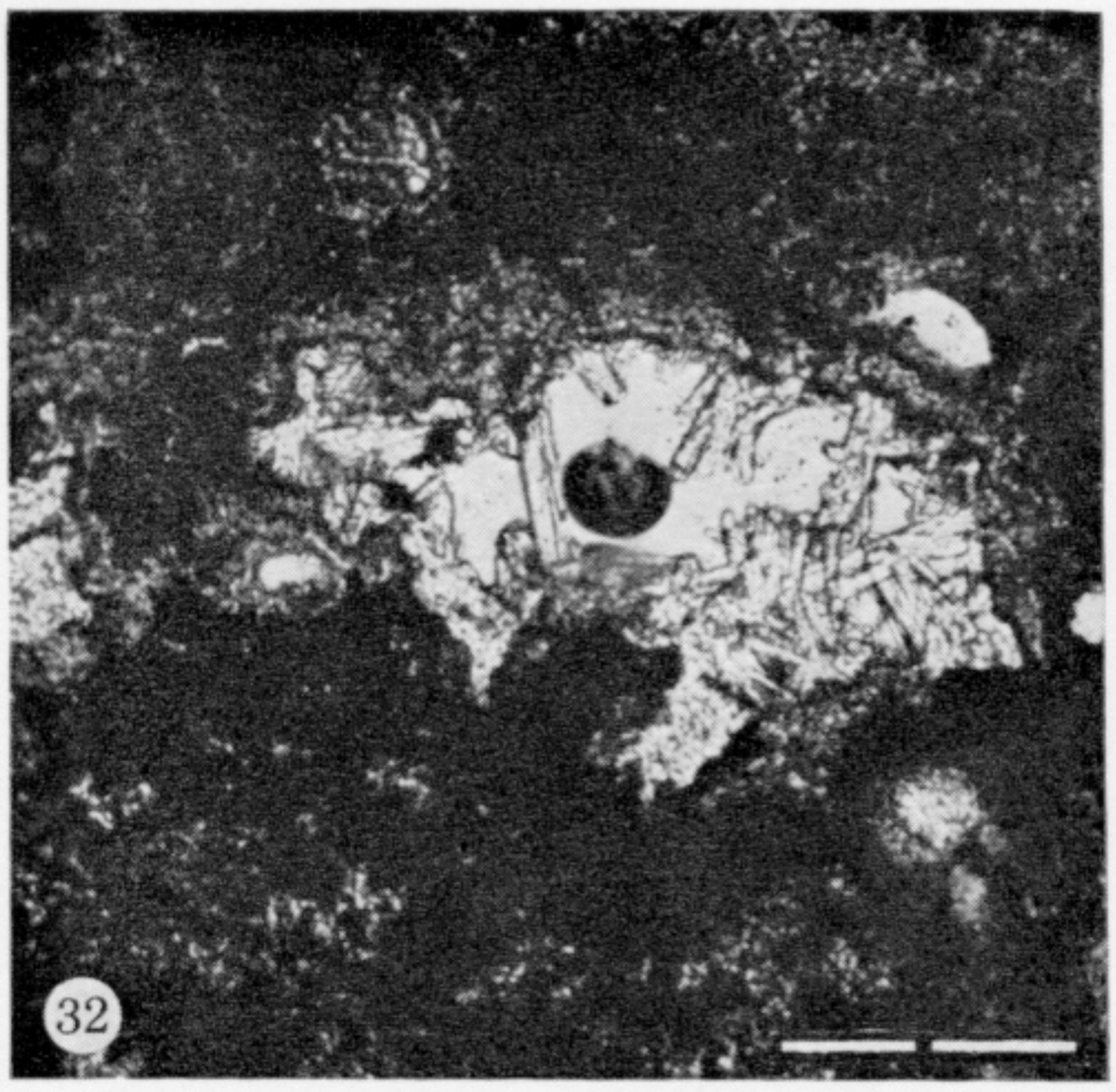

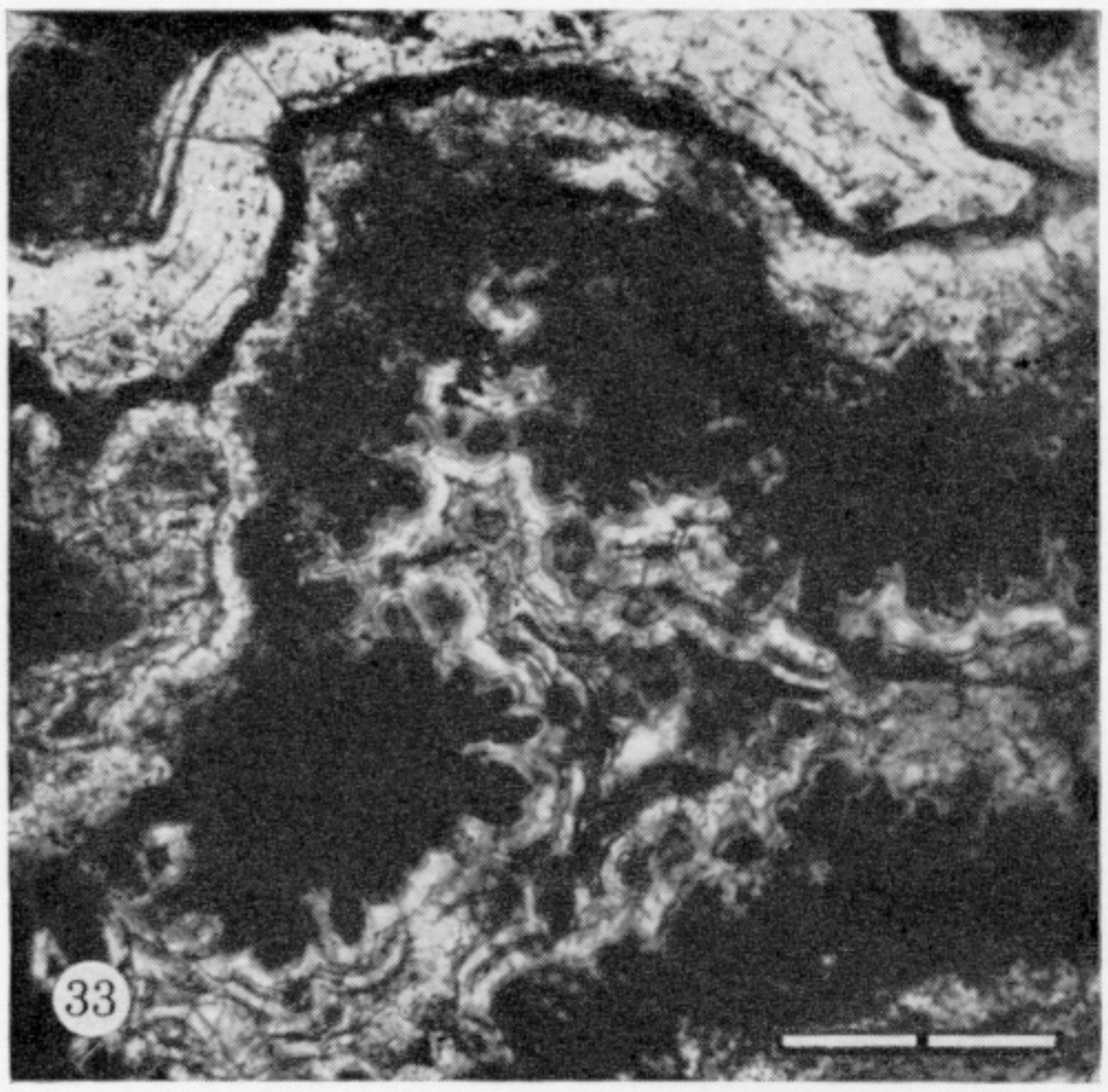

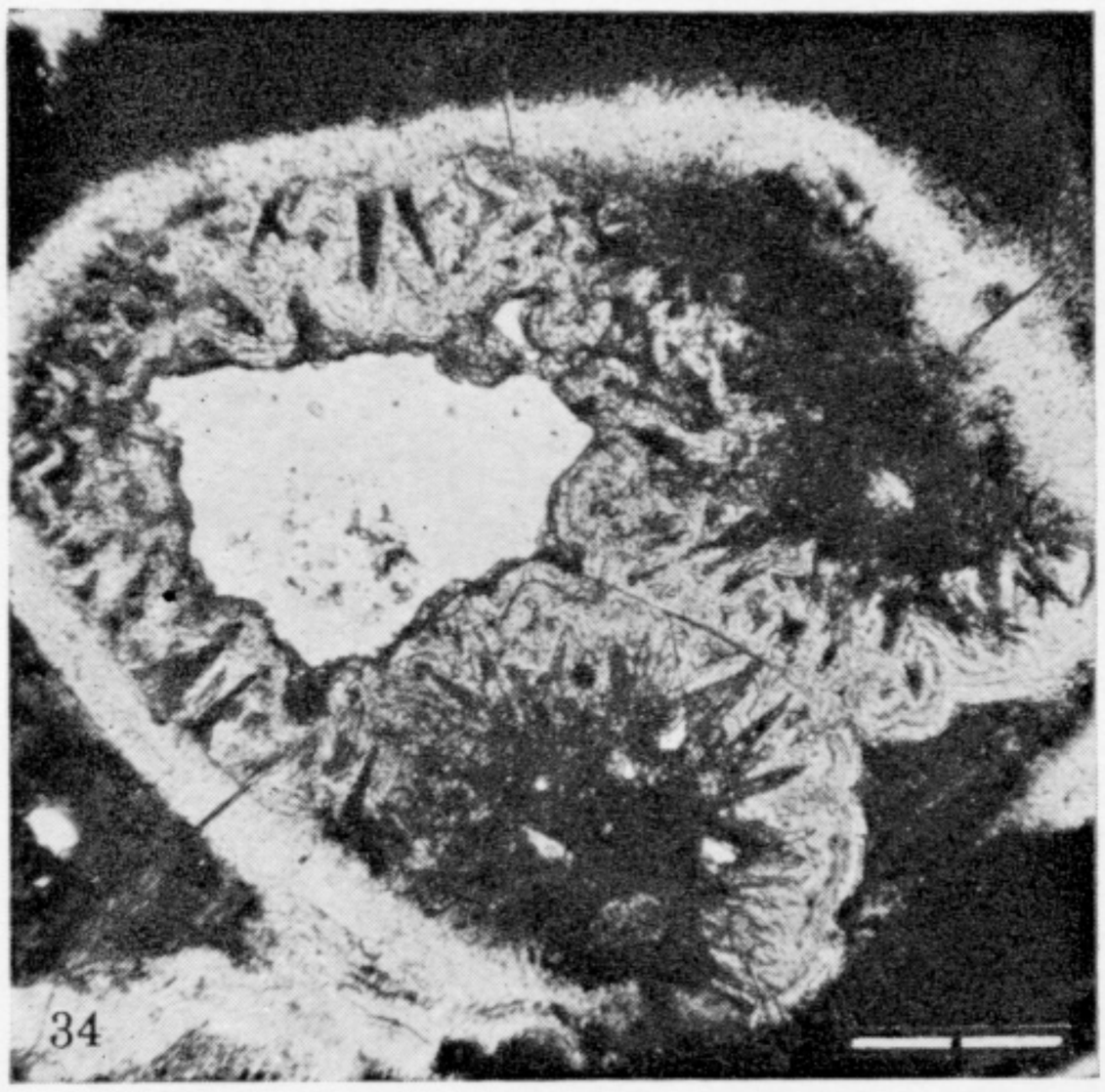

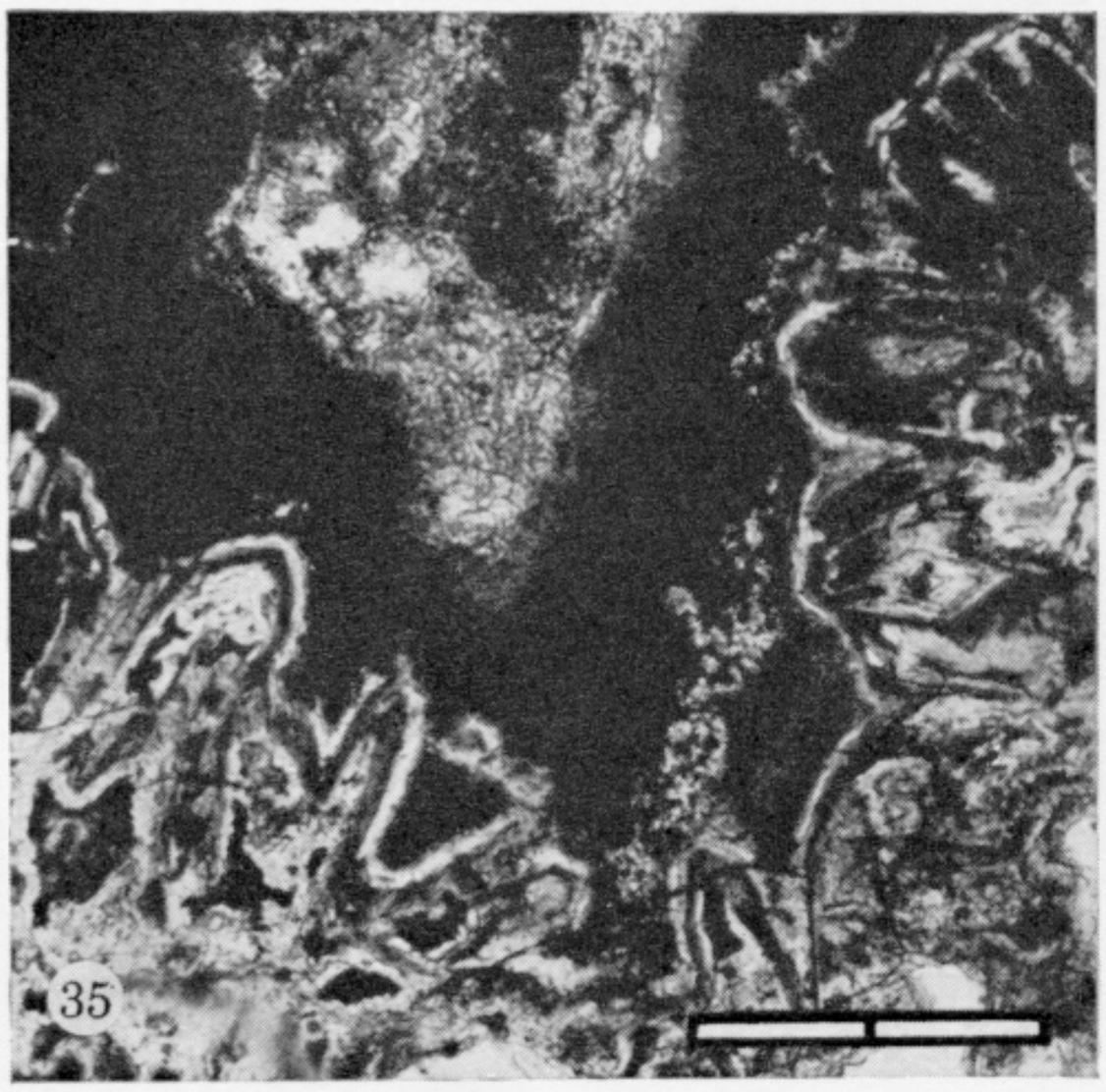

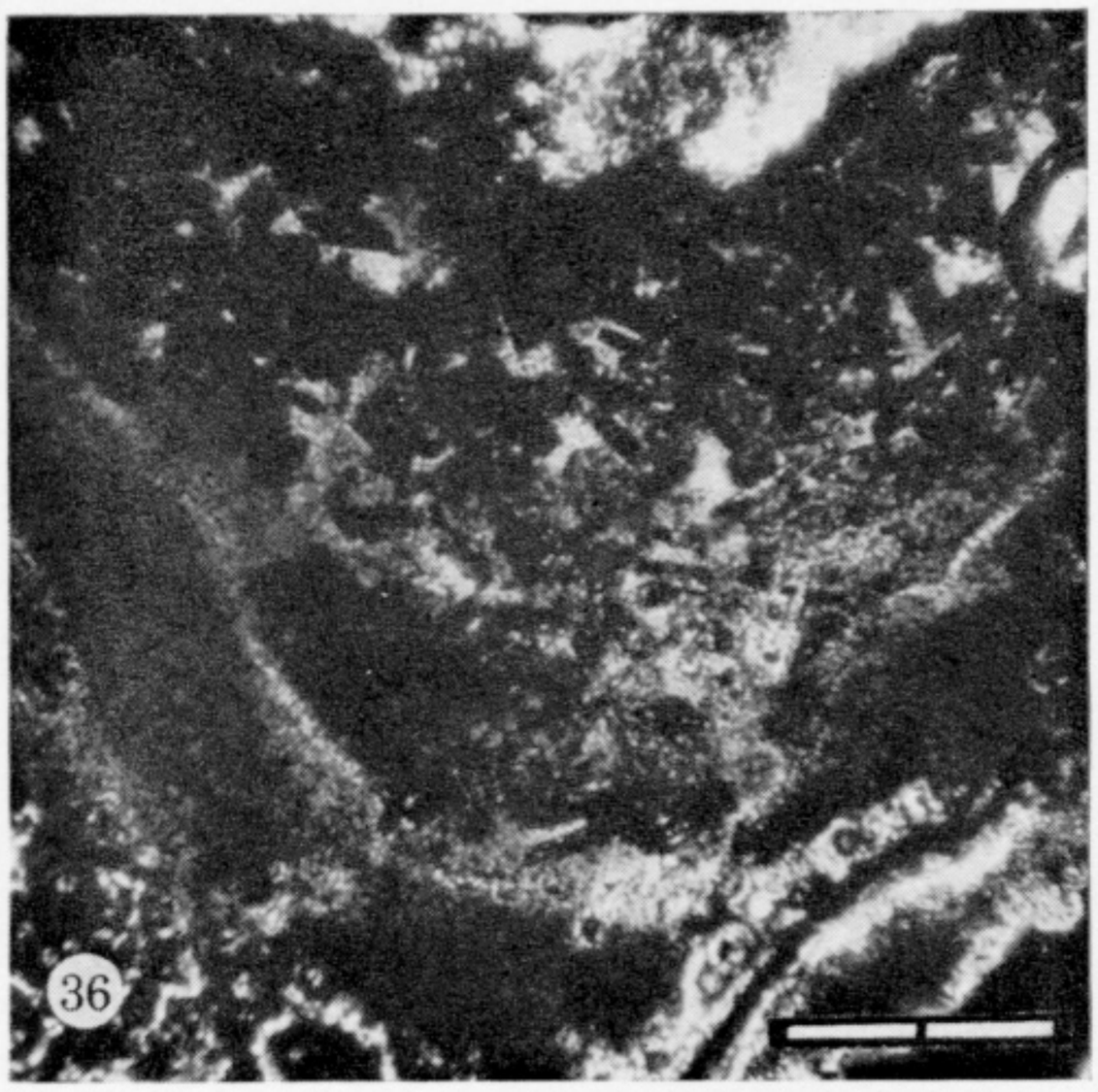

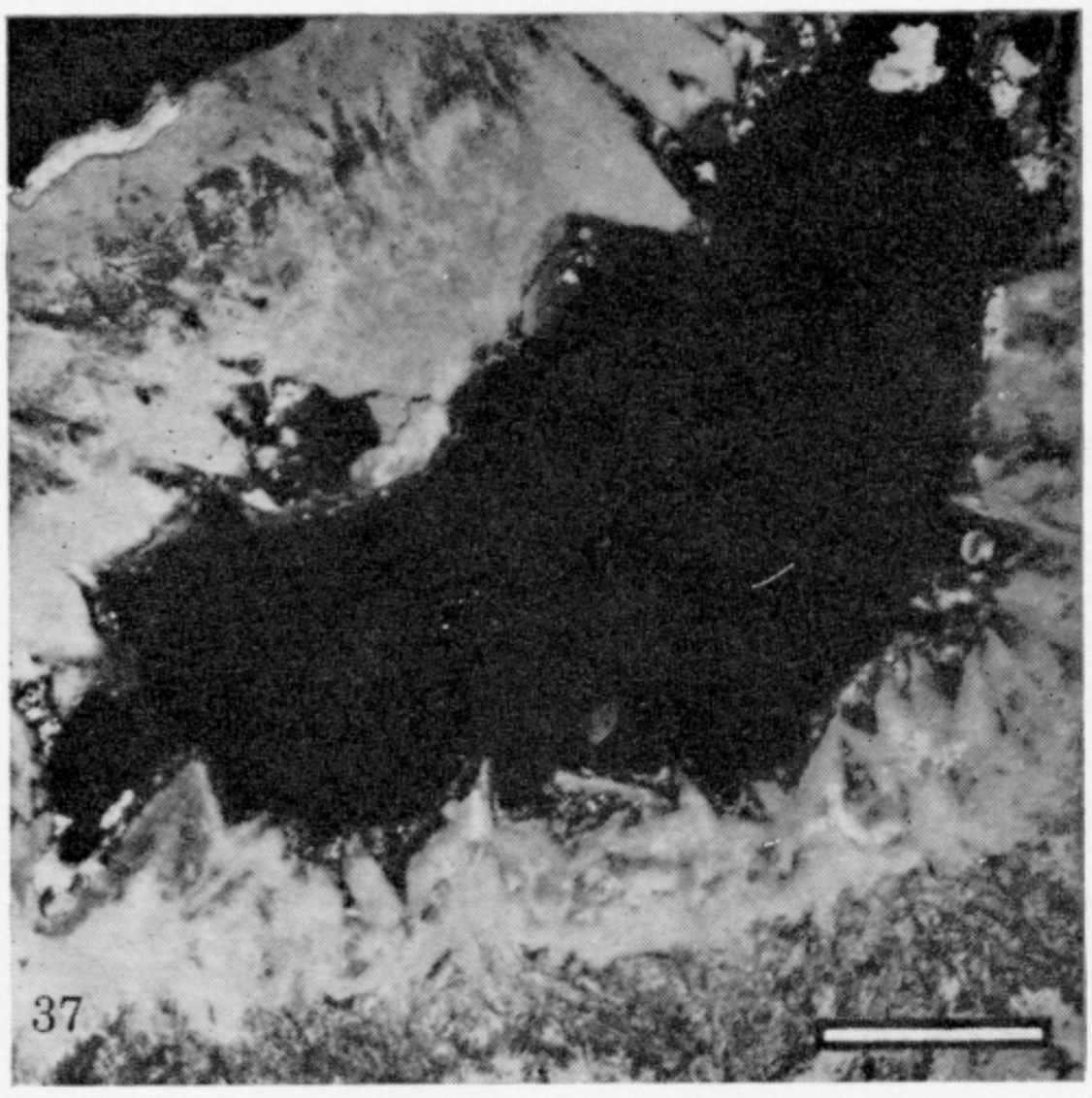

FIGURES 32–37. For description see opposite.

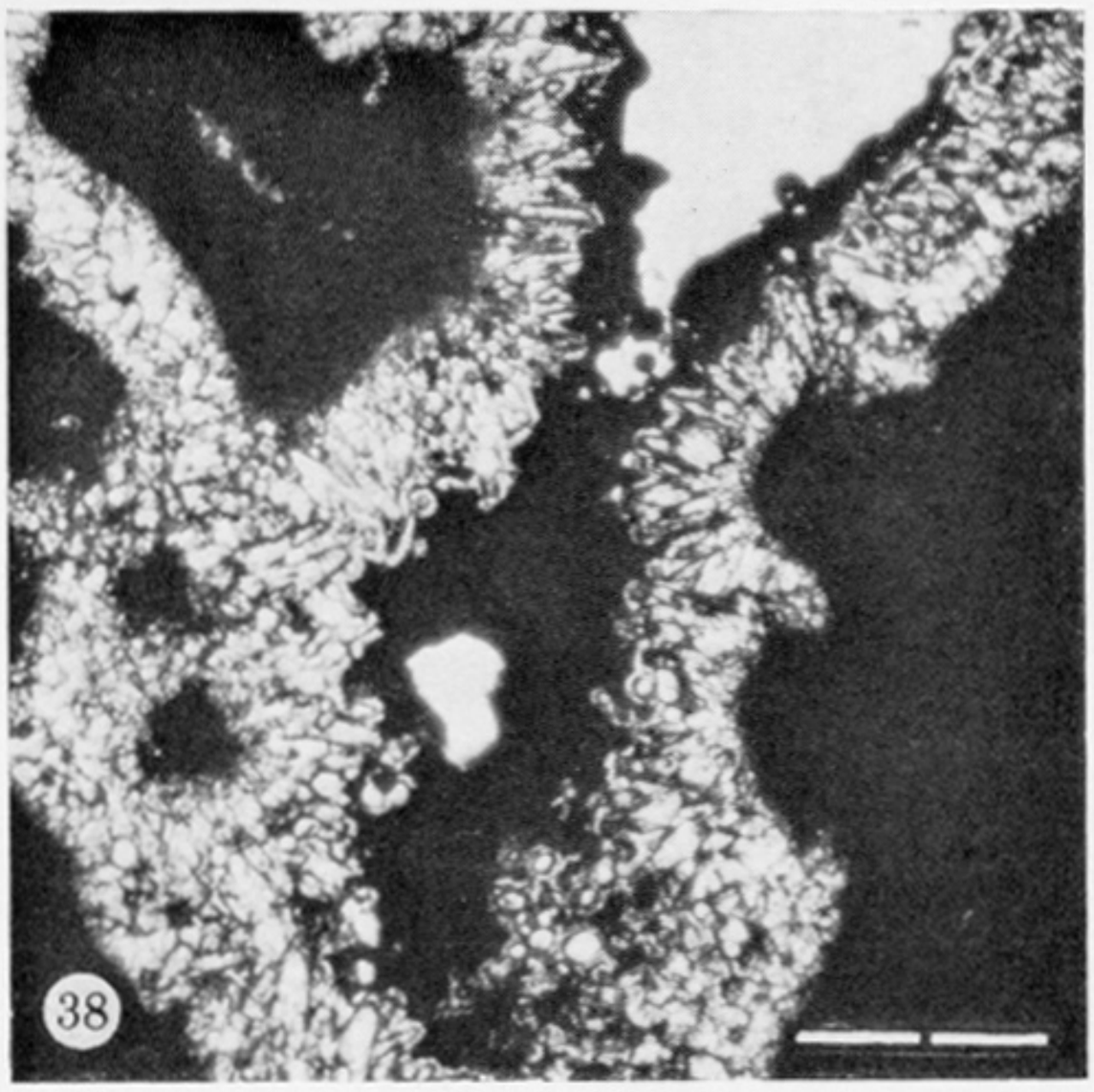

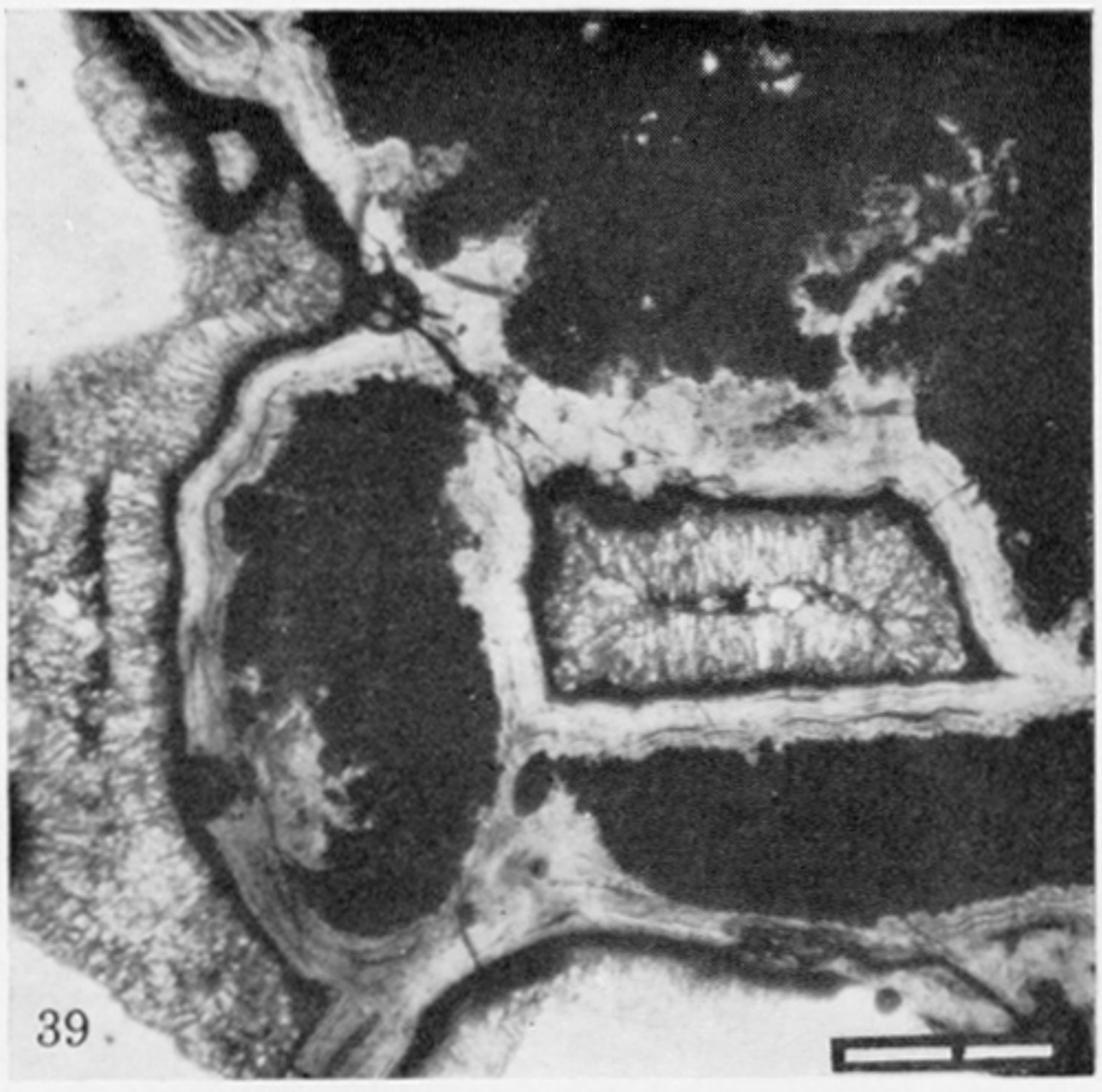

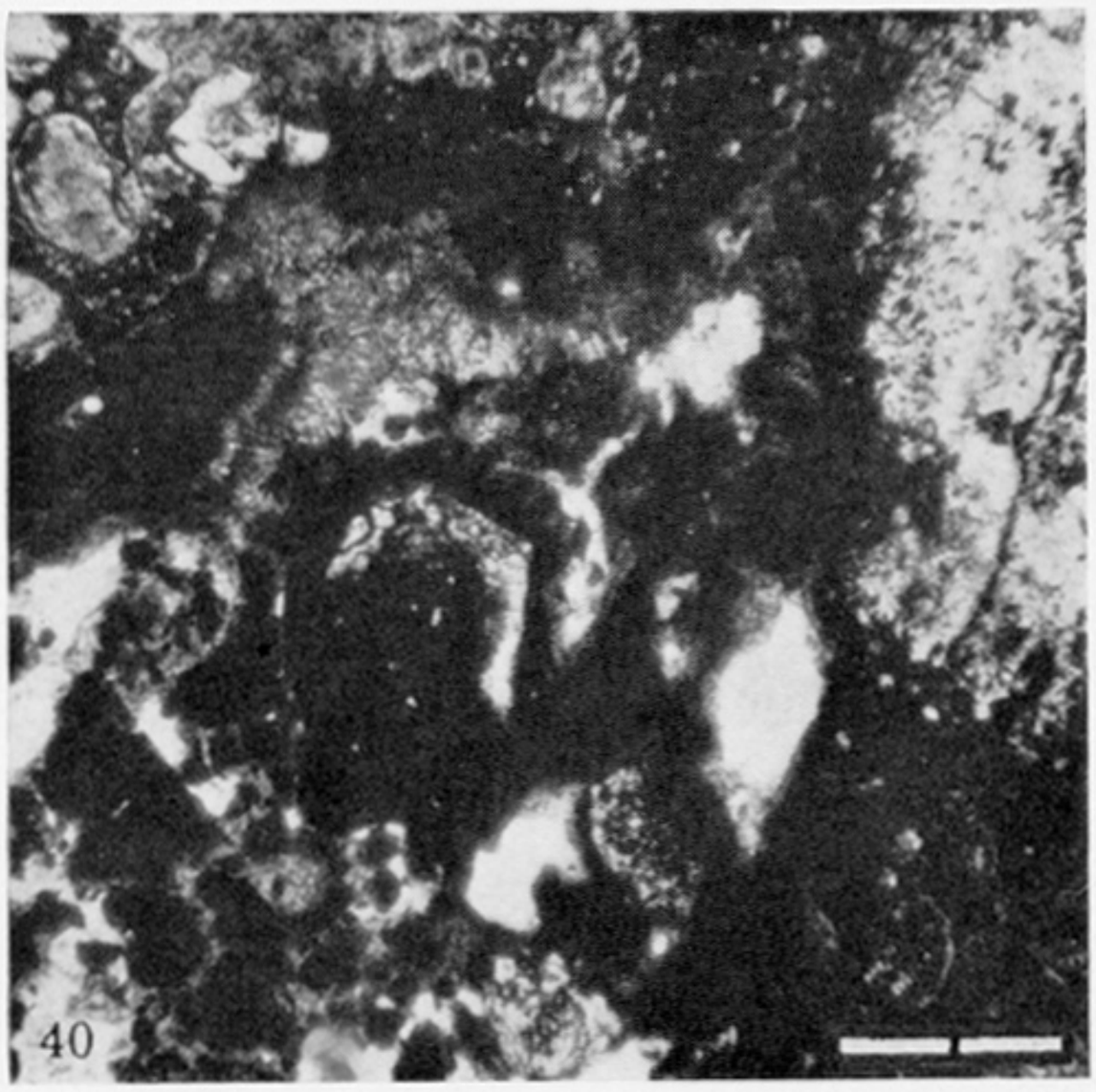

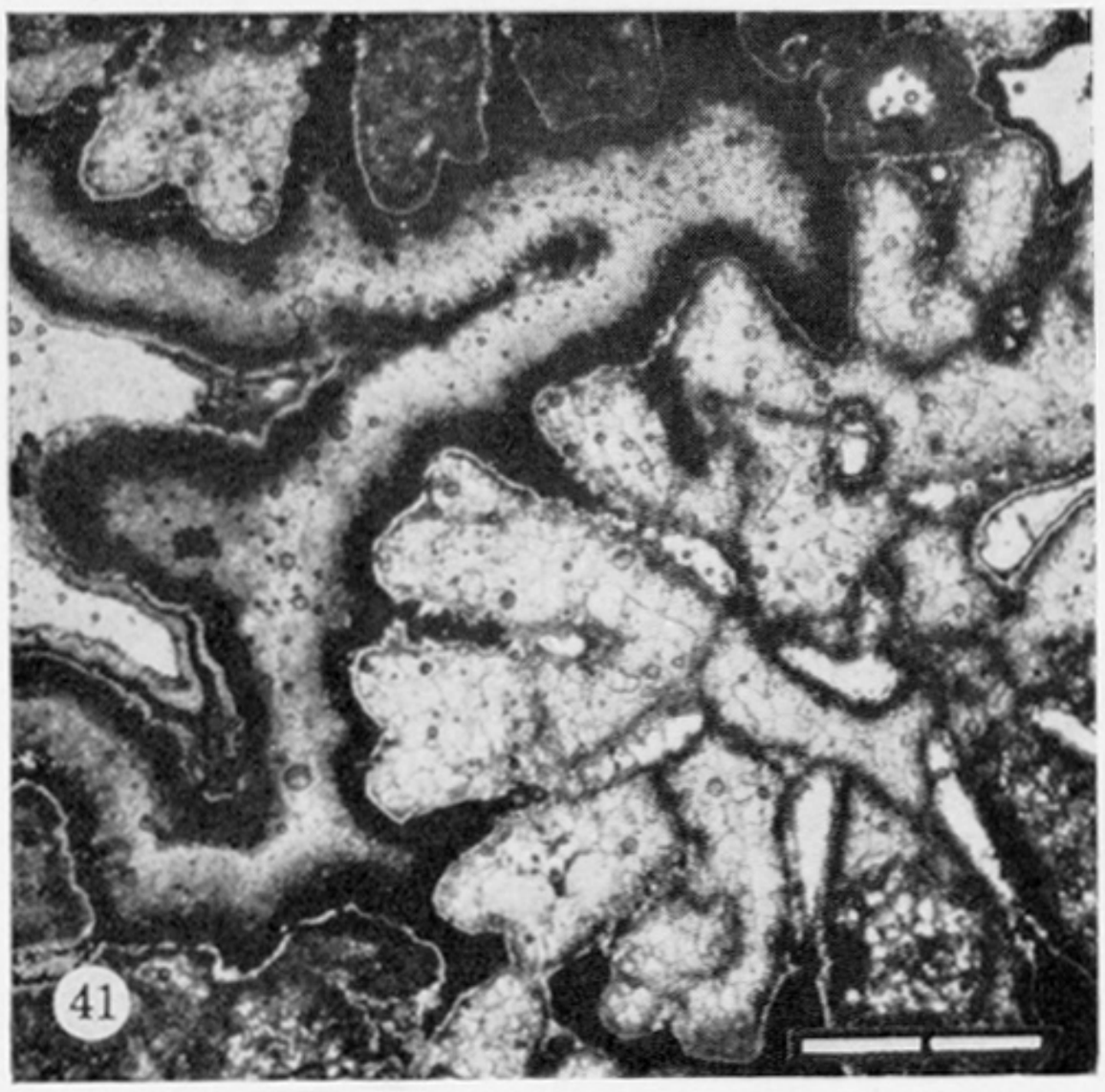

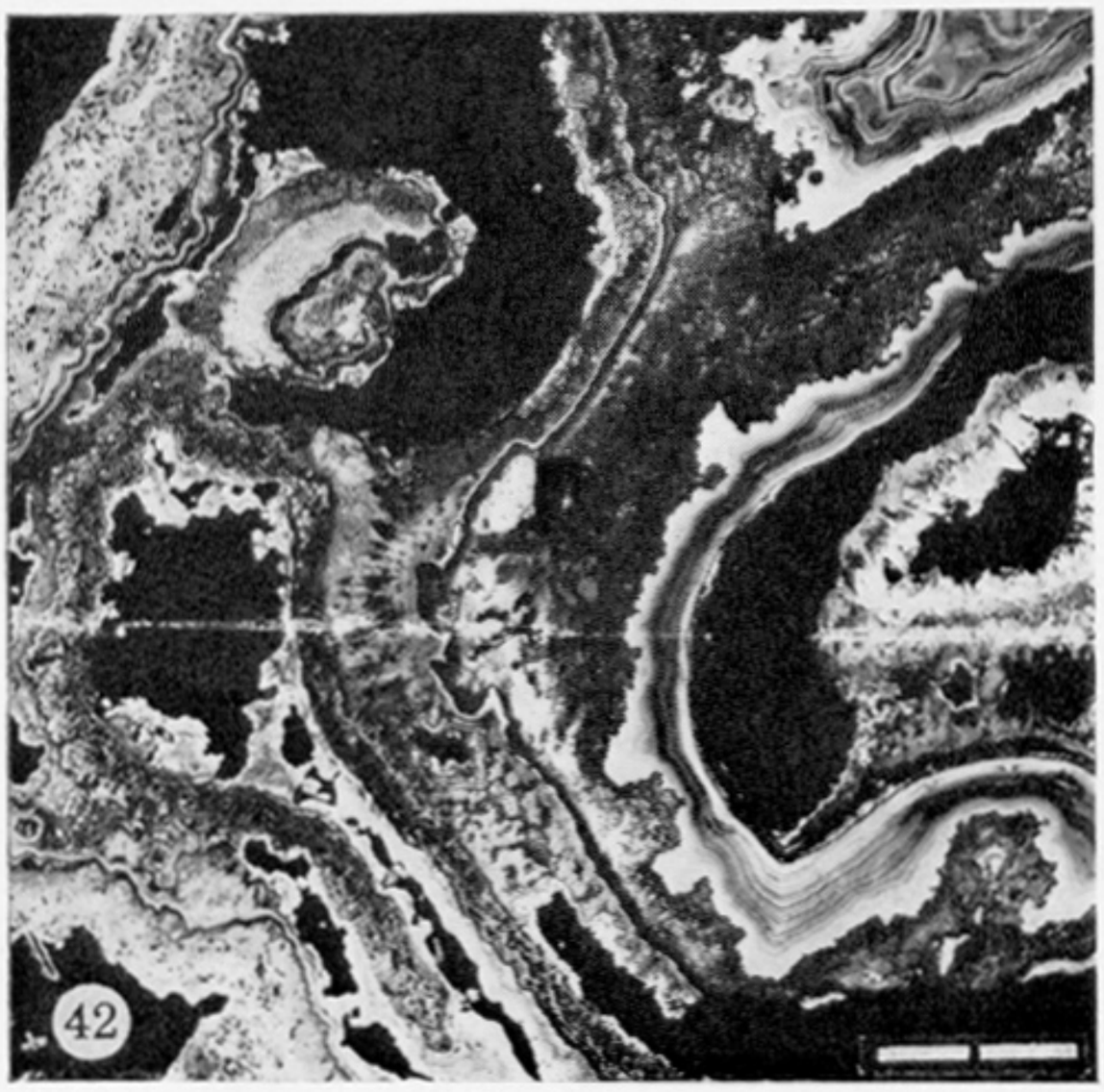

FIGURES 38–43. For description see opposite.